NOTE TO USERS

Validation and characterization of putative NHE6-interacting proteins identified by yeast two-hybrid screening and tandem affinity purification

Albena Davidova

Department of Physiology
McGill University
Montreal, Quebec, Canada
January 2007

A thesis submitted to the Faculty of Graduate Studies and Research in partial fulfillment of the requirements of the degree of Master of Science

Your file Votre référence
ISBN: 978-0-494-32689-3
Our file Notre référence
ISBN: 978-0-494-32689-3

ACKNOWLEDGMENTS

This work would not have been possible without the support of my supervisor Dr. John Orlowski, the help of my colleagues and the understanding of my husband, parents and friends.

I would like to thank first and foremost Dr. Orlowski for giving me the chance to do research in cellular biology despite my engineering background. This enriching experience had a big impact on my life, as it made me realize that despite the long hours of work and the frustrating days when nothing seems to work, my true vocation is to advance knowledge through research. Most importantly, I grant much credit to Dr. Orlowski for making every day (or almost) of my two years in his laboratory a day I was looking forward to. I believe that his overflowing enthusiasm, his genuine personality and his understanding and patience had a lot to do with it. I would like to thank him for always taking the time to answer my numerous questions and for guiding me through all the steps of my project.

I would also like to thank the other graduate students in the laboratory and our technician for being such good friends. My project wouldn't have started as well as it did without the assistance of Mrs. Alina Ilie who taught me almost all the laboratory techniques that I needed to know. She also helped me to interpret my results on several occasions, in addition to giving me a hand in the making of the GST-fusion constructs and the insertion of NHE6 into the TAPtag-containing vector. I would also like to thank Mr. Hans Zaun for always being available to answer my questions. Mr. Ewen Jones was very helpful in teaching me a rigorous scientific way of thinking, in advising me with the design and making of my DNA constructs and in my familiarisation with the confocal microscope. I am also grateful to Mr. Tushare Jinadasa for his assistance with computer issues and for his help in improving my immunoprecipitation technique. I would like to give credit to Mrs. Annie Boucher and Dr. Viktoria Lukashova for their support with different aspects of my project and with personal issues.

I would like to give credit to the following people from the Génome Québec Innovation Center: Dr. Marcos Rafael Di Falco for running all my samples through the mass spectrometer and for his assistance in troubleshooting my TAP experiments and Mr.

Leonid Kriazhev for running the aliquots of my purified samples through gel electrophoresis and for silver staining the gels.

I would like to thank the members of my supervisory committee for their time, their useful advices and their thought provoking questions, and especially Dr. Ursula Stochaj, who always encouraged me to think positively about my results and who has kindly agreed to be my internal examiner.

Last but not least, I would like to thank the graduate students' secretary, Ms. Christine Pamplin, for her professionalism and for her timely and efficient guidance with all the administrative requirements and paper work throughout my thesis.

TABLE OF CONTENTS

LIST OF TABLES

LIST OF FIGURES

LIST OF ABBREVIATIONS

Abbreviation	Meaning
2YT	2 x yeast-tryptone
AP-1/2	adaptor protein
APOD	apolipoprotein D
Arp2/3	actin related protein
ATCC	american type culture collection
ATP	adenosine tri phosphate
ATP5α or ATP5A1	mitochondrial ATP synthase, subunit alpha
BSA	bovine serum albumin
Cap1/2	capping proteins
CBB	calmodulin binding buffer
CCPs	clathrin coated pits
CEB	calmodulin elution buffer
CHO	chinese hamster ovary
CHP1/2	calcineurin B homologous protein
CLIC-1	chloride intracellular channel 1
CPA	cation proton antiporter
CRB	calmodulin rinsing buffer
CS	calmodulin sepharose 4B beads
DEX	dexamethasone
DHT	dihydrotestosterone
DOCK3	dedicator of cytokinesis 3
DTT	dithiolthreitol
EDTA	ethylenediaminetetraacetic acid
EGTA	ethylene glycol tetraacetic acid
ERC	endocytic recycling compartment
ERK	extracellular signal-regulated kinase
FBS	fetal bovine serum
GFP	green fluorescent protein
GST	glutathione s-transferase
HEK 293	human embryonic kidney 293
IgG	immunoglobulin G
IPTG	isopropyl-β-D-thiogalactopyranoside
kDa	kilodaltons
LE	late endosome
M2P	affinity purification with M2 anti-flag beads
MLCK	myosin light chain kinase
MS	mass spectrometry
MW	molecular weight
NHE	sodium/proton exchanger
NHERF1/2	sodium/proton exchanger regulatory factor
OD	optical density
OK	opussum kidney
PBS	phosphate buffer saline
PFA	paraformaldehyde
PKA	protein kinase A
PTGDS	prostaglandin D2 synthase
PVC	pre-vacuolar compartment
PVDF	polyvinylidene difluoride
SCAMP	secretory carrier membrane protein
SDS	sodium dodecyl sulfate
SDS-PAGE	SDS-polyacrylamide gel electrophoresis
TAP	tandem affinity purification
TEV	tobacco etch virus
Tfn-R	transferrin receptor
TGN	*trans*-Golgi network
TM	transmembrane
UBE2V2	ubiquitin-conjugating enzyme 2, variant 2
Y2H	yeast two-hybrid
α-MEM	α-minimum essential medium

ABSTRACT

Na^+/H^+ exchangers (NHE) are integral membrane proteins that catalyze the electroneutral exchange of Na^+ (or K^+) for H^+. The nine human isoforms identified to date share the same topology of twelve membrane-spanning domains and a cytoplasmic regulatory tail, and diverge in their tissue expressions and subcellular localizations. This thesis focused on the identification and characterization of proteins interacting with the ubiquitous NHE6 isoform, which resides predominantly in recycling endosomes. Recent yeast two-hybrid (Y2H) screening of a human brain cDNA library using the regulatory tail of NHE6 as a probe resulted in the tentative identification of about 250 partial or full-length NHE6-interacting proteins. Thirty other potential NHE6-interacting partners were identified by isolating NHE6 complexes from embryonic kidney 293 cells by tandem affinity purification (TAP) and subjecting them to mass spectrometry analysis. The interaction between NHE6 and eight of these proteins (four from each Y2H and TAP analyses) was tested by co-immunoprecipitation, co-localization by immunofluorescence microscopy and *in vitro* GST-fusion protein pull-down assays. We show that apolipoprotein D interacts weakly with NHE6, while myosin light chain kinase and the mitochondrial ATP synthase subunit-α are true NHE6-binding partners. The remaining five proteins exhibited poor and/or non-reproducible association with NHE6.

ABRÉGÉ

Les échangeurs de Na^+/H^+ (NHE) sont des protéines membranaires intégrales qui catalysent l'échange électroneutre de Na^+ (ou K^+) contre H^+. Les neufs isoformes humains identifiés jusqu'à présent partagent la même topologie composée de douze domaines transmembranaires et d'une extension cytoplasmique ayant des fonctions régulatrices. De plus, ils ont des expressions tissulaires et localisations cellulaires distinctes. Le but de cette étude était d'identifier et caractériser des protéines qui interagissent avec l'isoforme NHE6, lequel se trouve surtout dans les endosomes de recyclage. Récemment, un système double hybride de la levure (Y2H) a été utilisé avec succès dans l'identification, à partir d'une banque ADNc du cerveau, de près de 250 protéines ou fragments de protéines qui s'associent directement à la portion régulatrice cytoplasmique de NHE6. La méthode TAP (Tandem Affinity Purification) a par ailleurs abouti à l'identification par spectroscopie de masse de trente autres protéines appartenant à des complexes associés à NHE6 qui ont été isolées de cultures de cellules embryonnaires du rein. L'interaction entre NHE6 et huit de ces protéines (quatre du Y2H et quatre du TAP) a été vérifiée par les méthodes suivantes : la co-immunoprécipitation, la colocalisation par microscopie confocale et l'association *in vitro* avec des protéines GST-fusion. Alors que nous n'avons observé qu'une faible interaction entre l'apolipoprotéine D et NHE6, nous avons trouvé que la kinase de la chaîne légère de la myosine ainsi que la sous-unité alpha de l'ATP synthétase interagissaient véritablement avec NHE6. Les cinq autres protéines n'ont montré qu'une association faible ou non reproductible avec NHE6.

INTRODUCTION

Na^+/H^+ exchangers (NHEs) are a family of electroneutral transporters that mediate the exchange across biological membranes of Na^+ and H^+ down their respective concentration gradients. Such exchange of sodium and proton has been observed in various organisms ranging from bacteria to yeast, plants and mammals (138). Thus far, nine human NHE isoforms have been identified and been shown to differ in their tissue distribution, subcellular localization and drug sensitivity. They are subdivided into two general categories according to their subcellular localization: plasmalemmal (NHE1-5) and organellar (NHE6-9). NHE1 is the most extensively studied NHE and was the first to be described (170). Its cDNA was used as a probe for low-stringency hybridization of various tissue cDNA libraries and resulted in the discovery of four other plasmalemmal NHEs (138). NHE1-5 play important roles in intracellular pH control (33) and cell volume homeostasis (81), and facilitate other cellular activities such as adhesion, migration (57,59) and proliferation (24,82). The more distantly related organellar NHEs (NHE6-9) were discovered only recently and remain poorly characterized. Their main role is thought to be the regulation of organellar pH, although they might participate in protein trafficking and transport of vesicles, similarly to their yeast homologue Nhx1 (36,36,129). Considering that virtually nothing is known about the regulation of organellar NHEs, we endeavoured to identify and characterize proteins that interact with NHE6, an organellar isoform predominantly found in recycling endosomes. This study is motivated by the reality that proper functioning of NHEs is critical for many physiological processes, thus an increased knowledge of their function will improve our understanding of the numerous pathologies associated with NHE malfunction, including hypertension, epilepsy, postischemic myocardial arrhythmia, gastric and kidney disease, diarrhoea, glaucoma (48,138) and attention deficit hyperactivity disorder (54).

1.1 Evolutionary origins of mammalian Na^+/H^+ exchangers

In a recent phylogenetic analysis Brett et al. (36) studied more than 200 genes encoding Na^+/H^+ exchangers to shed light on the specific physiological roles of each. According to this study, eukaryotic NHEs belong to the cation proton antiporter 1 (CPA1) gene family, which itself is part of the CPA superfamily along with the CPA2 and the NaT-DC families (36). The CPA1 family originated from bacterial NhaP genes and encompasses the NhaP/SOS1 and the eukaryotic NHE subfamilies. The latter is the best characterized of the CPA families and is divided in two clades based on cellular localization: plasmalemmal and intracellular. The plasmalemmal clade is further subdivided into "recycling" and "resident" subgroups, whereas the intracellular clade comprises the "endosomal/*trans*-Golgi network (TGN)", "plant vacuolar" and "NHE8-like" clusters. From their extensive phylogenetic analysis, Brett *et al.* concluded that the eukaryotic NHE gene family originated as intracellular exchangers, such as the yeast *Saccharomyces cerevisiae* endosomal exchanger ScNhx1, the plant *Arabidopsis thaliana* vacuolar exchanger AtNHX1 and the slime mold DdNHE, the earliest member of the NHE8-like clade. According to Brett *et al.*, the cell surface or plasmalemmal NHEs would have emerged from these ancient intracellular NHEs to fulfill functions specific to higher eukaryotes.(36)

The human organellar NHE6, NHE7 and the most recently discovered NHE9 have high amino acid sequence identity (55-70%) (130) and are closely related to their endosomal homologues ScNhx1 from yeast, and AtNHX5/ AtNHE6 from plants (36). While the experimental evidence is limited, these NHE isoforms are thought to control organellar pH and volume homeostasis through functional coupling to the luminal H^+ gradient established by the vacuolar H^+-ATPase (36,80). The role of the "NHE8-like" clade is even less well understood. Its similarity to the other organellar isoforms is quite low (about 25%) (130,138) and its homologues are found only in animal cells, suggesting a unique physiological role.

Similar to NHE8, plasma membrane NHEs are exclusively present in animal cells (36) and have around 25% (138) sequence similarity to organellar NHEs. The recycling plasmalemmal NHE3 and NHE5 are found in worms, insects, fish and animals, whereas

the resident plasma membrane NHE1, NHE2 and NHE4 are present exclusively in vertebrates (36). From these observations, Brett at al. deduced that recycling plasma membrane NHEs appeared before the resident plasma membrane isoforms. The latter have evolved simultaneously with the Na^+/K^+-ATPase (136), which creates the extracellular Na^+ gradient responsible for their activation (138).

1.2 General structure of mammalian Na^+/H^+ exchangers

Despite their difference in amino acid sequence identity, computer modeling and hydropathy analysis predict that all NHEs share the same topology of twelve membrane-spanning α-helixes at the N-terminus and a cytoplasmic C-terminal domain of varying lengths and amino acid sequences (138). Thus far only the topology of NHE1 was extensively studied. Wakabayashi et al. performed accessibility studies of individually substituted cysteines in a cysteinless NHE1 mutant (204). Even though their model does not closely fit the original model obtained by hydropathy analysis, they confirm the presence of twelve membrane-spanning domains.

The cation exchange occurs through the transmembrane N-terminal region (205), which is of similar length for plasmalemmal and organellar NHEs (388 to 451 amino acids)(37). Some parts in the transmembrane region are critical for the function of all NHE isoforms. For instance, the hydrophobic loop between transmembrane segments 9 (TM9) and 10 (TM10) is predicted to form a re-entrant membraneous loop and appears to be essential in ion translocation (129,171). Certain residues in this loop, such as yeast Nhx1 Glu355 (equivalent to human Glu391) (129) are conserved and equally important for cation translocation in organellar and plasmalemmal NHEs. Other residues (Phe357 and Tyr361) uniquely conserved in organellar NHEs are critical for functions specific to organellar NHEs and can not be substituted by corresponding amino acids from plasma membrane NHEs without loss of function (129). In addition to the loop between segments 9 and 10, the transmembrane regions TM3 and TM4 are important for ion selectivity and drug sensitivity (138) and contain five residues (Gly142, Leu166, Pro167, Phe182, Asn185) conserved among all eukaryotic NHEs (36). In that same region, Leu163 in human NHE1 is known to be important for amiloride sensitivity (47,101,227)

and is substituted with the polar asparagine in the "endosomal/TGN" NHEs (36), and may partially account for observed differences in drug sensitivity.

While the transmembrane N-terminal region is mostly conserved in length and in amino acid sequence amongst NHEs isoforms, such is not the case for the more divergent C-terminal regulatory region. It contains putative as well as demonstrated binding sites for regulatory proteins, components of the cytoskeleton and recognition sites for phosphorylation by various kinases (72,138,227). In addition to its extensive sequence divergence among isoforms (36), the C-tail is significantly shorter in organellar NHEs, with 199±46 amino acids compared to 365±52 amino acids in plasmalemmal NHEs (36). Although it is generally accepted that the C-tail faces the cytoplasm, there is some evidence to suggest that part of this region in NHE1 (102), NHE3 (25,72,102) may face the extracellular milieu. Likewise, the yeast ScNhx1 tail contains sites that are N-glycosylated, which suggests partial luminal exposure (211). Moreover, recent topological studies on the plant AtNHX1 revealed that almost its entire C-tail faces the vacuolar lumen (219).

Further analysis of the primary structure of the NHEs reveals that they contain putative glycosylation sites. For instance, NHE1 is both N- and O-glycosylated in the extracellular loop between TM segments 1 and 2 (49,88), whereas NHE2 is only O-glycosylated (196). Out of the remaining plasmalemmal paralogues, only NHE3 was studied for post-translational modifications, but did not reveal any glycosylated residues (26,49). Other studies point to the possibility that the organellar isoforms NHE6 (125), NHE7 (133) and NHE8 (79) are N-glycosylated.

There is little information concerning the tertiary or quaternary structures of mammalian NHEs. A few biochemical studies suggest that NHE1 and NHE3 form homodimers through interactions of their transmembrane regions (69), which might be important for intracellular pH sensitivity and consequently Na^+/H^+ exchange (91). In addition, biophysical and kinetic studies of Na^+/H^+ exchange on renal brush border vesicles show evidence for the presence of NHEs as tetramers (21,140). Further evidence to support the hypothesis that NHEs exist as higher-order complexes is the dimerization of the *Escherichia Coli* Na^+/H^+ antiporter NhaA as revealed by its three-dimensional crystal structure (216).

1.3 Cation selectivity, transport kinetics and drug sensitivity

The plasmalemmal NHEs have a single binding site for Na^+ as indicated by their hyperbolic dependence on the extracellular Na^+ concentration (138). They can also translocate other monovalent cations such as Li^+ and NH_4^+ but less efficiently (10). The plasmalemmal isoforms do not translocate K^+. Interestingly, the organellar isoforms such as NHE7 (133), the plant AtNHX1 (199), and the yeast ScNhx1 (37) can transport not only Na^+, Li^+, NH_4^+, but also K^+ and presumably function mainly as K^+/H^+ antiporters in vivo, given that K^+ is the predominant intracellular alkali cation. Although plasmalemmal NHEs reveal a single binding site for Na^+, some of them contain a regulatory H^+ binding site other than the H^+ translocating site, as shown by their greater than first-order dependence on H^+ concentration (10,141).

Plasmalemmal NHEs are inhibited to different degrees by several pharmacological compounds such as amiloride and its analogues (46,50,227), benzoylguanidinium-based derivatives (50,175) and moderately by cimetidine, clonidine and harmaline (137,188,225). Most probably due to the difference in the regions responsible for drug sensitivity and binding (52,133,138), the organellar NHEs are less sensitive to amiloride inhibition (52,133). Conversely, the NHE7 isoform and possibly other organellar NHEs are inhibited by other compounds such as quinine (133).

1.4 Mammalian plasmalemmal Na^+/H^+ exchangers

As previously discussed, plasmalemmal and organellar NHEs diverge in their evolutionary origins and consequently in their primary structure, cation selectivity and drug sensitivity. The main difference is that plasma membrane NHEs act as Na^+-driven H^+ exchangers, thereby alkalinizing the cytoplasm, while the organellar NHEs function as H^+-driven, K^+ (Na^+) exchangers, alkalinizing the lumen and acidifying the cytoplasm (38). There are other important differences in tissue distribution, function and regulation, which will be treated separately for plasmalemmal and organellar NHEs.

1.4.1 Tissue distribution, cellular localization and function

NHE1 is ubiquitously expressed and accumulates in discrete domains on the plasma membrane such as in lamellipodia in fibroblasts (83), on the basolateral membrane of epithelia (27) and in the intercalated disks and t-tubules of cardiac myocytes (154). A recent study also suggests that NHE1 is present in the nuclear membrane of mammalian cells at varying degrees depending on cell type and species (30), although this observation is questionable as immunofluorescence was the only technique used in this paper and no other studies confirm this finding. NHE1 has two main roles: to relieve cells from excess acidification resulting from metabolic activity and to maintain cell volume through Na^+ influx coupled to Cl^- and H_2O uptake (138). It also fulfills some specialized functions depending on its localization on the cell membrane. In addition, NHE1 is an important regulator of cell adhesion and migration in fibroblasts. It interacts with the cytoskeletal-associated proteins ezrin, radixin and moesin, inducing the remodelling of the cortical actin network and the reshaping of focal adhesions (57-59).

The isoforms NHE2-4 are expressed at highest levels in epithelia of the kidney and gastrointestinal tract (138). While NHE4 is located in the basolateral membrane in renal epithelia (41,153,155), NHE2 and NHE3 are found in the apical membranes of discrete nephron and intestinal segments (26,93,153). In addition, NHE3 is also detected in endosomes (28,44), where it actively contributes to vesicular pH regulation (5,51) and is stored until a signal triggers its translocation to the apical surface. On the whole, NHE4 is thought to fulfill similar functions as NHE1 in the few cell types (*e.g.* mesangial cells) where the latter is missing, whereas NHE2 functions in fluid secretion, while NHE3 participates in absorption (138).

Amongst the plasmalemmal NHE isoforms, NHE5 distinguishes itself by its predominance in multiple regions of the brain (13,19). It is classified as a recycling plasmalemmal NHE (36), like NHE3 with which it shares the closest amino acid sequence similarity (~50%) (138). In addition to the plasma membrane, NHE5 is found in somatodendritic vesicles and synaptic-like microvesicles in PC12 cells, and is internalized by clathrin-mediated endocytosis into recycling endosomes of CHO cells

(189). Its role is unknown, but it likely serves to regulate the luminal acidity of its associated vesicles.

1.4.2 Regulation of plasmalemmal Na^+/H^+ exchangers

A broad range of growth factors and peptide hormones indirectly activate NHE1 through the phosphorylation of its C-tail by different kinases, including the mitogen activated extracellular signal-related kinase $p90^{rsk}$, Nck-interacting kinase and p160-rho-associated kinase. While, the mechanisms by which these kinases enhance the transporter's activity are still unknown, the binding and phosphorylation sites for some of them have been revealed. For instance, $p90^{rsk}$ phosphorylates S^{703} thereby promoting the binding of the scaffolding protein 14-3-3 (111,190), whereas the Nck-interacting kinase binds to the middle of NHE1's tail and mediates signalling events from receptor tyrosine kinases independently of $p90^{rsk}$ (111,223). Conversely, the phosphorylation site of the p160-rho-associated kinase, which participates in integrin triggered signalling that orchestrates cell adhesion (192,193), is still unknown. In addition to kinases, NHE1 is regulated by Ca^{2+} binding proteins. For instance, binding of Ca^{2+}-calmodulin to the C-terminal tail of NHE1 causes an increase in transport activity possibly by relieving auto-inhibition (203). Three other Ca^{2+} binding proteins called calcineurin B homologous proteins (CHP) bind to the juxtamembrane region of NHE1 cytoplasmic tail (3), two of which (CHP1 and CHP2) were found to interact with NHE3 as well (142,143).

Amongst isoforms NHE2-4, only the regulation of NHE3 has been studied extensively. The control of NHE3 activity mainly depends on hormones and physical factors such as osmolarity (139), which trigger diverse molecular mechanisms including phosphorylation (119,126,215,232), binding of accessory regulatory proteins (201,207,208) and trafficking of NHE3-containing endosomes from their storage pools to the surface and vice versa (28,44,51,106). An important regulatory mechanism of NHE3 activity is its downregulation through protein kinase A (PKA) phosphorylation in response to parathyroid hormone and dopamine (16,17,95,214,231). In addition, the effects of PKA phosphorylation are thought to be indirectly affected by two scaffolding proteins termed Na^+/H^+ exchanger regulatory factor 1 and 2 (NHERF1, NHERF2)

(209,210,228). Interestingly, both NHERF1 and 2 bind to ezrin (161,226), which acts as a link between membrane proteins and actin (224) and which can provide anchorage to PKA (62). In addition, treatment of epithelial cells with the *Clostridium difficile* toxin B, which disrupts Rho-GTPase mediated signalling, causes a cytoplasmic redistribution of ezrin and a decrease in NHE3 activity through internalization (89). Taken together, the above findings suggest that NHE3's activity is tightly controlled by its association with the cytoskeleton.

The regulation of NHE5 remains poorly understood, but a few studies show that activation of protein kinase A or C and hyperosmolarity decrease rat NHE5 activity in Chinese hamster lung fibroblast PS120 cells (12). Like NHE3, NHE5-containing vesicles are regulated by phosphatidylinositol 3'-kinase and by F-actin assembly (189). In addition, a recent study reveals that NHE5 associates *in vitro* and *in vivo* with the scaffolding/adaptor protein β-Arrestin 2, which is possibly responsible for its internalization by clathrin-mediated endocytosis (187).

1.5 Organellar Na^+/H^+ exchangers

Like their plasmalemmal counterparts, the different organellar NHE isoforms have distinct tissue distributions and intracellular localizations. Their precise roles and regulatory mechanisms remain poorly characterized, but some evidence supports their involvement in vesicular pH homeostasis, which in turn influences proper protein processing and vesicular trafficking. For better understanding of the potential contributions of mammalian organellar NHEs to cellular processes, some notions of vesicular pH control, endocytosis and molecular sorting in the endocytic pathway will be described first.

1.5.1 Mechanisms of endocytosis

All cells internalize extracellular fluid and receptor-bound ligands through endocytosis. In fibroblasts for example, this dynamic process can exceed an internalization rate of 50% of cell surface area per hour (184). Two main endocytosis

mechanisms co-exist: clathrin-coated vesicles formation and internalization mediated by lipid rafts/caveolae. Clathrin-mediated endocytosis is responsible for receptor-ligand internalization and is well understood. Conversely, the raft/caveolae endocytosis associated with integrin signalling and virus internalization is still ill-defined (151) and will not be discussed.

Clathrin-mediated endocytosis begins with the formation of clathrin-coated pits (CCPs) and the accumulation therein of receptor-ligand complexes. The clathrin coat is a lattice of hexagons and pentagons of the protein clathrin (149), whose functional unit is the triskelion. The CCPs grow and eventually bud off the membrane with the assistance of the protein dynamin, thus forming clathrin-coated vesicles. The assembly of the clathrin cages is promoted by adaptor proteins, which contain binding sites for both the cytoplasmic domains of transmembrane proteins and for clathrin (42,166,195). Until recently, only two adaptor complexes were known: AP-1, found on clathrin-coated buds of the *trans*-Golgi network (TGN) and AP-2, localizing to the plasma membrane coated pits (4,167). In the last few years many more adaptor proteins have emerged, including AP-3 (179), AP-4 and a range of other cargo-specific adaptors (165,173,182,194). Considering the variety of ligands and adaptor complexes it is not surprising to see a diverse range of adaptor protein recognition motifs (123), some of which are present not only in the cytoplasmic domain of cell surface receptors and TGN proteins, but also on vesicle membrane proteins, such as the lysosomal-assocoated membrane protein LAMP-1 (104). In addition to cytoplasmic motifs on transmembrane proteins, adaptor complexes also recognize membrane proteins responsible for vesicle docking and fusion such as v- or t-SNARE families (169), thus regulating vesicle fusion in addition to vesicle formation.

Recent studies show that the actin cytoskeleton is an important player in the endocytic process. In mammalian cells, actin poisons partially block endocytic uptake and the formation of coated vesicles (77,108), whereas in the yeast *Saccharomyces cerevisiae*, endocytosis is blocked completely by actin assembly inhibitors (14,15). Recently, Kaksonen et al. proposed a model whereby actin provides the force for membrane invagination by pulling directly on the vesicle coat with the assistance of

Actin-related-protein-2/3 (Arp2/3) complex, the Arp2/3-complex activator, capping proteins (Cap1/2), myosins and others (98).

1.5.2 Molecular sorting in endosomes

The clathrin-mediated endocytic system is a complex network of vesicles and tubules, whose role is to sort the proteins targeted for degradation from those, which are to be recycled. Four types of endocytic organelles have been established based on their function, although the distinction is not clear-cut due to the dynamics of the system. Indeed, recent studies reveal a variety of specialized endosome-derived vesicles each having a distinct subset of membrane proteins. The mechanisms by which these proteins are targeted and maintained at the proper compartment are just beginning to be clarified.

Sorting endosomes or early endosomes are the first structures to which the incoming endocyting vesicles fuse. The sorting endosomes form a dynamic network of tubules and vesicles, whose slightly acidic pH (6.0) (97,158) triggers the dissociation of receptor-ligand complexes. From the early endosomes, the proteins are sorted to three main destinations: the plasma membrane, recycling endosomes or late endosomes. In a recent study, Lakadamyali et al. observed two types of sorting endosomes by live cell imaging: a dynamic population that matures rapidly and moves on microtubules and a slowly maturing static population (107). By monitoring the trafficking pathways followed by different ligands, they concluded that the sorting process begins prior to fusion with early endosomes and depends on the mobility and composition of endocytic vesicles. According to this study, vesicles containing ligands targeted for degradation fuse with dynamic early endosomes and have adaptors other than AP-2, while those with recycling ligands, such as transferrin, are sent to all sorting endosomes and are eventually enriched in the slowly maturing type. This study completes the generally accepted model of sorting within early endosomes, which states that in the absence of signal, the internalized receptors and membrane proteins accumulate in tubular regions of the early endosomes, while the soluble ligands and the proteins targeted for degradation accumulate in the vesicular regions (116). Given their greater surface-area-to-volume ratio, the tubular regions bud off more readily than the vesicular parts, thus forming

recycling compartments (67,117). This simple mechanical geometry-based segregation efficiently recycles several membrane proteins. For example, despite the absence of a signal for recycling, the transferrin receptor (Tfn-R) exits the early endosomes with a $t_{1/2}$ of 2 minutes and efficiency greater than 99% (67,117).

The sorting endosomes have a half-life of about 8 minutes in CHO cells (116). During this "active life", they continuously fuse with incoming primary endocytic vesicles and recycle receptors by tubule pinching. A still to be defined molecular mechanism triggers the maturation of the sorting endosomes. They gradually acquire properties of late endosomes (LEs): absence of fusion with incoming endosomes, drop in pH and acquisition of acid hydrolases. The hydrolases initiate the degradation of the accumulated internalized substances as the newly formed LEs migrate on microtubules (7) towards the lysosomes. The transfer of LEs to lysosomes is dynamic and the distinction between the two subsets of vesicles is difficult. Nonetheless, lysosomes can be recognised by their higher density on Percoll compared to LEs (104). At this final step in the endocytic pathway, the digested material is processed, while the non-digestible substances are concentrated until the lysosome is reactivated by the fusion to a new LE.

From the sorting endosome, the recycling molecules follow two routes back to the cell surface. Some are delivered directly after the pinching off of the tubular structures. Others are sent to the endocytic recycling compartment (ERC), a long-lived organelle composed of tubular structures associated with microtubules (94,121,221,222). For instance, up to 75% of the Tfn-R is found in the ERC (198) and its transit time therein can take 5-10 min (53,174). It is not clear what determines the proportion of receptors that follow the direct recycling route from sorting endosomes relative to the slower recycling route via the ERC. Most of the molecules in the ERC are recycled back to the surface, although some are sent to other organelles of the endocytic/exocytic network, mainly the TGN. The complexity of the protein sorting system in the ERC is equivalent to the TGN and is still poorly understood.

The complexity of vesicle trafficking and protein sorting in the endocytic and exocytic pathways requires the assistance of an array of regulatory molecules. For example, Rabs are a family of small GTPases that regulate many membrane-transport steps, including the formation of the sorting endosome by Rab5 (66,109,118) and the

recycling to the plasma membrane from the ERC and the TGN by Rab11 (43,162). Other regulators of vesicle trafficking are SNARE complexes, which are responsible for vesicle fusion (168). The complex vesicular trafficking between organelles would require the assistance of coat proteins for vesicular formation and proper delivery. As a matter of fact, clathrin-coated buds have been observed to originate from early endosomes in fibroblasts and in neurones (185,213). Indeed, clathrin might play a role in the formation of transport vesicles (197) or in the morphology of endosomes (23). This intense activity around vesicles of the endocytic pathway could not occur without the assistance of an array of kinases (152) and signalling molecules (122). Indeed, recent discoveries reveal that endocytosis and cellular signalling are tightly interconnected.

1.5.3 pH Homeostasis of cellular organelles

The control of pH inside organelles is of critical importance for a number of processes, including receptor-ligand dissociation in early endosomes, protein degradation in lysosomes or secondary protein modifications in the Golgi. The vesicular pH decreases progressively along the endocytic pathway. In early endosomes it is nearly neutral (pH 6.5), whereas in lysosomes it is less than 5.5 (55). Conversely, in the secretory pathway, the pH decreases as the cargo transits towards the cell surface: in the endoplasmic reticulum it is nearly neutral (103), while the acidification is maximal at the *trans*-Golgi network (56,114).

The V-type H^+-ATPase, which transports protons in the presence of ATP, is the main pump responsible for the acidification of organelles in eukaryotes (146). If the V-ATPase attained chemical equilibrium, the vesicular lumen would reach a pH of 3 (55). Nevertheless, the pH varies along the endocytic and secretory pathways pointing to the existence of vesicular pH regulating mechanisms. The molecular nature of organellar pH control is still unknown, but the generally accepted model is the "pump and leak" model. At steady state, the rate of proton pumping by the V-ATPase is counteracted by an equivalent efflux of protons through various channels and transporters, such as the H^+ channel, the Cl^-/H^+ exchanger and the organellar NHEs. The existence of this proton leak was deduced originally from the observed alkalinization of organelles following the

inhibition of the V-ATPase (55,70,103). In addition, the measured leak was highest for the ER and decreased for more acidic organelles, which suggests that the pH of vesicles is determined mainly by their proton permeability. The variation of organellar pH could be also partly due to a different delivery and assembly of V-ATPases across endocytic vesicles (74), but not to a direct pH regulation of the V-ATPase's activity (172), nor to the establishment of membrane potential, as counterions such as K^+ flow freely out of the Golgi (172). These observations indicate that the proton leak pathway is the predominant mechanism of organellar pH control in which the NHEs most probably play a crucial role.

1.5.4 *Saccharomyces cerevisiae* Nhx1 and *Arabidopsis thaliana* AtNHX1

The most extensively studied organellar NHE is the yeast ScNhx1, which is 31% identical and 60% similar to human NHE6 (34) and is found in the pre-vacuolar compartment (PVC) (equivalent to late endosomes) in yeast, where cargo is sorted prior to its delivery to the vacuole/lysosome (131). Initially, it was proposed to be mainly responsible for conferring salt tolerance by working against the H^+ gradient established by the V-ATPase to sequester Na^+ into the vacuole (131). In 2000, Bowers et al. provided evidence that the role of ScNhx1 was not restricted to ion and endosomal volume homeostasis, but also to vesicular traffic control (34). However, it is only recently that other groups showed that ScNhx1 directly regulates vesicular trafficking via intracellular pH control (37,129). Indeed, ScNhx1-null cells exhibited trafficking defects such as sensitivity to the protein synthesis inhibitor hygromycin B and abnormal accumulation of the G-protein coupled receptor Ste3-GFP in the late endosome, which could be alleviated by treatment with weak bases (37). Despite the considerable knowledge on the *S.cerevisiae* endosomal NHE structure and function, not much is known about its regulation, except the observation that Gyp6, a GTPase activating protein involved in Ypt6-mediated retrograde traffic to the Golgi, is a negative regulator of ScNhx1 (6). This agrees with the other studies, which link endosomal pH regulation by ScNhx1 to vesicle and protein trafficking regulation.

The plant *Arabidopsis thaliana* has two classes of organellar NHEs: the vacuolar AtNHX1 and the endosomal class comprising AtNHX5 and AtNHX6 (144). The

vacuolar Na^+/H^+ antiporter AtNHX1, equivalent to the yeast ScNhx1, is important for maintenance of proper $Na^+(K^+)$ concentration and confers salt tolerance in plants (8,9,230). It also plays a role in vacuolar pH regulation (220), thus possibly affecting protein trafficking and targeting similarly to ScNhx1 in yeast. As previously mentioned, the AtNHX1 C-terminal region is in the vacuolar lumen (219) and similarly to yeast and mammalian NHEs, it is essential for regulating antiporter activity, as deletion of the C-tail results in a two-fold increase in Na^+/K^+ selectivity (219). Recently, Yamaguchi et al. showed that AtNHX1 is regulated by the luminal calmodulin-like protein AtCaM15 through interaction with its C-tail (218). They propose that under normal physiological conditions, i.e. low vacuolar pH and high Ca^{2+} concentration, AtCaM15 inhibits AtNHX1 through binding of its regulatory tail (218). However, during salt stress, the vacuolar pH rises (84) causing a release of AtCaM15 from the AtNHX1 tail, thereby activating AtNHX1 with a concomitant increase in vacuolar Na^+ influx. Such regulation by calmodulin-like proteins is common for plant and animal type IIB Ca^{2+}-ATPases (39,87) as well as for ion channels/exchangers (181,234), notably the mammalian NHE1 (202,203).

1.5.5 Tissue distribution, cellular localization and function of mammalian organellar Na^+/H^+ exchangers

NHE6, the first organellar NHE to be characterized, is ubiquitous, but found at highest levels in human heart, brain and skeletal muscle (134). It has a short brain splice variant (669 amino acids) and a longer liver splice-variant (701 amino acids) with a 96-base insertion between the transmembrane regions TM3 and TM4 that makes the loop more hydrophobic and adds an N-glycosylation site (125). Originally, NHE6 was proposed to be in mitochondria (134), based on fluorescence microscopy studies which revealed some co-localization of vesicles containing green fluorescent protein tagged NHE6 with MitoTracker Red dye. However, this initial observation was disputed by more compelling evidence showing the localization of NHE6 in endocytic vesicles. Indeed, some observations reveal that it has an ER signal peptide and goes through the secretory pathway when overexpressed in COS7 cells (125). In addition, Brett et al. (38)

demonstrated that NHE6 predominantly localizes to recycling endosomes (recycling vesicles and endocytic recycling compartment). They transiently transfected epitope-tagged NHE6 in CHO and OK cells and observed a scattered vesicular distribution in addition to a concentrated juxtanuclear localization, which significantly overlapped with the Tfn-R, but with no other organellar marker (38). Surface biotinylation experiments and fluorescently lableled cells at 4°C revealed that a small fraction (5%) transiently appeared on the cell surface (38). A recent study suggests that most of NHE6 localizes to early recycling endosomes, as opposed to the perinuclear ERC (130), but this finding is not supported by co-localization studies done by other groups ((38), Ilie A. and Orlowski J., unpublished). There is no information on the function of NHE6, but given its homology with the yeast ScNhx1, it can be deduced that it functions as a pH regulator in sorting and recycling endosomes/ERC to control the rate of receptor recycling to the plasma membrane. Although other NHEs likely contribute to endosomal pH regulation, such as NHE3 and NHE5, the role of NHE6 is unique for several reasons. NHE6 has different tissue distributions from NHE3 and NHE5 (48,134,139). In addition, even though NHE3 is functional in recycling endosomes, it acidifies the endosomal lumen (51,75), contrary to the organellar homologues such as NHE7 and ScNHX1, which have been shown to alkalinize the lumen (133,199).

NHE7 has a high sequence similarity to NHE6 (70%) and although it is ubiquitous, it is predominantly expressed in certain regions of the brain, in skeletal muscle and in secretory tissues (133). It is mostly localized to the *trans*-Golgi network, but part of it is found in early endosomes. In addition, it shares common compartments with NHE6, the nature of which remains to be determined. NHE7 functions as a non-selective monovalent cation/H^+ exchanger, although it has a high affinity for K^+ (133) and most likely acts as a pH and K^+ regulator in the Golgi.

As previously mentioned, NHE8 has limited similarity (25%) to other organellar NHEs. Northern blot analysis shows that it is ubiquitous with the highest expression in kidney, testis, skeletal muscle and liver (79,130). Nakamura et al. found that NHE8 localizes mainly in tubular and some vesicular perinuclear structures, next to the *cis*-Golgi marker GM130, whereas there was no co-localization with ER, sorting endosomes, LE and lysosomes (130). By contrast, *in situ* hybridization studies done by Goyal et al.

on human tissues revealed an enrichment of NHE8 signal in brush-border membranes (similarly to NHE3) (79). In a subsequent study, they showed that NHE8 co-localizes with γ-glutamyltranspeptidase and megalin in epithelia of proximal tubules, suggesting that it is both on the microvillar surface and in the coated-pit region (78). Based on these observations, it is possible that NHE8 mediates apical membrane transport in the proximal tubule and that it is subject to endocytosis and recycling. Another study revealed that NHE8 is also restricted to the apical membrane of intestinal epithelia and that there is a higher NHE8 mRNA expression in young compared to adult animals, while NHE2 and NHE3 are expressed at low levels in early life (217). Thus, NHE8 might be important for intestinal Na^+ absorption during early life.

NHE9, the most recently identified NHE, localizes to late recycling endosomes and partially overlaps with NHE6 according to Nakamura et al. (130). It was discovered as a potential gene linked to attention deficit hyperactivity disorder (ADHD), which is the most commonly diagnosed disorder in children (54). In a particular family affected by the disorder, there was a pericentric inversion on a part of chromosome 3, which resulted in silencing of NHE9, and Dedicator Of Cytokinesis 3 (DOCK3) (54). While NHE9 is ubiquitous with highest expression in heart and skeletal muscle, followed by placenta, kidney and liver, DOCK3 is found at highest levels in the frontal, temporal and occipital lobes of the brain (54). It is known that normal function of neuronal cells depends on control of ion concentration, as seen in NHE1-knockout mice which display ataxia and seizures (22,85), and NHE9 might be essential for fulfilling this role in neurons.

1.6 Research rationale and experimental plan

Although several reports indicate that organellar NHEs contribute to vesicular pH homeostasis and trafficking, the underlying molecular mechanisms are poorly understood. In one recent study, Lin *et al.* (113) demonstrated that members of the secretory carrier membrane protein (SCAMP) family, notably the SCAMP2 isoform, bind directly to human NHE7 and modulate its shuttling between the *trans*-Golgi network and recycling endosomes. This association appears to be NHE selective, in as much as SCAMP2 did not associate with NHE6. By contrast, virtually nothing is known about the factors that

regulate NHE6 and is the main focus of this thesis. Given our current understanding of other NHEs, it is reasonable to hypothesise that there are novel cytoplasmic proteins that interact, either directly or indirectly, with NHE6 and modulate its catalytic activity and/or trafficking.

To accomplish this, a doctoral candidate in the laboratory, Alina Ilie, recently used yeast two-hybrid methodology to screen a human brain cDNA library with the entire C-terminal tail of NHE6 (amino acids 499 to 669). After the final screening, approximately 90 cDNAs were identified as putative NHE6-interacting proteins. These included small GTPases, cytoskeletal proteins, kinases, ion channels, other transmembrane proteins, proteins associated with lipid metabolism, the nucleus, lysosomes and mitochondria, as well as those of unknown function (Ilie, A. and Orlowski J., unpublished data). Intriguingly, some of these proteins are luminal, which raises the possibility that part(s) or the entire NHE6 tail might face the lumen, especially considering the presence of an N-glycosylation site in the tail at amino acids 655 to 658. Although no studies on the orientation of NHE6 tail have been done, evidence for N-glycosylation at two sites on the tail of its yeast homologue ScNhx1 implies a luminal or partly luminal localization (211).

The present challenge is to determine which of the proteins identified by the yeast two-hybrid methodology are *bona fide* interacting partners *in vivo*. Hence, the main goals of my thesis project were two-fold: (1) to validate the interaction of NHE6 with a subset of the putative interacting partners identified by the yeast two-hybrid screen mentioned above using alternative biochemical and cellular methods; and (2) to develop a complementary experimental approach that would further identify NHE6-interacting proteins. To this end, I developed and implemented a proteomics strategy involving Tandem Affinity Purification (TAP), in combination with mass spectrometry analysis (TAP-MS), that was specifically adapted to enrich for integral membrane protein complexes containing NHE6 and its associated proteins. The advantage of this approach is that it allows one to identify interacting proteins (direct and indirect) of interest under more physiological conditions.

With respect to the proteomics approach, the first step was to adapt and test the TAP-MS method for mammalian membrane proteins, such as NHE6, as this method was

optimized and used for studying soluble proteins in yeast and mammals. To this end, NHE6 tagged with the hemagglutinin epitope ($NHE6_{HA}$) was inserted into a vector containing the TAP tag and used to make stably expressing $NHE6_{HA\text{-}TAP}$ human embryonic kidney (HEK 293) cell lines. Lysates from these $NHE6_{HA\text{-}TAP}$ stably expressing cells were used for the TAP troubleshooting experiments.

The second step was to upscale the adapted TAP-MS method to produce enough purified material for detection with mass spectrometry and to obtain an accurate and complete list of NHE6-interacting complexes. With this objective in mind, multiple TAP experiments were done to verify the reproducibility of the method. In addition, control experiments using HEK293 free of $NHE6_{HA\text{-}TAP}$ were done to minimize false positives.

The third step was to test the interactions of NHE6 with a limited number of putative interacting partners using the following techniques: co-immunoprecipitation and co-localization by confocal immunofluorescence microscopy. Four promising interacting partners from the yeast-two hybrid screening results were selected based on the following criteria: the number of distinct positive clones for each protein, the likelihood that the two proteins will physically meet based on their subcellular localizations, and the physiological relevance of the interaction. In addition, four other proteins were chosen from the list of positive-interacting partners identified by TAP-MS, mainly based on the potential relevance of the physiological interaction. Prior to testing the interactions with the aforementioned methods, the putative interacting partners were cloned, epitope-tagged with the *myc* epitope and co-transfected in mammalian cells. Alternatively, antibodies specific to the tested protein were purchased and used to measure endogenous protein levels.

The final step was to further analyse and characterize the interaction of NHE6 with one or two confirmed binding partners using the following methods: GST-fusion pull-down assays to identify the binding site of the interacting-partner on the NHE6 C-tail and inhibition of the binding partner to monitor the effects on NHE6 function.

MATERIALS AND METHODS

2.1 Materials and other reagents

The following materials and reagents for the tandem affinity purification were used: EzView Red ANTI-FLAG M2 Affinity Gel, 3X FLAG peptide, EzView Red Glutathione Affinity Gel and CelLytic M Cell Lysis Reagent, all purchased from Sigma-Aldrich (Saint Louis, MI), in addition to Calmodulin Sepharose 4B beads (GE Heath Care Life Sciences, Baie d'Urfé, QC), RapiGest-SF (Waters, Milford, MA) and AcTEV Protease (Invitrogen, Burlington, ON). The myosin light chain kinase specific inhibitor ML-7, Hydrochloride was purchased from EMD Biosciences (San Diego, CA).

All the materials for tissue culture were purchased from: VWR International Co. (Mississauga, ON), Fisher Scientific (Whitby, ON) or Invitrogen (Burlington, ON). The following materials were used for western blotting: polyvinylidene difluoride (PVDF) membrane (Millipore, Billerica, MA), Enhanced Chemiluminescence detection kit (GE Healthcare, Baie d'Urfé, QC), SuperSignal West Femto Maximum Sensitivity Substrate (Pierce Biotechnology, Rockford, IL), x-ray Kodak film (Amersham Biosiences, Baie d'Urfé, QC). All other chemicals were purchased from Fisher Scientific (Whitby, ON), Bioshop, Sigma-Aldrich (Oakville, ON), Invitrogen (Burlington, ON), VWR International Co. (Missisauga, ON), BD-Biosciences (Missisauga, ON), and Qiagen (Missisauga, ON).

2.2 Antibodies

The following mouse monoclonal antibodies were used: anti-hemagglutinin (HA) (Covance, Berkely, CA), anti-myc (Upstate Biotechnology, Lake Placid, NY), anti-apolipoprotein D (Abcam, Cambridge, MA), anti-ATP synthase H^+ transporting, complex F1, subunit α (anti-ATP5α) (Abcam, Cambridge, MA), anti-ATP synthase H^+ transporting, complex F1, subunit β (anti-ATP5β) (Mitosciences, Eugene, Oregon), anti-myosin light chain kinase (anti-MLCK) (Sigma-Aldrich, Saint Louis, Missouri), anti-calmodulin (Upstate Biotechnology, Lake Placid, NY). The following rabbit polyclonal

antibodies were used: anti-HA (Covance, Berkeley, CA and Abcam, Cambridge, MA), anti-myc (Upstate, Temecula, CA), anti-ubiquitin (Upstate, Lake Placid, NY). The following secondary antibodies were used for immunoblotting: horseradish peroxidase-conjugated goat anti-mouse and horseradish peroxidase-conjugated goat anti-rabbit from Jackson ImmunoResearch Laboratories (West Grove, PA). The following fluorescent secondary antibodies were used for immunofluorescence microscopy: Alexa Fluor 488 - conjugated anti-mouse and anti-rabbit, as well as Alexa Fluor 568 - conjugated anti-mouse and anti-rabbit and were purchased from Molecular Probes (Eugene, OR).

2.3 Cloning from cDNA libraries and design of DNA constructs

The construct for the human long myosin light chain kinase (MLCK) inserted into a pEGFP-C2 vector between EcoRI and ApaI sites was generously provided by Dr. Anne Bresnick from the Department of Biochemistry of the Albert Einstein College of Medicine of Yeshiva University. For the tandem affinity purification experiments, the cDNA of C-terminally HA-tagged NHE6 was inserted into the multiple cloning site of a pMZS3F vector between EcoRI and XbaI sites, using primers JO-1340 and JO-1341. This resulted into an in-frame C-terminal fusion with a modified TAP tag composed of a calmodulin binding domain followed by a tobacco etch virus cleavage site and a ending with a 3XFlag peptide at the C-terminus. GST fusion constructs were done by inserting the cDNA of NHE6 C-tail fragments between BamHI and EcoRI sites of a pGEX-2T vector. The following GST fusion proteins were made, with corresponding primers used for adding the BamHI and EcoRI sites shown in brackets: GST fused to NHE6 amino acids 499 to 669 (JO-1364, JO-1294), GST fused to NHE6 amino acids 499 to 523 (JO-1294, JO-1426), GST fused to NHE6 amino acids 499 to 567 (JO-1294, JO-1424), GST fused to NHE6 amino acids 499 to 600 (JO-1294, JO-1425), GST fused to NHE6 amino acids 499 to 623 (JO-1294, JO-1427) and GST fused to NHE6 amino acids 608 to 669 (JO-1290, JO-1294). The cDNA for the selected NHE6 putative interacting proteins identified by the Y2H methodology and studied in this thesis were obtained from the following sources: prostaglandin D2 synthase (PTGDS) was available as a full-length clone from the Y2H, apolipoprotein D (APOD) was obtained from the American Type

Culture Collection (ATCC) (Manassas, VA), the chloride intracellular channel 1 (CLIC-1) and the ubiquitin-conjugating enzyme 2, variant 2 (UBE2V2) were cloned from a heart cDNA library using primers JO-1371/JO-1372 and JO-1367/JO-1368 respectively. The cDNAs from all these proteins were inserted in the multiple cloning site of a pCMV-Tag3B vector, which contains an N-terminal myc tag. PTGDS was inserted between BamHI and EcoRI sites using primers JO-1379 and JO-1380. CLIC-1 was inserted between BamHII and XhoI sites using primers JO-1384 and JO-1385. UBE2V2 was inserted between BamHI and EcoRI sites using primers JO-1386 and JO-1387. APOD was inserted between EcoRI and HindII sites using primers JO-1394 and JO-1395. The sequences of each of the above primers are provided in Appendix A.

2.4 Tissue culture and transfections

Cells were grown at 37°C in a humidified 5% CO_2-containing atmosphere. They were fed with an α-minimum essential medium (α-MEM) containing 25 mM $NaHCO_3$ and complemented with 10% fetal bovine serum (FBS) and 1% penicillin/streptomycin. When working with stable cells selected through Neomycin (G418) resistance, the media contained in addition 400 mg/l of G418. For immunoprecipitation experiments, 70% confluent cells were transfected with 10 μg DNA and 2.5 μl Lipofectamine per 1 μg DNA in serum-free α-MEM. After 4 hours, the serum-free media was replaced with regular media and the transfected cells were left to grow overnight. For microscopy experiments, the cells were grown on UV sterilized (for 30 min) glass coverslips in 6-well plates. CHO cells were plated directly on the coverslips, whereas when using HEK 293 cells, the coverslips were first coated with poly-L-lysine. The transfections were done on 40-50% confluent cells with 1-1.5 μg DNA and 2.5 μl Lipofectamine per 1 μg DNA in serum-free media.

2.5 Tandem affinity purification method

Stable cell lines of $NHE6_{HA\text{-}TAP}$: HEK 293 cells were cultured in regular α-MEM in 10-cm culture dishes until 70% confluency. One plate was transfected with 10μg pMZS3F-

$NHE6_{HA}$, a control plate was transfected with 10μg empty pCMV. After 48 hours, the cells were split 1/160 and grown in α-MEM containing 800 μg/l of Neomycin (G418). The media was changed every third day for two weeks until single colonies of stable $NHE6_{HA\text{-}TAP}$ started appearing. About 15 viable clones were grown and tested for $NHE6_{HA\text{-}TAP}$ expression by Western blotting. Two of them were selected for the experiments: a strongly overexpressing $NHE6_{HA}$ and medium-to-low overexpressing.

Tissue culture and cell lysing: For one TAP experiment, 6 batches of 6 x 175 cm^2 culture flasks of stable HEK 293 cells were lysed. All the manipulations were done on ice or in a 4°C refrigerated room. The cells were rinsed 3 times in cold phosphate buffer saline (PBS) (pH 7.4) and collected by scraping (5 ml PBS per 175 cm^2 dish) in 15-ml Falcon tubes. The cells were gravity centrifuged for 5 min at 1,000 g and the supernatant was discarded. One (1) ml of lysis buffer (50 mM Tris-HCl pH7.4, 150 mM NaCl, 2mM ethylenediaminetetraacetic acid (EDTA), 0.1% NP-40, 0.1% Triton X, 10% glycerol, 1 x protease inhibitors, 10 mM NaF, 0.25 mM Na orthovanedate, 5 nM Okadaic acid, 50 mM β-glycerolphosphate, H_2O to volume) was added to each falcon tube. The cells were resuspended by pipetting and transferred to eppendorf tubes. Two freeze-thaw cycles by alternating liquid Nitrogen with 36°C water bath were done to optimize the lysis efficiency. After 30 min of lysing, with occasional mixing, the non-dissolved cellular debris were collected to the bottom of the tube by spinning at 15,000 g for 20 min in a bench-top ultracentrifuge. The supernatants were transferred to new eppendorf tubes and pre-cleared for a minimum of 1 h with glutathione agarose beads.

1^{st} affinity purification: The lysates were spun at 700 g for 2 min and the supernatants were added to new eppendorf tubes containing 60 μl of 50% pre-washed M2 anti-Flag agarose bead slurry. Following a 4 h incubation with gentle rocking, the samples were spun at 700 g for 2 min to collect the M2 agarose beads with the bound $NHE6_{HA\text{-}TAP}$ complexes. The supernatant was discarded and the beads were washed 3 times in 1 ml per eppendorf tube of M2 wash buffer (50 mM Tris-HCl pH 7.4, 150 mM NaCl, H_2O to volume). Between spins, the samples were rocked for 5 to 10 min. The beads from 3 samples were collected together (total of 150 μl bead slurry or 75 μl beads) and incubated in 500 μl of 3XFlag elution buffer (200 ng/ml 3XFlag peptide in M2 wash buffer) over night.

2nd affinity purification: The second day, the beads were spun down and the 3XFlag eluate was transferred to a second affinity purification column made of 40 µl Calmodulin-Sepharose 4B bead slurry (50%) in an eppendorf containing 800 µl of Calmodulin Binding Buffer (10 mM Tris-HCl pH 7.4, 150 nM NaCl, 1mM Imidazole, 1mM Mg-acetate, 2 mM $CaCl_2$, 0.1% NP-40, 10 mM β-mercaptoethanol, H_2O to volume) and 10 µl of 1M $CaCl_2$. The incubation on this second affinity purification column was done over night. In the meantime, the 3XFlag elution was repeated by adding 500 µl of 3XFlag buffer on the anti-Flag M2 agarose beads and incubating all day. The second 3XFlag eluate was added to a Calmodulin Sepharose 4B column as well and left to incubate over night. The NHE6-protein complexes, which remained on the anti-Flag M2 agarose beads after both elution steps, were eluted with 3XFlag elution buffer supplemented with 0.025% RapiGest SF mild denaturing detergent. These eluates were concentrated and sent for mass spectrometry analysis.

Final elution of purified NHE6-bound complexes: The third day, the Calmodulin Sepharose 4B beads with the bound NHE6 complexes were spun down for 2 min at 700 g and the supernatant was discarded. The beads were washed 2 times with calmodulin binding buffer (CBB) and 3 times with calmodulin rinsing buffer (CRB) (50 mM ammonium bicarbonate pH 8, 75 mM NaCl, 1 mM Imidazole, 1 mM Mg-acetate, 2 mM $CaCl_2$, H_2O to volume). The samples were incubated by rocking for 5 to 10 min between spins. The Calmodulin Sepharose 4B beads from two samples were collected in a new eppendorf to which 500 µl of calmodulin elution buffer (CEB) (50 mM ammonium bicarbonate pH 8, 25 mM ethylene glycol tetraacetic acid (EGTA), 0.025% RapiGest SF) was added and incubated for 1 h. The tubes were spun, the final eluate was collected and the elution step was repeated again by adding fresh 500 µl of CEB. The final eluates were frozen at -70°C.

Sample preparation for mass spectrometry analysis: After all 6 batches of 6 x 175cm^2 HEK 293 stable cells were lysed and tandem affinity purified (one such TAP experiment lasted about a month), all the final eluates (12 ml total) were thawed from -70°C. The final eluates were transferred to Amicon-Ultra 4 centrifugal filter units with 5 kDa MW cut-off and centrifuged using a Beckman J-6B centrifuge at 3,500 g until concentrated down to a volume of 40 µl. The samples were digested with trypsin.

2.6 Mass spectrometry and data analysis

For each sample about 40 µl (half of the digested mixture) was injected into a reverse phase chromatography column mounted in line with an Electrospray Ionization ESI-TRAP mass spectrometer. Following data acquisition, the comparison between the acquired spectra and the theoretical tandem MS (MS/MS) spectra from the NCBInr database was done automatically by a computer program called MASCOT. The following parameters were used: MS/MS ion search of NCBInr database for *Homo Sapiens* taxonomy, fixed modifications-carbamidomethyl, variable modifications-oxidation, monoisotopic mass values, unrestricted protein mass, ± 1.5 Da peptide mass tolerance, ± 0.8 Da fragment mass tolerance, one (1) maximum missed cleavage. For each experimental MS/MS spectrum, the peptide from the database having the highest score was assigned (i.e. the best fit of experimental and theoretical spectra). The score was determined as follows: Score = -10 x log (P), where P is the probability of the assigned peptide being a random match. Only peptides with a confidence level of 95% of being a true match were considered (i.e. $p < 0.05$). The results were presented as a list of proteins. Under each protein were displayed its significant ($p < 0.05$) and non-significant ($p > 0.05$) peptides, as well as a list of other proteins sharing the same peptides. To facilitate the analysis of results from multiple sample injections (total of nine, three for each TAP, IP and control IP) and to eliminate redundant hits, the results from the three replicate experiments analyzed with the mass spectrometer were clustered together as shown in Appendix B. Proteins with similar names and sharing the same set of peptides were displayed as one entry. When a protein identified by Mascot was called differently in separate "runs", for example: "unnamed protein product", "RPN2", ribophorin II precursor-human" and "RPN2 protein", generally the most explicit name was chosen for the final list of proteins, "ribophorin II precursor-human" in this case. The proteins, whose peptide(s) were found in the control experiments more than once, were considered as non-specifically binding to the beads and were excluded from the list of interacting proteins.

2.7 Co-immunoprecipitation

All the procedures were done at 4°C. Confluent cells were washed three times in ice-cold PBS and drained from all liquids. Cells from two 10-cm dishes were harvested by scraping in 500 µl RIPA lysis buffer (0.5% Triton X, 1 x Complete protease inhibitors in PBS pH 7.4). The cell lysates were collected in eppendorf tubes (500 µl per tube) and incubated by rocking for 20 min. The insoluble cell debris were collected by spinning for 20 min at 15,000 g in a desktop centrifuge. The supernatant was pre-cleared by incubating with pre-washed protein G beads for one (1) hour. The pre-cleared lysate was incubated with antibody overnight. The second day, 100 µl of 50% pre-washed protein G sepharose bead slurry was added to each eppendorf tube. After an incubation of two (2) hours, the samples were centrifuged at 700 g for 2 min and the supernatant was discarded. One (1) ml of RIPA lysis buffer was added to each tube and washed by rocking for 10 to 15 min. This washing procedure was repeated five other times. After the supernatant from the last wash was aspirated, 50 µl of gel loading buffer containing 10% Dithiolthreitol (DTT), 45% 2 x Laemmli buffer (100 mM Tris-HCl pH 6.8, 4% SDS, 20% glycerol, 0.2% Bromophenol blue) and 45% RIPA buffer was added to each sample. The beads were vortexed, spun down briefly and heated at 50°C for 10 min. The samples were vortexed again and spun for 3 min at 8,000 g.

2.8 Western blotting

Samples were loaded on a SDS-polyacrylamide gel (usually 10%, but we have used 8% occasionally) and proteins were separated by gel elecrophoresis. The proteins were transferred on polyvinylidene difluoride (PVDF) membranes. The following day, the membranes were blocked for one hour with 5% skim milk in PBS and then incubated for one hour with the particular primary antibody dissolved in 5% skim milk in PBS-0.1% Tween. The blots were washed 4 times for 10 min with PBS-0.1% Tween prior to incubating for one hour with a horseradish peroxidase-conjugated secondary antibody at a dilution of 1:5,000 when using the enhanced chemiluminescence detection kit or 1:30,000 to 1:50,000 when using the SuperSignal West Femto Maximum Sensitivity Substrate.

The membranes were washed again 4 times with PBS-0.1%Tween, before adding the detection kit (1 to 5 min incubation) and exposing with x-ray Kodak films.

2.9 Confocal immunofluorescence microscopy

Cells expressing the construct(s) of interest were plated on glass coverslips two days prior to immunostaining. The whole procedure was done at room temperature and a quantity of 1.5 ml per well of the particular reagent was added at each step. The cells were rinsed 3 times with PBS, fixed for 15 minutes with 2% paraformaldehyde (PFA) and then permeabilized with 0.1% Saponin in PBS for 20 min. Upon removal of the PBS-0.1% Saponin, the cells were blocked as follows: a 10-min wash and a 30-min incubation with 10 mM Glycine in PBS-0.1% Saponin followed by two 10-min washes and a 1h incubation with 2% bovine serum albumin (BSA)-PBS-0.1% Saponin. The desired concentration of the primary antibody (ies) in 2% BSA-PBS-0.1% Saponin was added and the coverslips were incubated over night at 4°C. The next day, the primary antibody (ies) was(were) removed and the coverslips were washed 4 times for 10 min with 2% BSA-PBS-0.1% Saponin. All the manipulations with the secondary antibody (ies) were done with the lights turned off. Following the washes, the slides were incubated with the secondary Alexa Fluor antibody (ies) for 1 h at room temperature in the dark. Three final 10-min washes with 2% BSA-PBS-0.1% Saponin, followed by 2 rinses with water were done. The coverslips were mounted with an Aqua Poly/Mount mounting media and placed overnight at 4°C in the dark. The fluorescent signals were detected with a Zeiss 510 LSM Meta microscope using a 63X plan apochromat objective with oil.

2.10 GST-fusion pull-down experiments

Preparation of GST-fusion proteins: The pGEX-2T-GSTfusion constructs were transformed in BL-21 *E.coli* bacteria. Single colonies were grown over night in 3 ml of 2YT (16 g Bio-Tryptone, 10 g yeast extract, 5 g NaCl in 1 l H_2O) media with 100 µg/ml Ampicillin. Small scale production of GST-fusion proteins was done first to look for the best expressing colonies, which were used for subsequent big scale GST-fusion

constructs' production. Two (2) ml from the overnight inoculation culture were grown in 50 ml 2YT with Ampicillin (for small-scale 200 µl in 5 ml) in a 37°C shaker. When the cultures have reached an optical density at 600 nm (OD_{600}) of 0.6-0.7, the flasks were transferred to a 30°C shaker for 10 min. The cultures were then induced for 2.5 h in a 30°C shaker by adding Isopropyl-β-D-Thiogalactopyranoside (IPTG) to a final concentration of 0.4 mM. The culture mixtures were transferred to 50 ml Falcon tubes and centrifuged for 20 min at 3,000 g. The supernatant was discarded and the bacterial pellets were resuspended in 1 ml (500 µl for small scale) of GST lysis buffer (250 µl NP-40, 100 µl 0.5 M EDTA, 1 tablet Complete protease inhibitors, in 50 ml PBS) and transferred to eppendorf tubes. The bacterial lysates were sonicated 2 times for 20 s (on ice) and the insoluble debris were collected by centrifuging at 4°C for 30 min at 15,000 g. The supernatants were transferred to fresh tubes and stored by freezing at -70°C. To test the expression of each GST-fusion construct relative to GST-protein alone, a 100 µl aliquot (500 µl for small scale) was added to 50 µl of pre-washed Glutathione Sepharose beads and incubated by rocking for 2 h at 4°C. The beads were washed 6 times with 1 ml of GST lysis buffer, with 2 min spins at 700 g in between. Upon removal of the supernatant from the last wash, 40 µl of 1 x Laemmli gel loading buffer with 10% DTT was added to each tube. After vortexing, boiling for 5 min and spinning for 5min, the samples were run on 10% SDS-polyacrylamide gel and stained with Coomasie blue (40% Methanol, 10% Acetic acid, 0.25% Coomasie).

GST-fusion precipitation experiments: The equivalent amount of each GST-fusion protein, as determined by the above procedure, was added to 100 µl of pre-washed Glutathione Sepharose beads slurry (50 µl of beads) and incubated by rocking at 4°C for 2 h. At the same time, the protein to be tested for interaction with GST-fusion constructs was *in vitro* translated by incubating for 1.5 hours at room temperature in the following mixture: 1 µg of DNA, 40 µl of TnT rabbit reticulocyte expression mixtures with T7 promoter and 2 µl of ^{35}S-labeled methionine. Alternatively, the protein of interest was epitope-tagged and overexpressed in cells. After the two-hour incubation, the Glutathione Sepharose beads bound to the GST-fusion construct were washed 3 times with GST lysis buffer. Three (3) µl of *in vitro* translated product or 500 µl of cell lysates (2 x 10-cm dishes in 500 µl of RIPA buffer) were added to each GST-fusion construct.

The volume was brought up to 500 µl with GST lysis buffer and the mixtures were incubated for 2 h at 4°C. Six (6) 10-min washes with 1 ml GST lysis buffer were done with 2 min spins at 700 g in between washes. After the final wash, 40 µl of 1x Laemmli loading buffer/ DTT was added to each tube. The samples were vortexed, boiled 5 min, spinned 5 min and loaded on 10% SDS-Polyacrylamide gels. After elecrophoresis, the gels with radioactively lableled GST-fusion reaction mixtures were stained with Coomasie blue for 40 min and destained overnight in destaining solution (7% acetic acid, 7% methanol, 1% glycerol). The gels were placed in gel soaking solution (40% methanol, 10% glycerol, 7.5% acetic acid) for 3 h prior to drying with a Promega gel drying kit. The next day, the dry gels were placed in a Molecular Dynamics Storage Phosphor screen cassette for at least 2 days. The radioactive signal was detected with a Molecular Dynamics Phosphor imager Instrument. Alternatively, for experiments done with cell lysates, the proteins were transferred onto PVDF membranes and blotted as described earlier.

2.11 Subcellular fractionation by gravity centrifugation

All the steps were done at 4°C. Cells were washed 3 times in ice-cold PBS and collected by scraping (1 x 10 cm dish in 1 ml PBS). The intact cells were pelleted by spinning for 3 min at 8,000 g. The supernatant was discarded and the cell pellets were homogenized by passing 10 to 15 times through a 26.5-gauge needle in a 200 µl of cold sucrose solution (250 mM sucrose, 10 mM HEPES-NaOH pH 7.5, 1 mM EDTA, and protease inhibitors). The nuclei and other bulky cell debris were collected by centrifuging for 15 min at 700 g. A subsequent centrifugation of the supernatant for 10 min at 6,000 g resulted in a pellet containing large organelles and mitochondria. A last centrifugation for 1 h at 100,000 g in a Beckman Optima™ TL ultracentrifuge equipped with an L-100 rotor sedimented all remaining organelles and membranes, leaving in the supernatant only the cytoplasmic proteins. Prior to using the pellet fractions in GST-fusion experiments, they were dissolved in 500 µl of RIPA buffer with rocking for at least 1 h.

RESULTS AND DISCUSSION

3.1 Tandem affinity purification method development and results

The tandem affinity purification method was initially developed by Rigaut et al. in 1999 (164) to study protein-protein interactions in yeast. The original TAP tag, composed of two IgG binding domains of *Staphylococcus aureus* protein A and a calmodulin-binding peptide separated by a tobacco etch virus (TEV) cleavage site, was fused at the C-terminus of the protein of interest (164). Since then, different N- and C-terminal variations of the TAP tag were used successfully for studying not only protein-protein interactions in yeast, but also protein interactions between soluble mammalian proteins. However, there are virtually no TAP studies done on mammalian integral membrane proteins, which could be explained by the difficulty of extracting membrane proteins from the lipid bilayer, while maintaining the interactions within their associated protein complex (es). In an effort to adapt the TAP method to the purification of NHE6-bound protein complexes, the method as described by Anne-Claude Gingras and colleagues (76) was used as a starting point and several parameters were optimized thereafter, including lysis buffer and elution buffers composition, as well as duration of binding/elution steps and washes. A simplified graphical representation of the TAP procedure used in the present study, as well as the expression levels of TAP-tagged $NHE6_{HA}$ in two of the stable cell lines used in our experiments, are shown in Figure 1.

The pMZS3F expression vector used in the present study contains a modified TAP tag, composed of a triple flag epitope (3xFlag), followed by a calmodulin-binding peptide, separated by a TEV cleavage site. As such, the conditions for the first elution step of the Anne-Claude Gingras' method were not applicable given that it is based on purification through protein A and elution by TEV cleavage. The modified TAP tag has the advantage of not requiring TEV, which could inadvertently cleave NHE6 and/or its associated partners. The conditions and reagents suggested in the data sheet provided by Sigma-Aldrich upon the purchase of the 3xFlag peptide were used as a guideline for the affinity purification using the anti-Flag M2 Affinity Gel.

Figure 1: Tandem affinity purification method and $NHE6_{HA\text{-}TAP}$ expression in HEK 293 stable cell lines

A) Cartoon representation of the two affinity purification steps of the TAP method.

B) Different levels of expression of $NHE6_{HA\text{-}TAP}$ in various clones of stable HEK 293 cells. HEK 293 cells were transfected with pMZS3F-$NHE6_{HA}$ and individual colonies surviving a G418 selection were collected and grown to confluency in 10-cm dishes. Cells were lysed in TAP-lysis buffer and equal amounts of lysates for each clone were separated by SDS-Polyacrylamide gel electrophoresis (SDS-PAGE). The membranes were blotted with an anti-HA (1:5,000) antibody. The arrows indicate the clones selected for TAP experiments: a low expressing clone (1) and the high expressing clone (5).

C) Expression levels and localization of the HEK 293 $NHE6_{HA\text{-}TAP}$ expressing stable cell lines selected for study. Cells were grown on glass coverslips and fixed and permeabilized. $NHE6_{HA\text{-}TAP}$ was visualized by staining with a primary monoclonal anti-HA (1:2,000) and a secondary Alexa Fluor 568 - conjugated anti-mouse antibody (1:2,000). Panels **a** and **b** represent clones 1 and 5 respectively.

A)

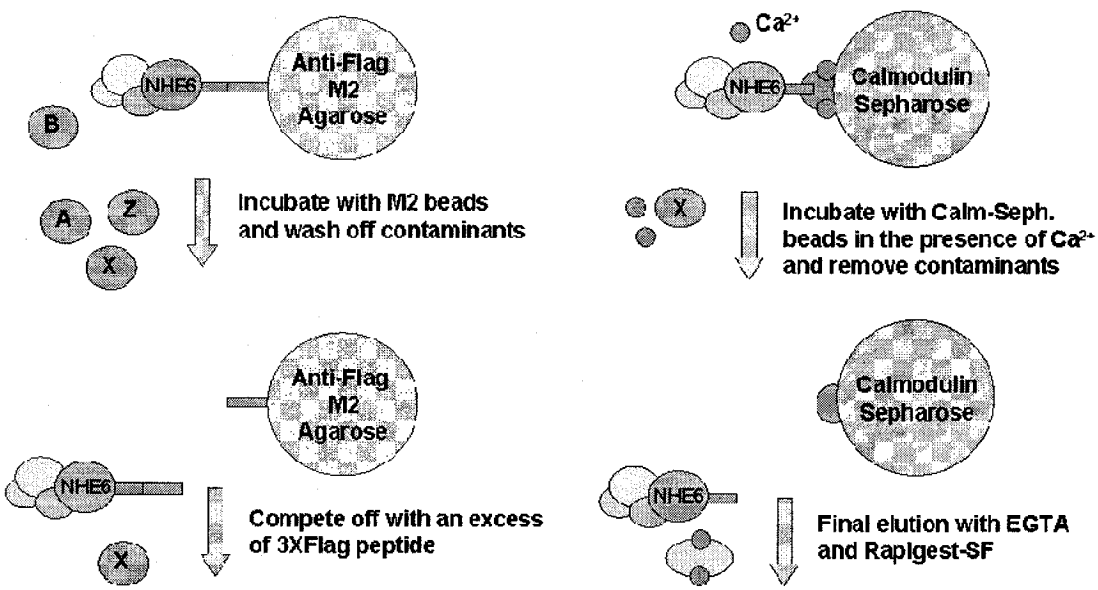
Anti-Flag M2 Agarose
NHE6
B
A
Z
X
Incubate with M2 beads and wash off contaminants
Ca2+
Calmodulin Sepharose
Incubate with Calm-Seph. beads in the presence of Ca2+ and remove contaminants
Compete off with an excess of 3XFlag peptide
Final elution with EGTA and Rapigest-SF

B)

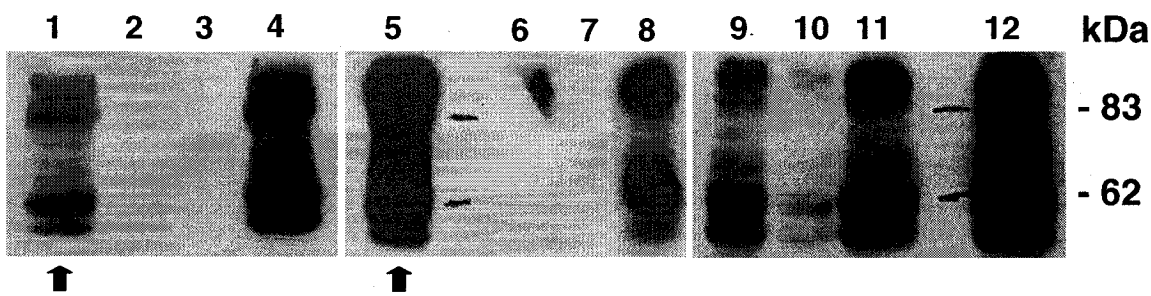
1 2 3 4 5 6 7 8 9 10 11 12
kDa
- 83
- 62

C)

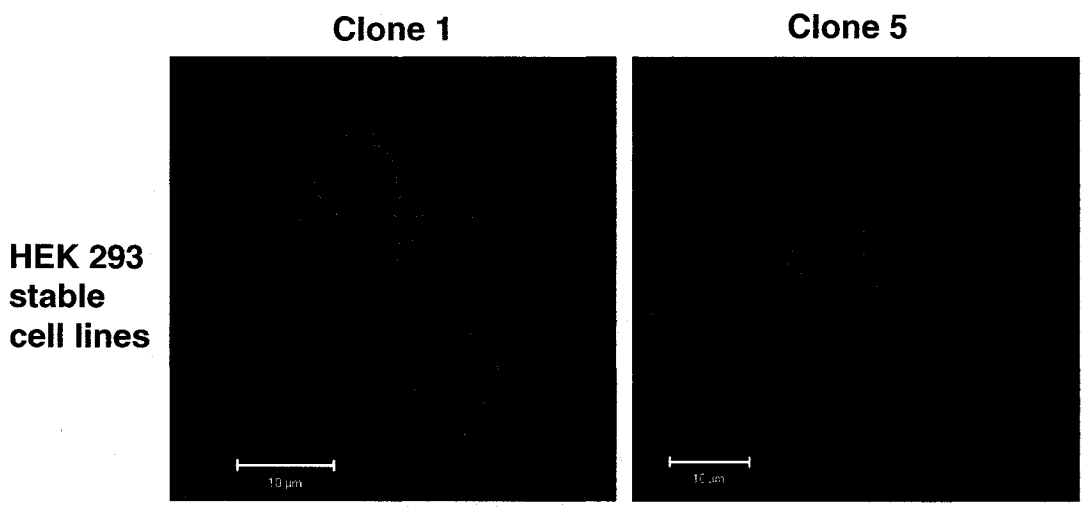
Clone 1
Clone 5
HEK 293 stable cell lines

The first step towards the TAP method optimization was the comparison between two lysis buffers: a modified version of the lysis buffer according to Anne-Claude Gingras' recipe and the commercial CelLytic lysis buffer. This test was inspired from a previous study done by Qiang et al. (112) who compared four different lysis buffers for their efficiency of extracting the polycystin-2 channel. They found that CelLytic was the best in extracting this integral membrane protein, which motivated us to test its efficacy for NHE6. Preliminary results using small scale preparations indicated that the CelLytic lysates gave stronger signals for $NHE6_{HA\text{-}TAP}$ than the traditionally used lysis buffer, when equal amounts of lysates were separated by SDS-Polyacrylamide gel electrophoresis (SDS-PAGE) and visualized by Western blotting (data not shown). However, when the entire medium scale TAP procedure (as described in Table 1) was done with both lysis buffers and the proteins at different purification steps were visualized on a silver-stained polyacrylamide gel, the final eluate using the CelLytic lysis buffer contained much less and much lower amounts of proteins than the Anne-Claude Gingras' recipe (data not shown). With the concern that CelLytic might disrupt too much the protein interactions, the latter lysis buffer was selected.

The major difficulties encountered were the poor recovery of $NHE6_{HA\text{-}TAP}$ bound complexes from both affinity purification columns. The problem was especially pronounced for the elution of the purified complexes from the Calmodulin Sepharose 4B beads, as virtually no proteins could be recovered unless the mild denaturing detergent RapiGest-SF was present. Considering that this reagent is relatively expensive, additional tests were done to determine the lowest amount that could be used without affecting protein recovery. The RapiGest-SF concentration was thus decreased from 0.1% (small/medium scale experiments) to 0.025% (large scale experiments) (Table 1).

Similarly, there was a significant loss of NHE6 protein on the M2 beads. To optimize this step, several approaches were used, amongst which the use of the TEV to cleave off the NHE6-bound complexes instead of competing it off with 3xFlag peptide. There was not a significant difference between these two means of elution as shown in Figure 2 A, thus the less compromising use of the 3xFlag approach was used. An increase in 3xFlag peptide concentration in the elution buffer did not significantly

Table 1: Comparison of the experimental conditions used for different scale tandem affinity purification experiments

		FINAL METHOD: Large scale				Medium scale			Small scale	
		6 batches of 6 tubes of 1 x 175 cm^2 dish				3 tubes of 4 x 10-cm dishes			2 x 10-cm dishes	
No	Step Description	Experimental conditions (vol. per Eppendorf tube)	Incub. time	No. of tubes	Total vol. (ml)	Method differences	No. of tubes	Total vol. (ml)	Method differences	Total vol. (ml)
1	**Preclearing the lysates**	20 µl agarose beads (glutathione)	>1 h	6	6		3	3.6		
	Incubating the precleared lysates on M2 beads	25 µl of M2 beads	>2 h	6	6		3	3.6	ON	0.5
2	**Supernatant from the M2 incubation**			6	6		3	3.6		0.5
	Three (3) washes after the M2 incubation	collect beads in 2 tubes (75 µl/tube)		2			1			
3	**M2 beads pre-elution**			2	1		1	0.5		
4	**Two (2) elutions with 3XFlag peptide**	add 500 µl M2 buffer with 200 ng/ul 3XFlag peptide	ON	2	2	one (1) elution 3xFlag	1	0.5	200 µl of 500 ng/ul 3XFlag	0.4
5	**M2 beads post-elution**			1	0.5		1	0.5		0.5
	Incubation on Calmodulin Sepharose (CS) beads	20 µl CS beads + 500 µl Eluate + 800 µl CBB + 10 µl $CaCl_2$ (1M)	ON	4	5.2	500 µl Eluate + 500 µl CBB + 400 µl CBB rinse; 3 h	1	1.4	3 h	1.4
	Two (2) washes with CBB	collect beads in 1 tube (80 ul beads)		1			1			
	Three (3) washes with CRB			1			1			
6	**CS beads pre-elution**			1	1		1	1		
7	**Final elutions (2 x 500 µl or 3 x 333 µl)**	CEB + 0.025% RapiGest-SF	1 h each	1	1	+ 0.1% RapiGest-SF; 20 min each	1	0.5	0.1% RapiGest 20 min each	0.4
8	**CS beads post-elution**			1	1		1	1		

improve the recovery. It was enhanced above all by augmenting the elution duration from 30 minutes to several hours through the use of two elution steps.

The above improvements resulted in an estimated final NHE6-protein recovery of nearly 20% of the NHE6 present in the lysate (Figure 2A). At this point, the method was deemed sufficiently optimized for a large-scale preparation. Although comparable NHE6 recovery was obtained in a medium scale purification experiment involving the lysis of twelve 10-cm dishes of cells (Figure 2B), a small difference between the medium and small-scale purification is in the presence of the core (faster migrating band) and glycosylated (slower migrating band) NHE6. It is possible that the core glycosylated form of NHE6 is more abundant than the fully glycosylated NHE6, which is not visible yet in Figure 2A due to a short exposure. A significant number of putative NHE6-associated proteins were recovered from a medium scale experiment as revealed by the protein bands in lane 7 on Figure 2C. One should keep in mind that these proteins are associated in complexes, thus only a fraction of them interact directly with NHE6. In addition, given the low amount of detergents in the lysis buffer, it is likely that many protein interactions were preserved throughout the purification.

At this point, the improved TAP method was considered to be adequate for the efficient purification of NHE6-associated complexes and their subsequent identification by mass spectrometry analysis. Unfortunately, the protein concentration in the final eluate was below the detection limits of the mass spectrometer, which could only detect and identify fragments corresponding to NHE6. There were two options for correcting the problem: modify the method to optimize the recovery or simply upscale the already established procedure. Due to time constraints, we chose the simpler solution and upscaled the TAP procedure ten-fold, resulting in the lysis of the equivalent of 120 10-cm dishes for each sample analyzed by mass spectrometry. A total of three large scale TAP experiments were done, two of which using the higher expressing NHE6 cell line (clone 5), and one using the lower expressing NHE6 cell line (clone 1). Even though in this last experiment twice as many cells were lysed (240 x 10-cm dishes) to compensate for the lower NHE6 expression, few peptides could be detected by mass spectrometry. This low NHE6 protein complex recovery is also illustrated in the silver stained gel (Figure 3), as there are virtually no purified proteins in the last lane (TAP Feb 10).

Figure 2: Relative amounts of proteins purified at different steps of the TAP procedure

A) Amounts of $NHE6_{HA\text{-}TAP}$ purified at different steps for a **small scale** TAP experiment. Equal volume fractions for each aliquot were separated by SDS-PAGE and the membranes were blotted with monoclonal anti-HA antibody (1:5000). The numbers on the top of each lane correspond to different aliquots: **1** – Precleared lysate, **2** – Supernatant from incubation on M2 beads, **3** – M2 beads prior to elution with 3xFlag peptide, **4** – 3xFlag peptide eluate, **5** - M2 beads post 3xFlag peptide elution, **6** – Calmodulin Sepharose beads prior to final elution, **7** – Final eluate, **8** – Calmodulin Sepharose beads post-elution.

B) Same as **A)** but for a **medium scale** experiment.

C) Proteins purified at different steps of a **medium scale** TAP purification. Proteins contained within aliquots of different volume fractions (as indicated) were separated by SDS-PAGE and visualized by silver staining. The numbers above each lane correspond to the same aliquots as in **A)**, except for **6b**, which is the supernatant from incubation with Calmodulin Sepharose beads.

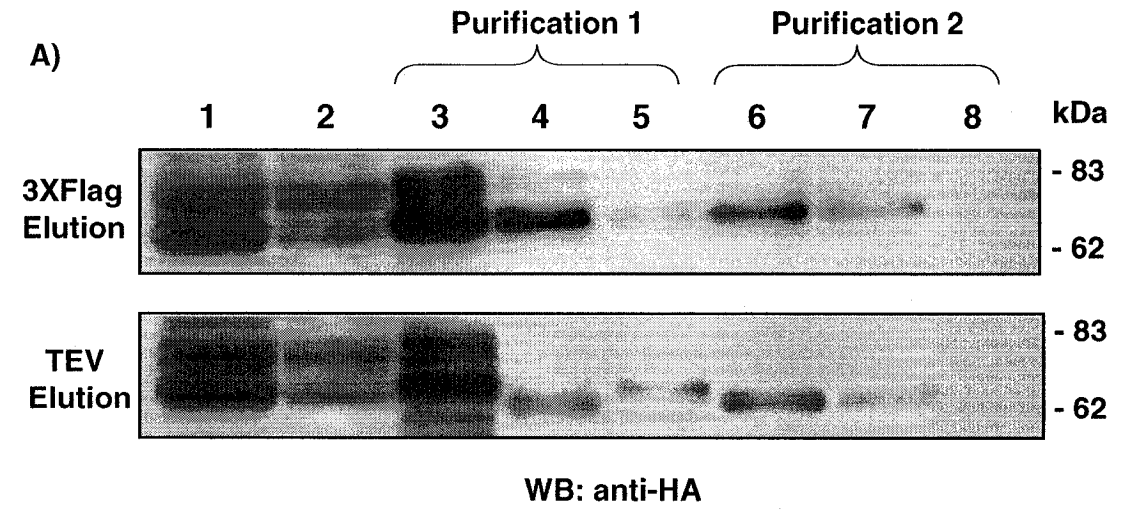
A)
Purification 1
Purification 2
1
2
3
4
5
6
7
8
kDa
3XFlag Elution
- 83
- 62
TEV Elution
- 83
- 62
WB: anti-HA

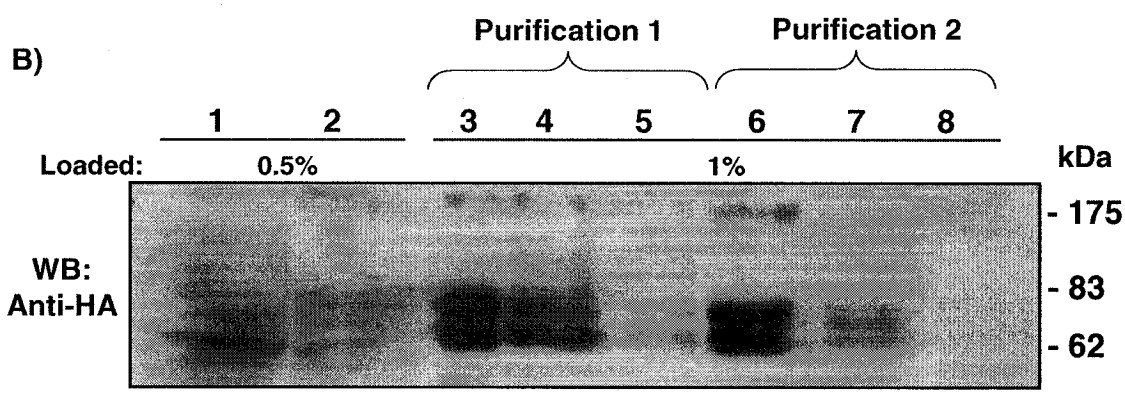
B)
Purification 1
Purification 2
1
2
3
4
5
6
7
8
Loaded:
0.5%
1%
kDa
WB: Anti-HA
- 175
- 83
- 62

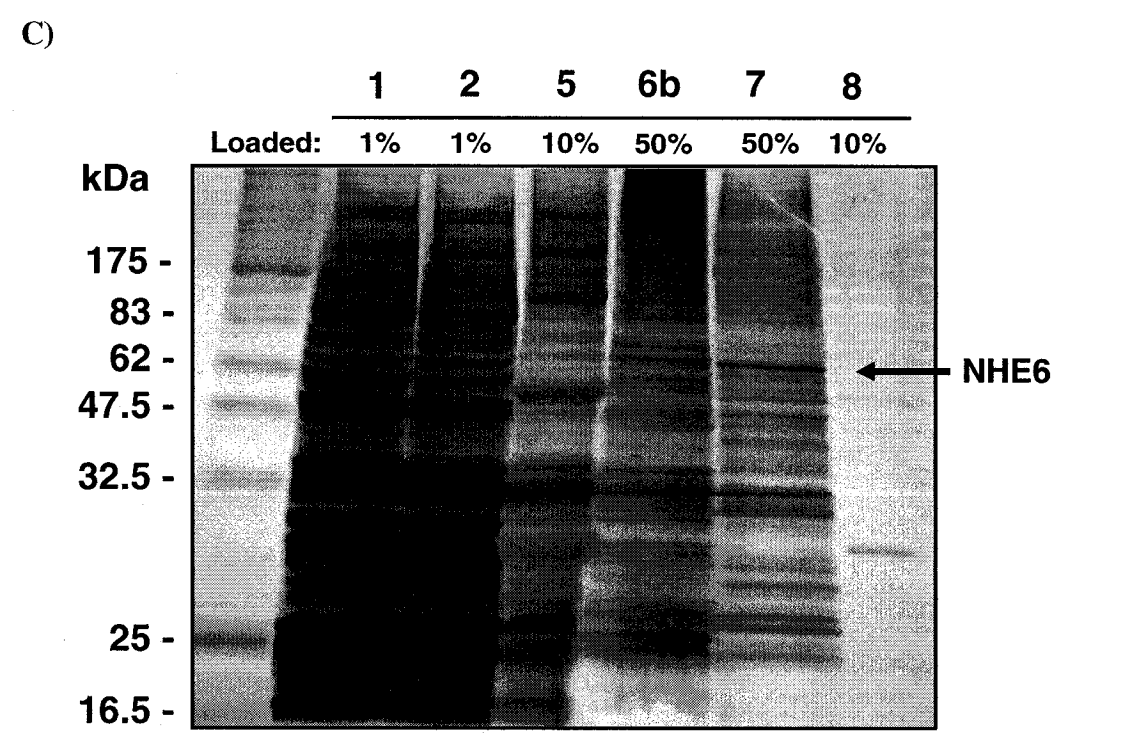
C)
1
2
5
6b
7
8
Loaded:
1%
1%
10%
50%
50%
10%
kDa
175 -
83 -
62 -
47.5 -
32.5 -
25 -
16.5 -
NHE6

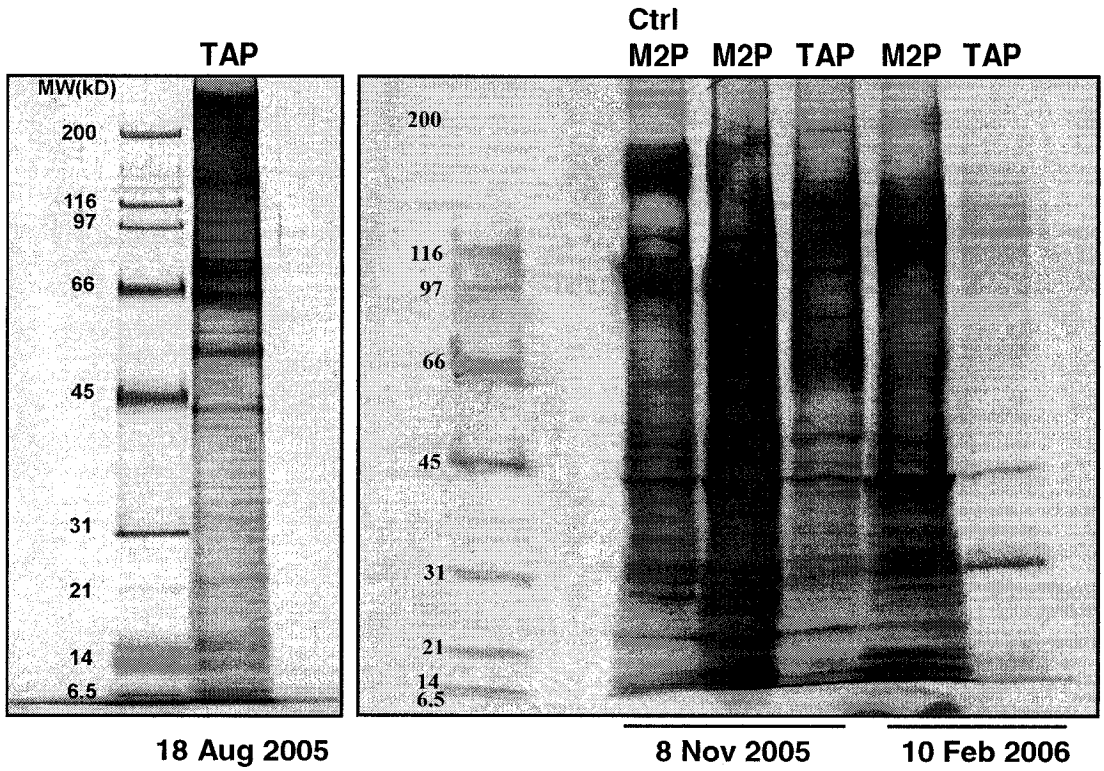

Figure 3: Aliquots of samples sent for mass spectrometry analysis visualized by silver staining

The tandem affinity purification was repeated three times (18 Aug 05, 8 Nov 05, 10 Feb 06) using $NHE6_{HA\text{-}TAP}$ stably expressing HEK 293 cells. For each of the three different experiments, three samples were sent for analysis: a negative control sample (ctrl M2P), a sample from one-step purification using M2 beads (M2P) and a sample from tandem affinity purification (TAP). For the first two experiments (18 Aug, 8 Nov), the equivalent of 130 x 10-cm culture dishes of highly overexpressed $NHE6_{HA\text{-}TAP}$ (clone 5) were lysed. For the third experiment (10 Feb), the equivalent of 260 x 10-cm culture dishes of low $NHE6_{HA\text{-}TAP}$ overexpressed (clone 1) cells were used. The proteins that remained bound to the M2 beads post-elution were removed with detergent and send for mass spectrometry analysis as well (M2P). As a negative control, cells from 20 x 10-cm dishes of HEK 293 cells transfected with empty plasmid were purified with M2 beads and eluted with detergent (ctrl M2P). For all samples, the final eluates were concentrated down to 40µl. A 5-µl aliquot was loaded on 4-12% Tris-Glycine gel and silver stained.

For each TAP experiment, eluates from one-step affinity purification by M2 anti-Flag beads and control samples were analysed by mass spectrometry. Given that nearly 50% of the NHE6-complexes remained bound on the M2 beads post 3xFlag elution, it was convenient to elute them in the presence of RapiGest-SF and to use this sample, called "M2P" for protein identification with mass spectrometry. In addition, for each TAP experiment a control purification of non-transfected HEK 293 cell lysates with M2 beads (ctrl M2P) was done to identify and thus disregard proteins, which bind non-specifically to the beads (only one of the three control experiments is shown in Figure 3).

The final list of NHE6-interacting proteins, displayed in Table 2, contains results combined from three separate mass spectrometry analyses; the first two being replicate runs from the same experiment (dated 18 August 2005) and the third one being a separate experiment (dated 8 November 2005). As expected, NHE6 was the most abundant protein and was present in all of the samples. A total of 76 NHE6-interacting proteins were identified, 28 of which were present in the TAP eluates and are written in bold. A detailed version of Table 2, which includes results from individual experiments, is provided in Appendix C. It gives information on the reproducibility of the technique. For instance, the reliability of the mass spectrometry instrumentation was tested by injecting twice the same TAP sample: on the 18th of August and on September the 2nd. Out of the 20 proteins identified in each of the two mass spectrometry analyses, 15 were the same. In addition, 18 proteins were identified in a separate TAP experiment (November 8th), 14 of which were present in either or both of the two previous analyses. Thus, the TAP technique used in this study is reasonably reproducible.

Amongst the putative NHE6-associated partners, several interesting candidates include elements of the cytoskeleton (actin, tubulin) and cytoskeleton-associated proteins (myosin light chain kinase, kinesin, cytoskeleton-associated protein 4) as well as proteins involved in vesicle trafficking such as the small GTPases (Rab7, Rab1B, Rab2B) and ubiquitin. Several integral membrane proteins were also identified, including two Ca^{2+} transporting ATPases and the monocarboxylate transporter. Regulatory molecules such as calmodulin were also found in our final eluates, although it remains to be verified if it fulfills similar functions in association with NHE6 like with other NHEs as previously

Table 2: NHE6HA-interacting proteins identified from replicate M2 affinity purification (M2P) and tandem affinity purification (TAP) experiments

Protein name	No. peptides		Function
	Total	Distinct	
Integral to membrane (organelles non-specified)			
NHE6	18	6	Na^+/H^+ antiporter activity
ATPase, Ca^{2+} transporting, cardiac muscle, slow twitch 2	4	2	calcium/proton transport, sarcoplasmic reticulum
cytoskeleton-associated protein 4 (CKAP4)	3	3	
VAMP (vesicle-associated membrane protein)-associated protein A	2	2	protein complex assembly, exocytosis, protein trafficking
ATPase, Ca^{2+} transporting, plasma membrane 4	2	2	calcium ion transport, metabolism
phosphatidylserine synthase 2	1		phospholipid biosynthesis
brain-selective and closely mapped on the counter allele of CMAP in cystatin cluster	1		biosythesis
transmembrane protein 41B (KIAA0033)	1		phosophoenolpyruvate-dependent sugar phosphotransferase system
microsomal glutathione S-transferase 1 (MGST1)	1		microsome, GST activity
monocarboxylate transporter 1 (MCT1)	1		organic ion transport
Acyl-CoA synthetase	1		lipid metabolism
basigin, EMMPRIN, CD147	1		cell surface receptor linked to signal transduction
neutral amino acid transporter	1		dicarboxylic acid transport
RAP1B, member of RAS oncogene family	1		protein transport, cell cycle regulation, signal transduction, immunoglobuin family
Endoplasmic Reticulum			
BiP protein	8	6	chaperone, lumen
ribophorin II precursor (RPN2)	6	4	N-linked glycosylation via asparagine
aldehyde dehydrogenase 3A2	6	4	membrane, lipid metabolism
ribophorin I	4	2	membrane, protein amino acid glycosylation
signal sequence receptor, delta (translocon-associated protein delta)	3	3	membrane, intracellular protein transport, Ca^{2+} binding
calnexin	3	2	lumen, chaperone
translocating chain-associating membrane protein (TRAM1)	2	1	translocation of secretory proteins
delta7-sterol reductase (D7SR); 7-dehyrocholesterol reductase (DHCR7)	1		membrane, cholesterol biosynthesis
oligosaccharyltransferase	1		membrane, N-linked glycosylation via asparagine
zinc metalloproteinase STE24 homolog	1		membrane ER, Golgi, proteolysis and peptidolysis
SURF-4 isoform, surfeit 4	1		membrane, unknown function
Mitochondria			
voltage-dependent anion channel 2 (porin)	5	4	outer membrane, anion transport
ATP synthase, H^+ transporting, mitochondrial F1 complex, α subunit (ATP5α)	2	2	inner membrane
tricarboxylate carrier protein	2	1	tricarboxylate/iron carrier
translocase of outer mitochondrial membrane 70 homolog A	2	1	integral to membrane, protein binding
leucine-rich PPR motif-containing protein	1		protein/RNA/DNA binding
B-cell receptor associated protein	1		inner membrane, regulation of transcription
prohibitin	1		inner membrane, DNA replication, cell cycle
chaperonin (HSP60)	1		matrix, protein folding
transmembrane protein, motor protein, mitofilin	1		inner membrane, unknown function
heat shock 70kD protein 9B	1		protein folding
peripheral benzodiazepine receptor	1		outer membrane, signal transduction, protein-mitochondrial targeting, also at plasma membrane
Nucleus			
heat shock 70kDa protein 1A	9	5	protein folding
ubiquitin	3	1	protein modification, cell cycle
HNRPH1	3	2	RNA binding
thymopoietin isoform β	3	3	lamino-associated polypeptide 2 / emerin
leucine-rich PPR motif-containing protein	1		protein/RNA/DNA binding
B-cell receptor associated protein	1		inner membrane, regulation of transcription
BCL2-associated transcription factor 1	1		regulation of transcription
lamin B receptor	1		integral to nuclear membrane, DNA binding

Protein name	No. peptides		Function
	Total	Distinct	
Cytoskeleton			
actin-β	26	11	
β-tubulin	20	9	
α-tubulin	15	5	
tropomodulin 3	1		actin capping protein complex
Cytosol			
heat shock 70kDa protein 1A	9	5	protein folding
myosin light chain kinase (MLCK)	5	2	serine/threonine protein kinase
protein phosphatase 1B1 43 kDa isoform	4	3	protein amino acid dephosphorylation
calmodulin	4	3	Ca^{2+} binding, cell cycle
B-ind1 protein	3	1	small GTPase mediated signal transduction
ubiquitin	3	1	protein modification, cell cycle
chain A, crystal structure of human carbonyl reductase 1 (Cbr1) in complex with hydroxy-Pp	3	3	short-chain dehydrogenase-reducatase, metabolism
small GTP binding protein Rab7	2	1	Golgi, protein transport, endocytosis
ancient ubiquitous protein 1(AUP1)	1		integrin signalling
RAB2B	1		ER, Golgi, intracellular protein transport
RAB1B	1		intracellular protein transport
kinesin-related protein	1		microtubule associated complex, microtubule-based movement
ribosomal protein S3	4	2	protein synthesis
ribosomal protein S18	3	2	protein synthesis
ribosomal protein L11	2	1	protein synthesis
PREDICTED: similar to 40S ribosomal protein S17	2	2	protein synthesis
similar to ribosomal protein L23 (RPL23)	2	1	protein synthesis
similar to ribosomal protein S14	1		protein synthesis
ribosomal protein L13 (RPL13)	1		protein synthesis
PREDICTED: similar to ribosomal protein S27	1		protein synthesis
Unknown function and/or location			
CHCHD2 protein	5	2	
DNA dependent protein kinase catalytic subunit	4	3	DNA repair
STMF151	2	1	
KIAA0090	2	1	
transmembrane protein, uncharacterized hypothalamus protein HTMP	2	1	
hypothetical protein LOC55379	1		
MBC3205	1		
UNQ501 protein	1		
KIAA0887 protein	1		
PREDICTED: similar to Enhancer of rudimentary homolog	2	1	regulation of cell cycle

described. We also had a few surprises, notably many mitochondrial and nuclear proteins for which a physiological interaction with NHE6 is difficult to envision.

As stated in the research rationale section, the TAP was done as a complementary approach to the yeast two-hybrid method and we expected to find some common as well as different NHE6-interacting proteins from the two methods. To our surprise, there were virtually no common proteins, except for β-tubulin and perhaps Rac1 found in the Y2H, which regulates the protein B-ind1, identified through TAP. Far from discrediting both methods, these seemingly divergent results should be rather viewed as complementary, considering the significant differences between the two approaches. Indeed, while the Y2H screening was done with a brain cDNA library, the TAP was done in completely different cells, namely a human embryonic kidney cell line. Given that these specialized cells fulfill totally different functions, it is likely that NHE6 does not interact necessarily with the same complement of proteins in both. Another explanation for the different results is the fact that the Y2H method detects direct protein interaction with the tail of NHE6, while the TAP allows one to identify proteins within NHE6-interacting complexes. Moreover, the Y2H method is somewhat artificial in that it only uses part of NHE6 to measure interactions with fragments of proteins, which might never encounter NHE6 under physiological conditions, thus resulting in many false positives. The advantage of the TAP method is that it is done under close to physiological conditions, thus having a lower false positive incidence (about 15%) compared to the Y2H method (45 to 80%) (68). On the other hand, many protein-protein interactions under physiological conditions are transient, thus it is possible that several weakly bound complexes are lost during the purification.

3.2 Overview of the experimental results obtained for eight putative NHE6-interacting proteins selected for study

This Master's thesis encompassed the study of eight different putative NHE6-interacting proteins, four of which were found through a yeast two-hybrid screening of a brain cDNA library and four others, through tandem affinity purification of NHE6 stably transfected HEK 293 cells. Table 3 contains a list of these proteins as well as a summary of the different experiments done to validate their interaction with NHE6. The highlighted proteins (APOD, ATP5A1 and MLCK) showed positive NHE6-interaction and were studied most extensively, as indicated by the large number of experiments. Each of them will be discussed in greater detail in subsequent sections. Although some of the remaining five proteins showed weak interactions with NHE6, none of them was studied further due to lack of confidence in the results and time constraints.

Table 3: Summary of the results from experiments testing the interaction between NHE6 and eight putative interacting partners

	Name of Putative NHE6 Binding Protein	Number of experiments			Experimental Result			Interaction?
		Co-IP	LSM3	GST	Co-IP	LSM3	GST	
Y2H	Apolipoprotein D (APOD)	6	3	2	weak	NO	weak	non-specific
	Prostaglandin D2 synthase (PTGDS)	3	1		weak	small		need more experimental evidence
	Ubiquitin conjugating enzyme variant 2 (UBE2V2)	1	1		yes	NO		
	Chloride intracellular channel 1(CLIC1)		1			NO		
TAP	ATP synthase H+ transporting, F1, alpha (ATP5A1)	6	2	4	positive	weak	positive	positive
	Myosin light chain kinase (MLCK)	3	2		positive	partial		positive
	Calmodulin	2			NO			need more experimental evidence
	Ubiquitin	3			NO			

3.3 Interaction between NHE6 and apolipoprotein D

Within the scope of this thesis, apolipoprotein D was the most extensively studied NHE6-interacting protein identified through the yeast two-hybrid screening. A total of 3 different clones from a brain cDNA library were found to directly interact with NHE6 C-tail, which made APOD a promising candidate. Apolipoprotein D is a 29-kDa glycoprotein with a β-barrel tertiary structure, found in association with high density lipoproteins in human plasma (120). It binds to a variety of molecules, including cholesterol (147), bilirubin (150), steroids (148) and arachidonic acid (127). Although its exact physiological role is unknown, it is proposed to be a multi-functional transporter of small hydrophobic molecules. It is found predominantly in adrenal glands, pancreas, kidneys, placenta, spleen, lungs, ovaries, testes, brain, peripheral nerves and cerebrospinal fluid (32,63). Apolipoprotein D is mostly expressed in fibroblasts found in proximity to blood vessels (159,180), as well as in astrocytes, oligodendrocytes and endoneurial fibroblasts (132,183). Intriguingly, high levels of apolipoprotein D are observed in several disorders, including breast cancer (86), prostate carcinomas (11) and neurodegenerative conditions such as Alzheimer's disease (191). In addition, it is upregulated in quiescent cells (159) and in regenerating peripheral nerves (35). Knowing that apolipoprotein D is a secreted protein and that part of, or the entire, NHE6 C-tail could be luminal, similarly to its yeast homologue ScNhx1, we hypothesised that NHE6 could serve as a receptor to internalize this lipocalin and its cargo.

This hypothesis could be tested by looking for the binding region of apolipoprotein D on NHE6 tail. To this end, an *in vitro* binding experiment was done between GST-fusion constructs of NHE6 C-tail fragments and *in vitro* translated apolipoprotein D lableled with radioactive methionine (APOD-^{35}S) (Figure 4). The latter showed interaction with all NHE6-GST fusion constructs, except for the extremity of the NHE6 C-tail ranging from amino acids 608 to 669. Even though the fraction of APOD(^{35}S), which bound to parts of NHE6 tail was minimal with respect to the total amount loaded (Figure 4, lane 1), it is probably a true interaction as no APOD(^{35}S) bound to GST protein alone (Figure 4, lane 2). Overall, the result from this *in vitro* binding experiment shows that APOD binds to the very beginning of NHE6 C-tail and its binding

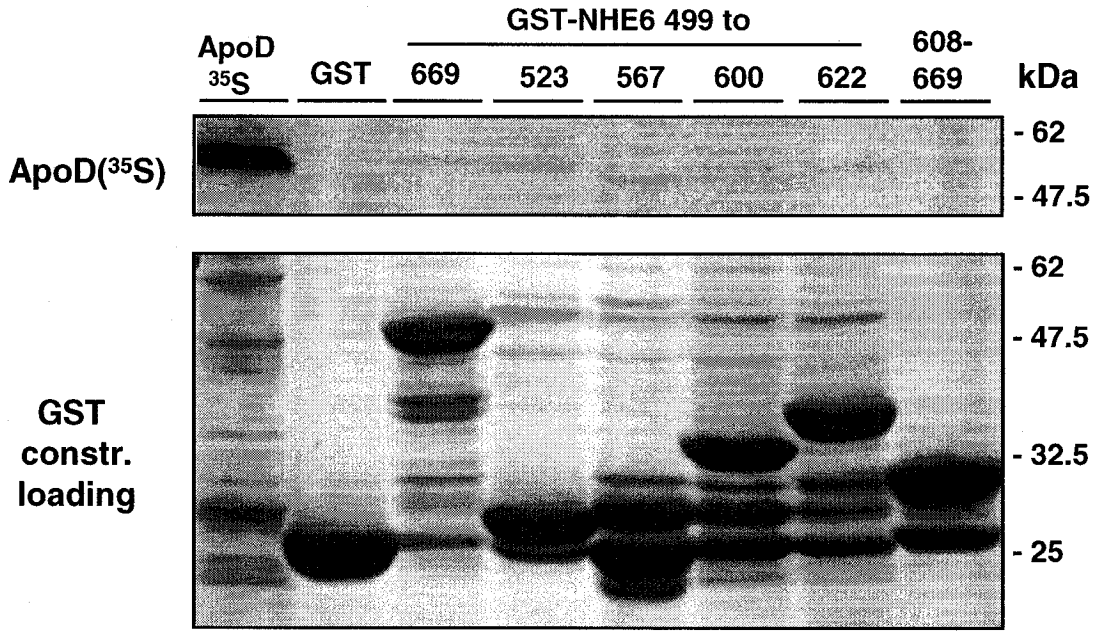

Figure 4: *In vitro* binding of APOD(^{35}S) with GST-fusion constructs of NHE6 regulatory tail

Apolipoprotein D was translated *in vitro* by adding 0.2 µg of pCDNA3-APOD into a 40 µl of rabbit reticulocyte TnT T7 Quick Coupled Transcription/Translation system in the presence of 2 µl ^{35}S radioactively labeled methionine. Three (3) µl of this *in vitro* translated mixture were added to each reaction tube containing a different NHE6 C-tail GST-fusion construct. Following an overnight incubation and extensive washing, the protein samples were run on a SDS-Polyacrylamide gel, which was stained with Coomasie blue to show equal GST-fusion construct loading (bottom panel). After drying, the gel was exposed for 3 weeks on a Molecular Dynamics Storage Phosphor screen cassette and visualized with a Phosporimager instrument.

region might extend up to amino acid 608. Although this observation supports the idea of a luminally oriented NHE6 regulatory tail, it does not account for the observed interaction between other NHE6-interacting proteins, such as Rack1, which reside in the cytosol and show a similar binding pattern to APOD (Ilie, A. & Orlowski, J., unpublished data). To resolve this discrepancy and to confirm that APOD interaction with NHE6 C-tail fragments is specific, *in vitro* binding experiments with different NHE6-GST fusion constructs is required.

To confirm the observations from the GST-fusion pull-down experiments, the interaction between $NHE6_{HA}$ and $APOD_{myc}$ was tested *in vivo* by co-immunoprecipitation. As indicated in Table 3, a total of 6 co-immunoprecipitation experiments were done for which a representative blot is shown in Figure 4A. In this particular experiment, $NHE6_{HA}$ and $APOD_{myc}$ were co- transfected in CHO cells and the immunoprecipitation was done with both anti-myc, top panel, and anti-HA, bottom panel, antibodies. Even though some $NHE6_{HA}$ came down along with the immunoprecipitated $APOD_{myc}$ (top panel, lane 4), it was but a small fraction from the total $NHE6_{HA}$ (top panel, lane 5). Similarly, the signal was at the verge of detection when the inverse experiment was done, whereby the SuperSignal West Femto Maximum Sensitivity Substrate was used to detect $APOD_{myc}$ (bottom panel, lane 4, middle band) bound to immunoprecipitated $NHE6_{HA}$. The results were even less convincing when the two proteins were co-transfected in HEK 293 cells, as no signal could be detected even in the lysates, which means that APOD is poorly expressed or secreted in these cells, under the experimental conditions used. To ensure that the observed interaction was real, several controls were done, including a sample in which non-specific IgG antibody was used to see if any of the two proteins bind non-specifically to the beads (lane 1) and a sample of non-transfected cells, in case the antibody used for blotting recognizes non-specific proteins. An additional control shows that the interaction with APOD might not be exclusive to NHE6, but could extend to other NHEs, such as NHE1 (lane 2). In summary, the co-immunoprecipitation experiments did reveal a weak interaction between the overexpressed epitope-tagged APOD and NHE6, but the question of whether the interaction is specific or physiologically relevant remains unanswered.

Figure 5: Testing the interaction between $NHE6_{HA}$ and $APOD_{myc}$ by co-immunoprecipitation and confocal microscopy

A) Interaction between $NHE6_{HA}$ and $APOD_{myc}$ by co-immunoprecipitation. $NHE6_{HA}$ and $APOD_{myc}$ were co-transfected in CHO cells. Twenty four hours (24) post-transfection, the cells were lysed and polyclonal anti-myc or anti-HA antibodies were added to the pre-cleared lysates. The immunoprecipitated proteins were separated by SDS-PAGE and transferred to PVDF membranes. The membranes were visualized with the Enhanced Chemiluminescence detection kit when blotted with a monoclonal anti-HA antibody (1:10,000) or with the SuperSignal West Femto Maximum Sensitivity Substrate when blotted with monoclonal anti-myc antibody (1:1,000). The same experimental conditions were used for the control experiments. The band indicated by the arrow represents APOD protein.

B) Comparison of the cellular distributions of $NHE6_{HA}$ and $APOD_{myc}$ in CHO cells. Cells were grown on glass coverslips and co-transfected with $NHE6_{HA}$ and $APOD_{myc}$. Twenty four (24) hours post-transfection, the cells were fixed, permeabilized and dually lableled with a rabbit polyclonal anti-HA (1:1,000) and a mouse monoclonal anti-APOD (1:100) primary antibodies, followed by Alexa Fluor 488 (green) - conjugated anti-rabbit (1:2,000) and Alexa Fluor 568 (red) - conjugated anti-mouse (1:2,000) secondary antibodies. Four representative images out of a z-stack containing a total of eight slices are shown. Each slice is 6 μm thick and was obtained at a different cell depth with respect to the coverslip's contact surface: slice one is 2^{nd} of 8, slice two is 3^{rd} of 8, slice three is 4^{th} of 8 and slice four is 6^{th} of 8. The scale bar represents 10 μm.

A)

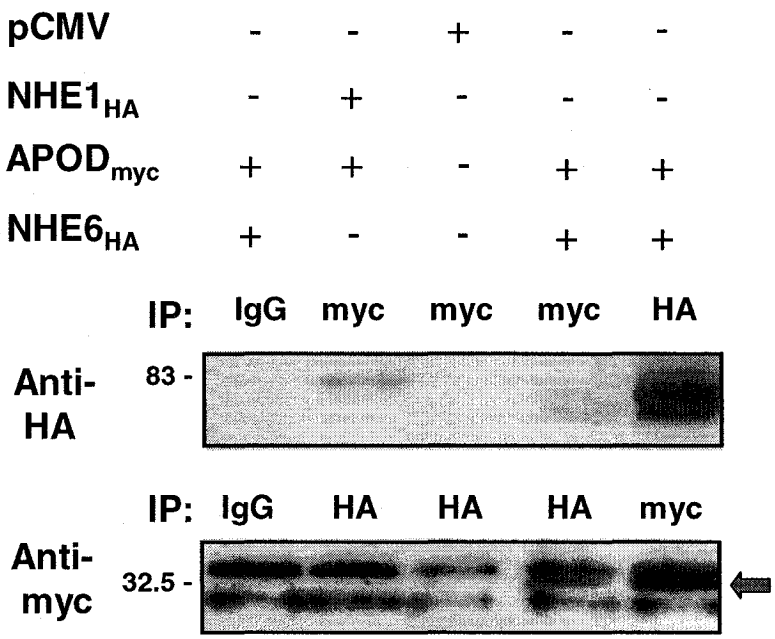
pCMV - - + - -
NHE1HA - + - - -
APODmyc + + - + +
NHE6HA + - - + +
IP: IgG myc myc myc HA
Anti-HA
83 -
IP: IgG HA HA HA myc
Anti-myc
32.5 -

B)

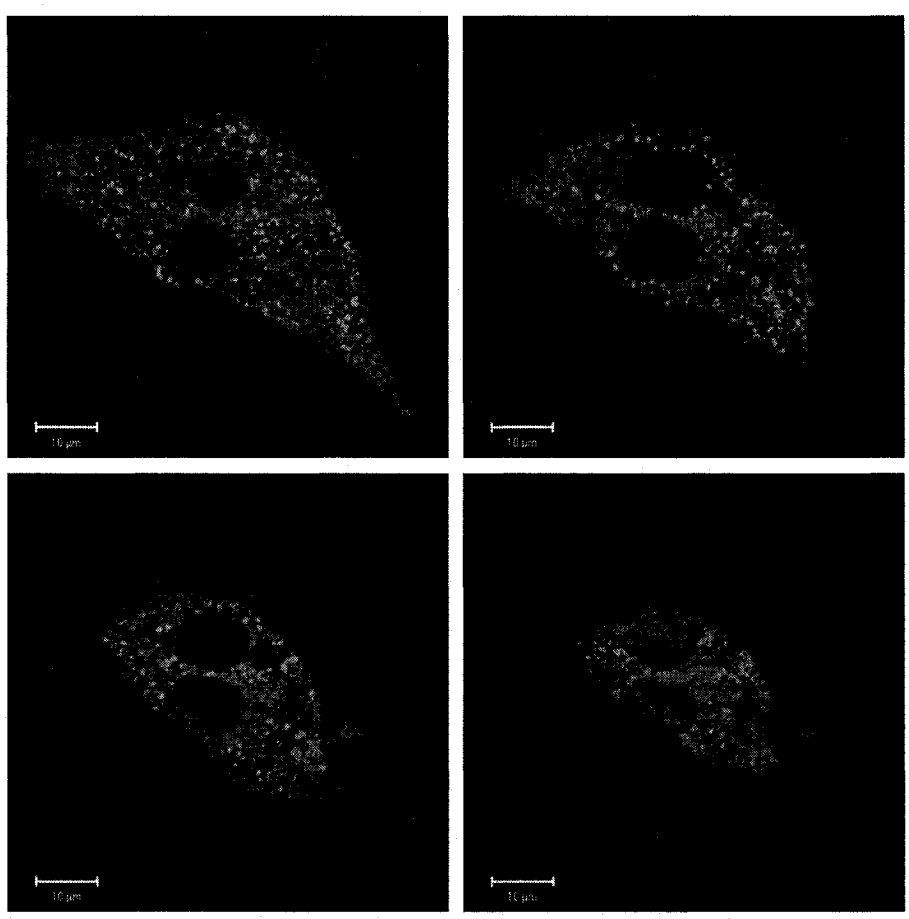

In an effort to answer this question, a different means of validating the interaction was used, namely to look for co-localization of the two proteins using laser scanning confocal microscopy. Figure 4B shows four slices at different depths of two CHO cells transiently co-transfected with $NHE6_{HA}$ and $APOD_{myc}$. No overlap of the two signals could be observed, as 24 h post-transfection, NHE6 and APOD localize in distinct set of vesicles. Considering that APOD is a secreted protein, it is presumably found in vesicles of the exocytic pathway. Knowing that APOD expression is increased in quiescent cells and presuming that the secreted protein will eventually get internalized through endocytosis, we expected to see some co-localization between $NHE6_{HA}$ and $APOD_{myc}$ in non-proliferating cells. To this end, CHO cells were co-transfected with both proteins and serum-free media was applied 24 h post-transfection. Cells were fixed and labeled 2, 4 and 6 days post-transfection and visualized using confocal microscopy. Contrary to our expectations, not one vesicle containing both proteins could be found and the APOD signal decreased with time (data not shown). A few possible explanations for this low APOD expression are that it significantly increases only after 2 to 3 weeks in HEK 293 cells (60) and/or that not all types of cells overexpress APOD at the same levels when subjected to stress conditions, such as serum starvation (60). The results from these co-localization experiments are inconclusive, as apolipoprotein D might well interact with NHE6 under appropriate physiological conditions which could not be reproduced in our experiments.

Taken together, these results suggest that under the experimental conditions used in this study, apolipoprotein D interacts weakly with NHE6 and that this interaction could be non-specific as indicated by a wide binding region, revealed by GST-fusion pull-downs, which overlaps with the cytosolic protein Rack1, and by an interaction with NHE1. Even though more questions have been raised than answered by these preliminary data, they constitute an important basis for the design of future experiments. Several approaches could be used to enhance the expression of apolipoprotein D and to mimic its activity in close to physiological conditions. For instance, COS cells, which have been shown to be good overexpressors of APOD when subjected to serum starvation (60) could be used. Alternatively, its levels could be increased by treating cells with dihydrotestosterone (DHT), dexamethasone (DEX) or retinoic acid, which have been

shown to stimulate APOD secretion (31,178), or simply by adding sufficient amounts of the purified protein to the cell culture media. Given that APOD was identified as an NHE6-interacting partner using a brain cDNA library and that it has been found in sites of peripheral nerve regeneration (35), it might be interesting to use native antibodies to monitor the levels of APOD and its possible association with NHE6 in human astrocytoma U373MG cells subject to post-injury recovery. It is not excluded that such experiments end up revealing that NHE6 assists in the internalization of APOD and its cargo, in particular cholesterol and its esters, thus contributing to post-injury nerve regeneration (35).

3.4 Interaction between NHE6 and ATP synthase, H^+ transporting, F1 complex, subunit α

It is puzzling that an important number of mitochondrial proteins were present in NHE6-associated complexes purified by TAP and M2P (Table 2), including transmembrane carrier proteins, ion channels and chaperones. Amongst all the mitochondrial proteins, only the ATP synthase, H^+ transporting, F1 complex, subunit α (ATP5α) was present in both TAP and M2P purifications. Even though, NHE6 was originally proposed to be a mitochondrial Na^+/H^+ exchanger (134), a number of studies provided evidence against this hypothesis (38,130). We were intrigued by this unexpected interaction between ATP5α and NHE6 and decided to further investigate it in quest of a novel function for one or both of these proteins.

As it name indicates, ATP5α is a subunit of the mitochondrial ATP synthase, responsible for the conversion of ADP to ATP driven by the translocation of H^+ from the intramembrane space to the mitochondrial matrix. The ATP synthase is made of two units: the F0 complex, situated in the inner mitochondrial membrane and the F1 complex, found in the space between the two mitochondrial membranes. The F1 complex functions as a stator and is composed of three α subunits alternating with three β subunits, which are anchored to the membrane via the a,b and δ subunits (1). The rotor consists of the F0 complex comprising the subunits γ, ε and c. The rotation of the γ subunit, driven by the proton flux, causes a deformation of the β subunit responsible for the binding and transformation of ADP to ATP (1). Interestingly, recent studies suggest that the function and location of the ATP synthase is not restricted to ATP-generation in mitochondria, since it was detected one the plasma membrane, where it can function as either ATP synthase or ATP hydrolase (18,115,128,145). Moreover, it was shown to act as a receptor for apolipoprotein A-I (115) and enterostatin (145) in addition to being inhibited by angiostatin (128).

The interaction between transfected $NHE6_{HA}$ and endogenous ATP5α was extensively studied by co-immunoprecipitation experiments in stably transfected AP-1 and HEK 293 cells, as well as in transiently transfected CHO cells. All the experiments resulted in a positive interaction between the two proteins irrespective of whether

antibodies against ATP5α or against the HA-epitope were used to immunoprecipitate. A representative western blot of these experiments is shown in Figure 6A. In this particular experiment, all the controls were negative, and this was not due to differences in immunoprecipitation efficiency or protein expression levels. However, in some experiments, NHE1 also showed to immunoprecipitate with ATP5α (data not shown), which raised a question about the specificity of the ATP5α-NHE6 interaction. To test this possibility, equal amounts of HA-tagged NHEs (except NHE4 and NHE7) were transfected in CHO cells and immunoprecipitated with an anti-HA antibody (data shown in Appendix D). When blotted against an anti-ATP5α antibody, $NHE6_{HA}$ gave the strongest signal, while NHE3, NHE5 and NHE9, which all coincidently transit or reside in recycling endosomes, gave moderate signals. The other NHEs and the controls showed no interaction with ATP5α. Even though these results suggest that the interaction of ATP5α is restricted to endosomal NHEs and most particularly to NHE6, this experiment was done but once and bears repeating before any definite conclusion is reached.

Virtually no co-localization between $NHE6_{HA}$ and endogenous ATP5α could be observed in $NHE6_{HA}$ stably expressing HEK 293 cells, in spite of the biochemical evidence for their interaction. Despite the absence of overlap, in most cells observed, NHE6-containing vesicles were found next to mitochondria, as if they were touching. This is nicely illustrated in Figure 6b, which shows several slices of the same cell. In addition, in a few locations, indicated by the arrows in the merged images, the two signals overlap. This piece of evidence is far from proving any real contact or exchange between mitochondria and vesicles of the endocytic pathway. Nonetheless, it supports the idea proposed by other researchers that in certain situations, such as in iron transport to the mitochondria, these two organelles could exchange material (212,229). Indeed, White et al discovered that haemoglobin deficient mice have an exon deletion in the gene Sec1511, which is homologous to the yeast vesicle docking protein SEC15 (212), this suggests that transport of iron from transferrin-containing vesicles to mitochondria requires vesicle docking. This observation is supported by the work of Zhang et al., who observed that the addition of Bafilomycin A1, which prevents endosomal acidification and consequently the dissociation of iron from the Tfn-R, and the inhibition of myosin light

Figure 6: Validating the interaction between $NHE6_{HA}$ and ATP5α by co-immunoprecipitation and immunofluorescence microscopy

A) Interaction between $NHE6_{HA}$ and ATP5α by co-immunoprecipitation. $NHE6_{HA}$ was transfected into CHO cells. Twenty four (24) hours post-transfection, the cells were lysed and polyclonal anti-HA or monoclonal anti-ATP5α antibodies were added to the pre-cleared lysates. A non-specific IgG antibody was used as a negative control. The immunoprecipitated proteins were separated by SDS-PAGE and transferred to PVDF membranes. The membranes were blotted with 1:8,000 monoclonal anti-ATP5α or 1:4,000 polyclonal anti-HA antibodies. The lysates contain $1/30^{th}$ of the total volume used for immunoprecipitation.

B) Cellular distribution of $NHE6_{HA}$ and endogenous ATP5α in $NHE6_{HA}$ stably expressing HEK 293 cells. The cells were grown on poly-L-lysine coated glass coverslips and fixed with 4% PFA. Upon permeabilization, the cells were dually labeled with a polyclonal anti-HA (1:1,000) and a monoclonal anti-ATP5α (1:300) primary antibodies, followed by an Alexa Fluor 488 (green)-conjugated anti-rabbit and an Alexa Fluor 568 (red) - conjugated anti-mouse secondary antibodies (1:2,000). Three representative images out of a z-stack containing a total of fifteen (15) slices are shown. Each slice is 6 μm thick and was obtained at a different cell depth with respect to the coverslip's contact surface: slice one is 2^{nd} of 15, slice two is 3^{rd} of 15 and slice three is 7^{th} of 15. The scale bar represents 5 μm.

A)

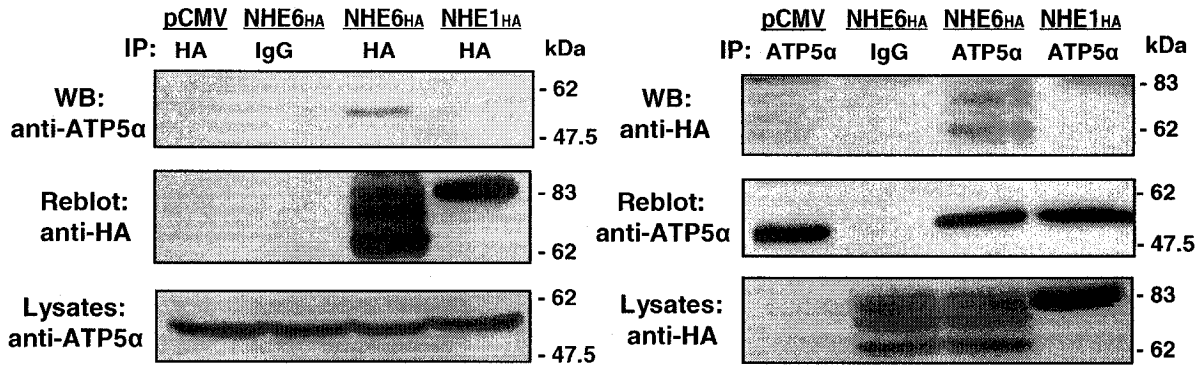
pCMV
NHE6HA
NHE6HA
NHE1HA
IP: HA
IgG
HA
HA
kDa
WB: anti-ATP5α
Reblot: anti-HA
Lysates: anti-ATP5α
- 62
- 47.5
- 83
- 62
- 62
- 47.5
pCMV
NHE6HA
NHE6HA
NHE1HA
IP: ATP5α
IgG
ATP5α
ATP5α
kDa
WB: anti-HA
Reblot: anti-ATP5α
Lysates: anti-HA
- 83
- 62
- 62
- 47.5
- 83
- 62

B)

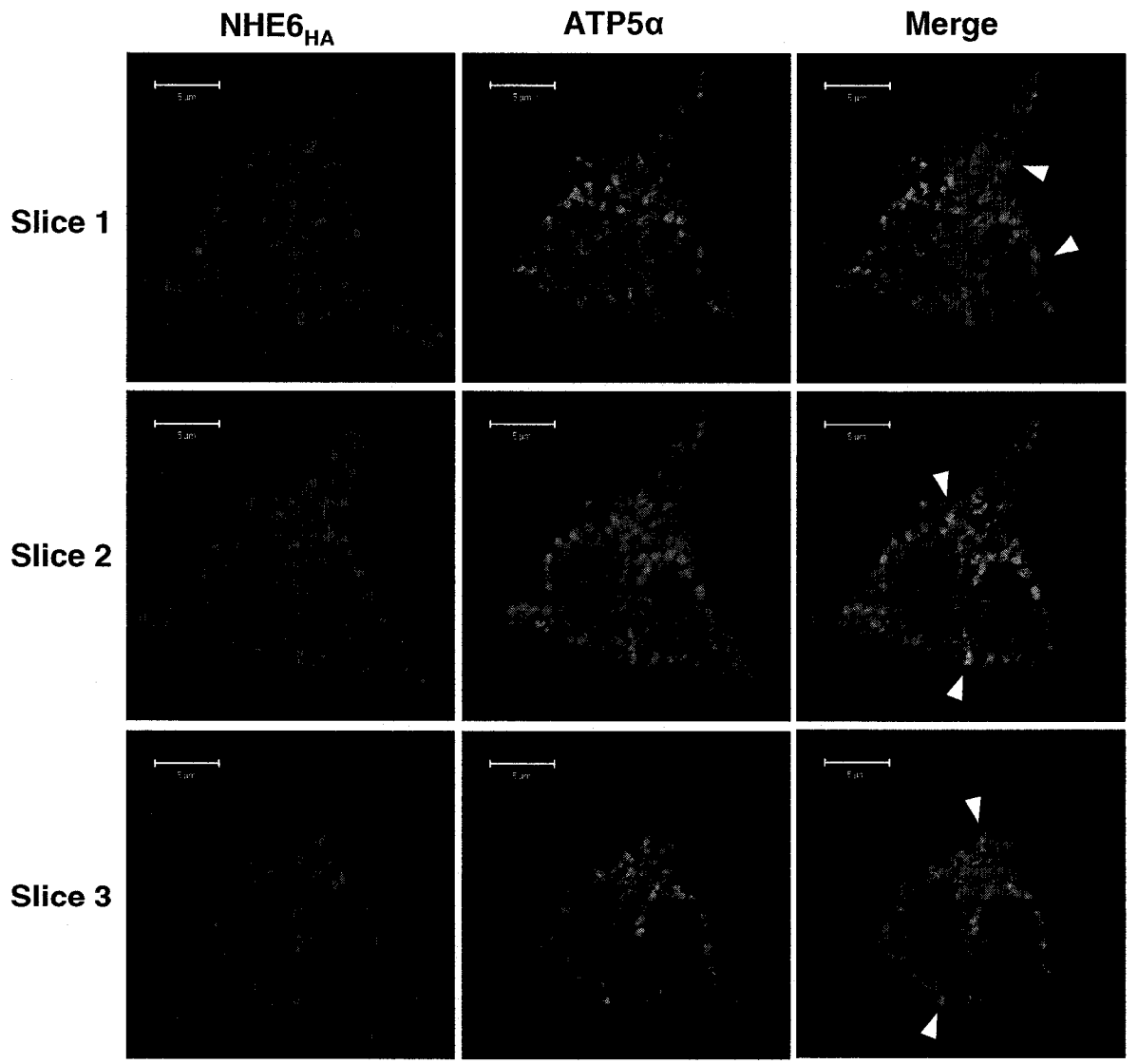
NHE6HA
ATP5α
Merge
Slice 1
Slice 2
Slice 3

chain kinase, involved in the movement of vesicles on microtubules, inhibited the transfer of endocytosed iron into heme (229). From these observations, and knowing that unlike other cell types, red blood cells do not accumulate cytosolic iron in the form of ferritin (2,156,163) Zhang et al. propose that the transfer of iron occurs through direct contact between endosomes and mitochondria in erythroid cells.

Even though the confocal microscopy images show that certain NHE6-containing endosomes are adjacent to and even touching mitochondria, this could not explain the interaction observed by immunoprecipitation. Considering that ATP5α is also found on the plasma membrane, co-localization studies were done on non-permeabilized cells to observe surface distribution of NHE6 and ATP5α. Unfortunately, these studies were not successful, as the signal for ATP5α was very weak, while the distribution of NHE6 seemed similar to its distribution in permeabilized cells (data not shown). The strong NHE6 signal could be caused by a partial permeabilization of the membrane by the PFA used for fixing, allowing the primary antibody to bind to vesicles underneath the plasma membrane. From these experiments, we could not determine if NHE6 and ATP5α interact on the cell surface.

To further characterize the interaction between NHE6 and ATP5α, we tested the binding of endogenous ATP5α from cell lysates with GST-fusion constructs of NHE6 C-tail fragments (Figure 7). A total of six GST-fusion constructs were tested, including the whole NHE6 tail. In addition, GST alone and NHE1 C-tail fused to GST were used as negative controls. The top panel in Figure 7, shows a stronger binding of ATP5α with NHE6 regulatory tail fragments of increasing size, up to amino acid 600 and no binding with the extremity of the C-tail. This variation in binding affinity is not caused by an uneven GST-fusion proteins or lysate loading (Figure 7, bottom two panels). From this data, one can deduce that the binding region of endogenous ATP5α from CHO lysates extends from the beginning of the regulatory tail (amino acid 499) of NHE6 up to amino acid 600, and that this entire fragment is necessary for efficient binding. This observation is not entirely supported by results obtained from a similar experiment done with HeLa lysates, which show the same binding region, but no increase in binding efficiency with growing fragment sizes. This suggests that the extremity of the C-tail, ranging from amino acids 499 to 523, might be sufficient for efficient binding. More in vitro binding

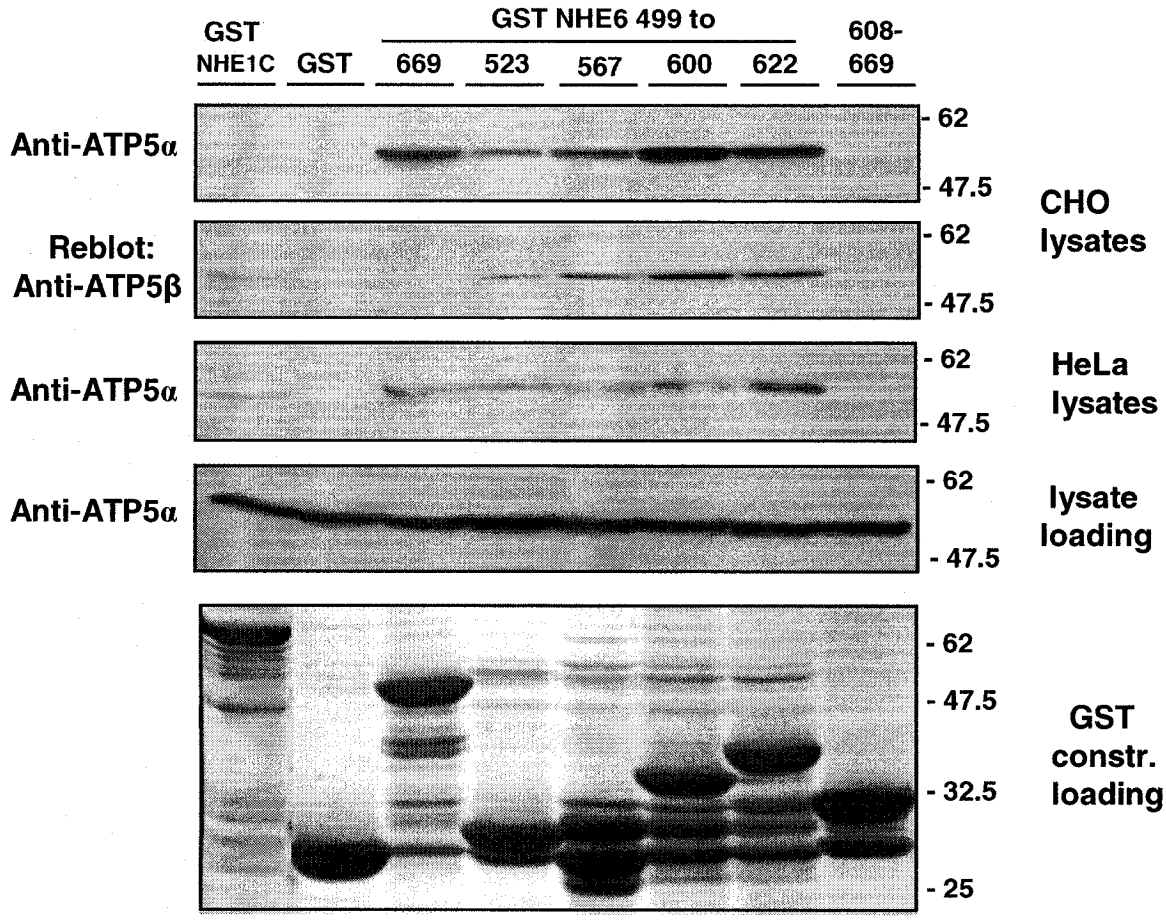

Figure 7: *In vitro* binding of ATP5α and ATP5β with GST-fusion constructs of NHE6 regulatory tail

Equal amounts of NHE6 C-tail GST-fusion constructs (bottom panel) were bound to Glutathione Sepharose beads during a two-hour incubation. Cell lysates (CHO or HeLa) from two (2) 10 cm dishes were added to each NHE6 C-tail GST-fusion construct and incubated overnight. After extensive washing, the protein samples were separated by SDS-PAGE and transferred to PVDF membranes. The membranes were blotted with endogenous anti-ATP5α (1:6,000) and anti-ATP5β (1:2,000) antibodies.

experiments with different GST-fusion constructs are currently being done to clarify this issue and determine the exact binding site. In addition, given that these experiments are done with cell lysates, it is impossible to say whether ATP5α binds directly to NHE6 C-tail or whether it does so through an intermediate within the same complex. One way to verify this would be through GST-binding studies with *in vitro* translated ATP5α.

Considering that we identified ATP5α as an NHE6-interacting protein via the TAP method, we expect that it does so in a protein complex. Upon examination of the results from the tandem affinity purification (Table 2), no other mitochondrial proteins, thus no other subunits of the ATP synthase, could be seen. It is possible that they were bound weakly and were lost through the numerous washes. Nonetheless, this is improbable, as they were not present even in the single step affinity purification using the M2 beads. We were also intrigued that the beta subunit did not show up in our immunoprecipitation experiments. Suspecting that *in vivo*, ATP5β does not interact with NHE6, we were curious to see if this still holds *in vitro*. To this end, we reblotted with an endogenous antibody against ATP5β the same membrane used for GST-fusion pull down experiments with ATP5α (Figure 7, second panel). We were perplexed to see a similar, although fainter, binding pattern to ATP5α, but no interaction of ATP5β with the whole NHE6 regulatory tail. At this stage, it is premature to draw definite conclusions from this observation, although, it is safe to assume that the ATP synthase alpha and beta subunits do not interact with NHE6 in the same way. It seems that ATP5α interacts with NHE6 separately from the ATP synthase complex, thus fulfilling some novel function.

This possibility was further investigated by performing cell fractionation through gravity centrifugation and looking for ATP5α in cell parts other than mitochondria, in particular the plasma membrane and the cytosol. Indeed, as previously mentioned, the ATP synthase is functional at the plasma membrane. In addition, its alpha subunit has a shorter splice variant, which gets translated from methionine 51 on and as a result lacks the mitochondrial targeting signal. We suspected that a certain fraction of the ATP5α is therefore not delivered to the mitochondria, but remains in the cytoplasm, where it fulfills a still-to-be-determined function. There is a precedent for ATP5α cytoplasmic accumulation associated with neurofibrillary degeneration in Alzheimer's disease, although it is unclear by what mechanism (177). To find if it accumulates in the

cytoplasm of other cells, we sheared CHO and HEK 293 cells by repeated passage through a 26.5 gauge needle and subjected the mixture to gravity centrifugation to separate the mitochondrial fraction from the plasma membrane and cytosolic fractions. Previous gravity centrifugation studies in our laboratory showed that the pellet obtained from a 10-min centrifugation at 6,000 g contains large organelles, including mitochondria (Virdee & Orlwoski, unpublished data). This fraction, called P6, therefore contains mitochondrial ATP5α. A subsequent 1-hour centrifugation at 100,000 g resulted in the separation of the plasma membranes (P100) from the cytosol (S100). Western blots of these lysate fractions using antibodies against α and β can be seen in Figure 8. As we expected, a signal for ATP5α, but not ATP5β was detected in the cytoplasm. However, we were surprised that the molecular weight of this cytoplasmic protein was 70 kDa and not 53 kDa. A possible explanation is that the anti-ATP5α antibody recognises a 70 kDa chaperone, which shares a high sequence similarity with ATP5α, since they have a common evolutionary origin (73). Furthermore, in the few *in vitro* binding studies of these cell fractions, no interaction could be detected between the cytosolic 70 kDa protein and GST-fused NHE6 C-tail (data not shown). Before reaching a definite conclusion about the nature of this cytoplasmic protein recognized by the anti- ATP5α antibody, more *in vitro* binding studies with increased amounts of the cytoplasmic fraction need to be done. In addition, this cytoplasmic protein could be immunoprecipitated using the anti- ATP5α antibody and its sequence determined by mass spectrometry. Other than in the cytoplasm, the ATP5α, but not the ATP5β is found in the P100 fractions from CHO and HEK 293 cells. This suggests that in some subcellular compartment, other than the mitochondria and the cytoplasm, the ATP5α functions independently of the ATP5β.

Overall, the results from the above experiments support the possibility that the alpha subunit of the mitochondrial ATP synthase interacts with the regulatory tail of NHE6 somewhere in the region spanning amino acids 499 to 600 and that it does so independently of the ATP5's beta subunit. This opens the possibility for a novel function of ATP5α in a cellular compartment other than the mitochondria. The localization of this ATP5α, as well as the reason behind its interaction with NHE6 remain to be revealed.

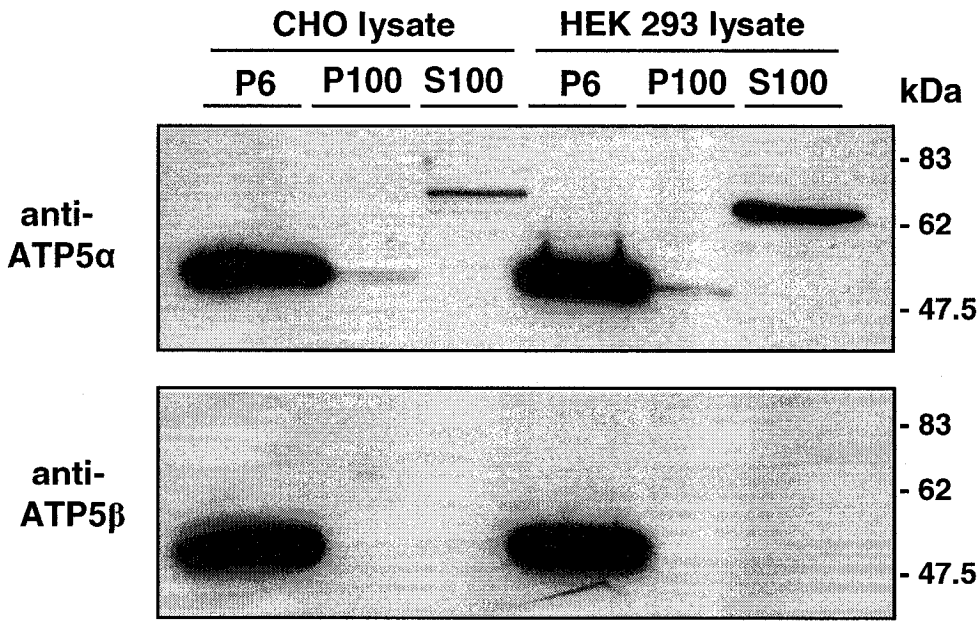

Figure 8: Distinct expressions of ATP5α and ATP5β in cell lysates fractions separated by differential gravity centrifugation

Cells were sheared by multiple passages through a 26.5 gauge syringe in an isotonic sucrose-containing solution. The liberated organelles and sheared membranes were subsequently separated through a series of consecutive gravity centrifugation steps. The fractured cells were first centrifuged at 700 g for 15 min to separate the nuclei from the remaining cell components. The resulting supernatant was then centrifuged for 10 min at 6,000 g to separate the bulky organelles, including mitochondria (**P6**) from the cytosol and fractionated membranes. The supernatant was then subjected to a final centrifugation of 1 h at 100,000 g to separate the cytoplasm (**S100**) from the membranes and light organelles (**P100**). Equal volume fractions of aliquots from each centrifugation step were separated by SDS-PAGE and blotted with anti-ATP5α (1:8,000) and anti-ATP5β (1:2,000) antibodies after transferring to PVDF membranes.

3.5 Interaction between NHE6 and myosin light chain kinase

Myosin light chain kinase (MLCK) was found in the final eluates from both the one-step affinity purification on the anti-FLAG M2 agarose beads (M2P) and the tandem affinity purification (Table 2). We were interested to investigate the interaction of NHE6 with MLCK mainly because of its regulatory function and the commercial availability of its specific inhibitor ML-7. These attributes of MLCK are advantageous as they allow broadening the range of experimental possibilities, considering that no functional assay for measuring NHE6 activity has been developed yet.

Myosin light chain kinase is activated upon the binding of Ca^{2+}/calmodulin (186) and phosphorylates Ser19 and Thr18 of the regulatory light chain (RLC) of myosin II (96). Myosins are a superfamily of motor proteins that hydrolyse ATP to generate unidirectional movement along actin filaments, causing muscle contraction, cytokinesis, movement of vesicles and even membrane trafficking and signal transduction (20,124). To date 17 different classes of myosins have been identified (45,92) among which myosin type II is the most extensively studied. Myosins contain a motor region, a neck region and a tail region. The motor region is highly conserved in all myosin classes and has an ATP-binding pocket and an actin-binding motif (61,160). The neck region is a helix of variable length, which has binding sites for myosin regulatory light chain and calmodulin (176). There is an extensive variability in the tail regions of different myosins and they are believed to determine the cellular localization and function of the myosin (176). Myosin heavy and regulatory light chains were present in NHE6-interacting complexes in the TAP experiment, but were considered as false positives, as they bound non-specifically to the beads in the control experiments. Nonetheless, given the presence of actin and calmodulin in the TAP eluates (Table 2), we supposed that NHE6 forms a complex with calmodulin, MLCK, myosin and actin and as a result participates in vesicle movement along actin filaments.

Prior to all other experiments on MLCK, the antibody against the endogenous MLCK was tested on CHO and HEK 293 cell lysates, to make sure that it recognises protein bands of the right size. There are many variants of the myosin light chain kinase of different molecular weights depending on species (135) and cell type (100). There are

two kinds of MLCK according to cell type: the skeletal muscle MLCK and the non-muscle, smooth muscle MLCK. The skeletal muscle MLCK, whose molecular weight varies between 75 and 90 kDa according to species (135), is composed of a kinase catalytic domain and a regulatory domain that contains Ca^{2+}/calmodulin-binding sites and autoinhibitory sequences (100). As it name indicates, its expression is restricted to skeletal muscle, while the non-muscle/smooth muscle type is expressed in skeletal, cardiac, smooth muscle and other tissues (90,110,233). Non-muscle and smooth muscle cells express several splice variants of MLCK (110), which can be subdivided into two types: a high molecular weight transcript of approximately 210 kDa and a low molecular weight one of 108-125 kDa (100). The short smooth muscle MLCK differs from the skeletal muscle MLCK in the sequence of its catalytic core and regulatory segment, in addition to having actin binding sites and three Ig domains (100). The long non-muscle MLCK includes the short MLCK plus a 900 amino acid N-terminal extension (206) containing two additional actin-binding motifs and six immunoglobulin (IgG) motifs (99). This 210 kDa form is the predominant MLCK in non-muscle and cultured cells (29,71,200). This coincides with our observations in cultured HEK 293 cells, which express the 210-kDa non-muscle MLCK at significantly higher levels than the shorter isoform (Figure 9A). Interestingly, the antibody recognized other bands, which could be the short non-muscle MLCK, transcript variants or non-specific proteins. There was no MLCK signal in CHO cells, indicating that it is either expressed at very low levels or that the antibody does not recognise MLCK from this species.

Several co-immunoprecipitation experiments were done to test the interaction between transiently or stably expressing $NHE6_{HA}$ and endogenous or transiently expressing GFP-tagged MLCK in HEK 293 cells. In all the experiments, an anti-HA antibody (monoclonal or polyclonal), was used to immunoprecipitate $NHE6_{HA}$ and the interacting MLCK was observed by blotting with a monoclonal anti-MLCK antibody. The reverse experiment was attempted, but the anti-MLCK antibody did not reveal itself to be potent for immunoprecipitation. There was variability in the strength of interaction between $NHE6_{HA}$ and MLCK, which could be attributed to the use of different batches of anti-HA antibodies or to the decreasing efficiency of the endogenous anti-MLCK antibody, as it was getting older. The strongest interaction between stably expressed

Figure 9: Validating the interaction between $NHE6_{HA}$ and MLCK by co-immunoprecipitation

A) Expression of different endogenous MLCK transcript variants in CHO (lane 1) and HEK 293 (lane 2) cells. Cell lysates were subjected to SDS-PAGE and endogenous MLCK was visualized by blotting with an anti-MLCK (1:7,000) antibody.

B) Co-immunoprecipitation of transiently co-transfected $NHE6_{HA}$ and $MLCK_{gfp}$ in HEK 293 cells. Two 10-cm dishes of confluent cells, per sample, were lysed and used for immunoprecipitation with a monoclonal anti-HA antibody (lane 2), or non-specific IgG (lane 1). The protein samples were subjected to SDS-PAGE and transferred to PVDF membranes. The signal was visualized by Western blotting with either a monoclonal anti-MLCK (1:5,000) antibody (top and middle panels) or a polyclonal anti-HA (1:4,000) antibody (lower panel).

C) Co-immunoprecipitation of stably expressed $NHE6_{HA}$ and endogenous MLCK in HEK 293 cells. Two 10-cm dishes of confluent cells, per sample, were lysed and used for immunoprecipitation with a monoclonal anti-HA antibody (lanes 2 and 6), or non-specific IgG (lane 4) as a negative control. The protein samples were subjected to SDS-PAGE and transferred to PVDF membranes. The signal was visualized by Western blotting with either a monoclonal anti-MLCK (1:7,000) (top panel) or a polyclonal anti-HA (1:3,000) antibody (bottom panel). Cells transfected with pCMV were used as a negative control (lanes 1 and 2).

A)

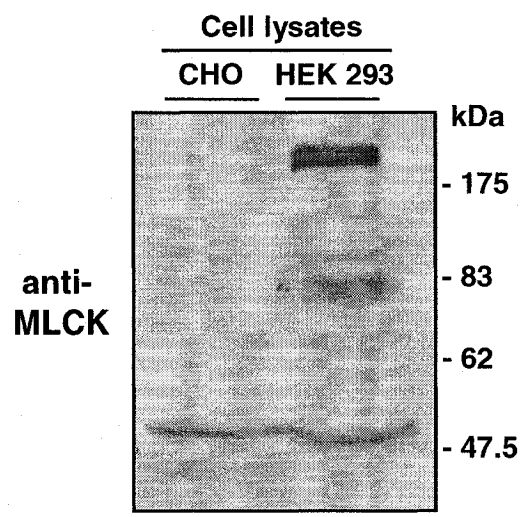
Cell lysates
CHO
HEK 293
kDa
anti-
MLCK
- 175
- 83
- 62
- 47.5

B)

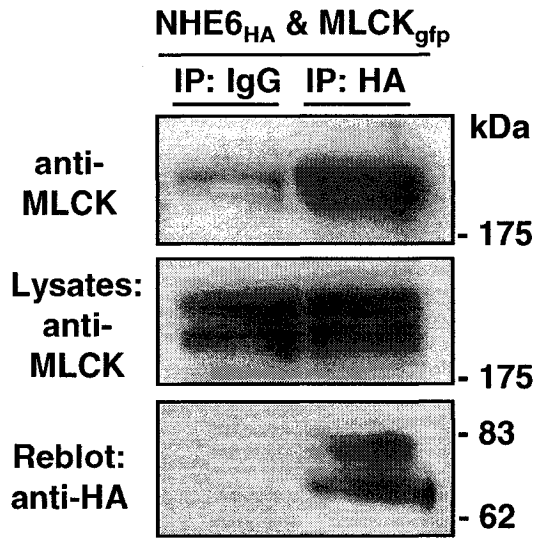
NHE6HA & MLCKgfp
IP: IgG
IP: HA
kDa
anti-
MLCK
- 175
Lysates:
anti-
MLCK
- 175
Reblot:
anti-HA
- 83
- 62

C)

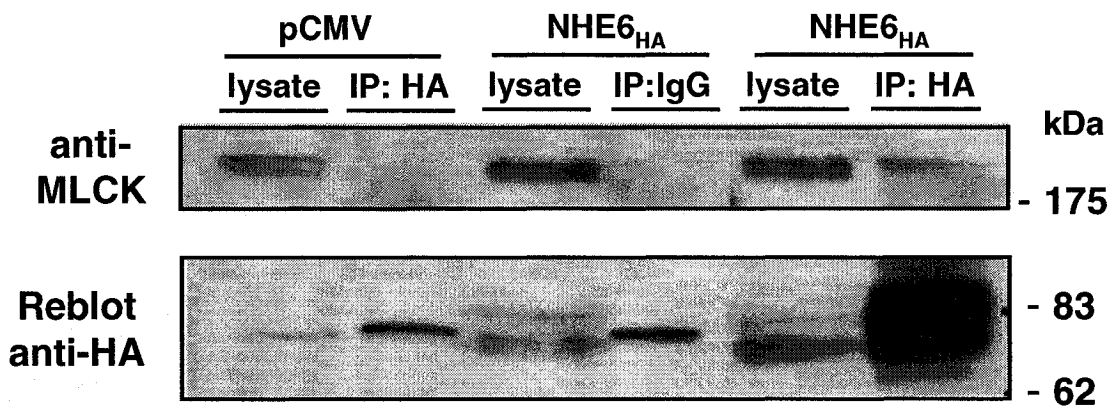
pCMV
NHE6HA
NHE6HA
lysate
IP: HA
lysate
IP:IgG
lysate
IP: HA
kDa
anti-
MLCK
- 175
Reblot
anti-HA
- 83
- 62

$NHE6_{HA}$ (clone 5 made for the TAP) and endogenous MLCK was observed when a monoclonal anti-HA antibody was used to immunoprecipitate (Figure 9C). This suggests that the monoclonal anti-HA antibody is better for immunoprecipitation than its polyclonal counterpart. When both $NHE6_{HA}$ and $MLCK_{gfp}$ were transiently transfected in HEK 293 cells, the immunoprecipitation signal was strong, but there was also a weaker signal in the control experiment, indicative of non-specific binding of myosin to the beads (Figure 9B). Such non-specific binding of myosin occurred in the earlier TAP/M2P experiments and is not uncommon.

The interaction between NHE6 and MLCK was tested in $NHE6_{HA}$ stably expressing HEK 293 cells with transiently transfected $MLCK_{gfp}$. Figure 10 shows representative localization of these proteins in four different cells. Considering that the cells were not confluent, the majority of them were very flat and had many processes as revealed by the distribution of the green fluorescent signal emitted by the MLCK presumably associated with the actin cytoskeleton. A small percentage of cells, like the cell in panel B exhibited a different MLCK localization pattern with virtually no protrusions. This cell could be in a different stage of the cell cycle, post-mitotic for instance. Indeed, the activity of the long MLCK has been shown to be cell-cycle dependent, as it is phosphorylated differently during interphase and mitosis (64) and displays two-fold decrease in activity during mitosis (157).

Figure 10B displays magnified sections of representative cells shown in panels B and C from Figure 10A. This closer look revealed that the localization pattern of some $NHE6_{HA}$-containing vesicles closely follows the MLCK signal and its associated actin fibers, especially in protrusions (Figure 10B, merged signals in panel a). In panel b in Figure 10B, even a yellow co-localization signal could be seen in certain parts of the cell. Overall, these confocal microscopy images indicate a close relationship between the cellular distributions of $NHE6_{HA}$ and $MLCK_{gfp}$ especially in plasma membrane protrusions.

The interaction between the two proteins was further tested by the use of the MLCK specific inhibitor ML-7 prior to fixing and labelling cells for microscopy or lysing cells for immunoprecipitations. The results from these experiments are shown if Figure 11. We expected to see a different distribution of $MLCK_{gfp}$, and consequently $NHE6_{HA}$

Figure 10: Subcellular localizations of $NHE6_{HA}$ and $MLCK_{gfp}$ visualized by immunofluorescence microscopy

A) $NHE6_{HA}$ stably expressing HEK 293 cells were transiently transfected with $MLCK_{gfp}$. The fixed and permeabilized cells were labeled with a monoclonal anti-HA (1:2,000) primary antibody, followed by an Alexa Fluor 568 (red) – conjugated anti-mouse (1:2,000) secondary antibody. Four representative images of different cells are shown. The scale bar represents 10 μm.

B) Selected parts from the images in panels **B** (image series **a** and **b**) and **C** (image series **c**) from **Figure 10 A)** were magnified for a better representation of regions where the signals for $NHE6_{HA}$ (red) and $MLCK_{gfp}$ (green) co-localize or follow similar patterns. The scale bars represent 2 μm for image series **a** and **b** and 5 μm for image series **c**.

A)

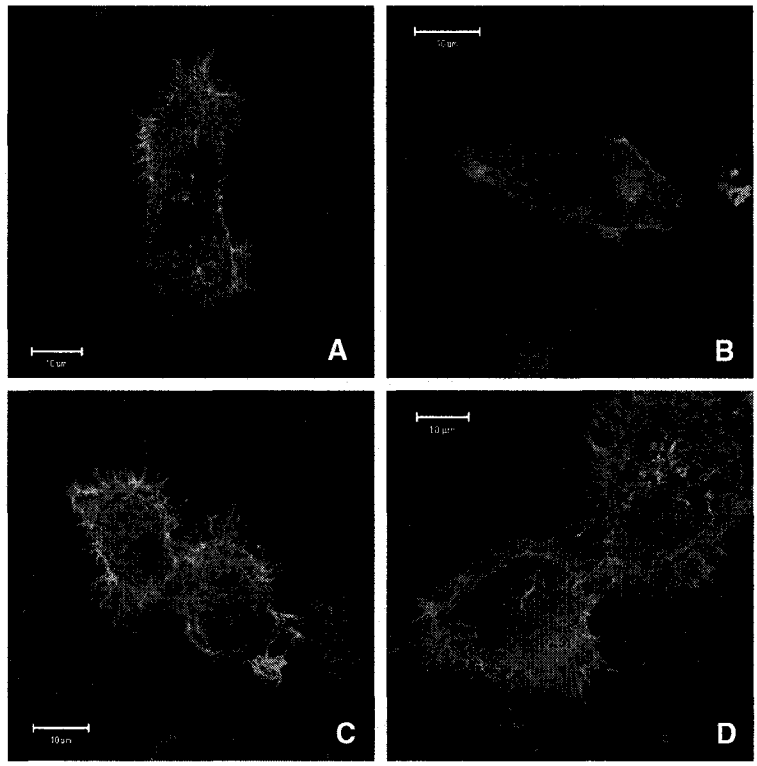

B)

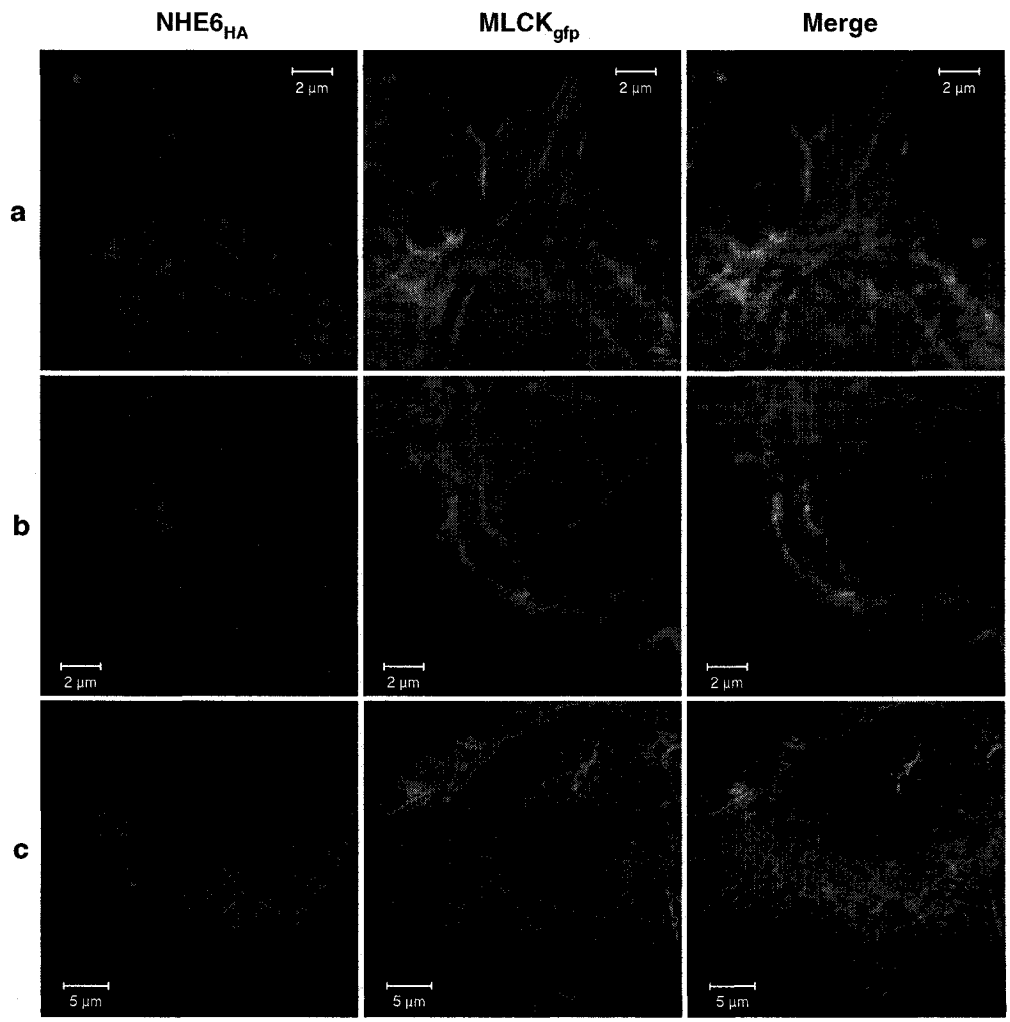

Figure 11: Effect of the MLCK-specific inhibitor ML-7 on the interaction between $MLCK_{gfp}$ and $NHE6_{HA}$

A) $NHE6_{HA}$ stably expressing HEK 293 cells were transiently transfected with $MLCK_{gfp}$. Twenty four (24) hours post-transfections, the cells were treated for 30 min with 30 μM of ML-7 (second series of images) or just DMSO (top series of images). The fixed and permeabilized cells were labeled with a monoclonal anti-HA (1:2,000) primary antibody, followed by an Alexa Fluor 568 (red) – conjugated anti-mouse (1:2,000) secondary antibody. For each condition, three representative 6 μm thick slices from a z-stack are shown. The images are presented starting with the closest image to the coverslip interface and going up through the cell. For the cells not treated with drug, slice 1 is 1st of 9, slice 2 is 3rd of 9 and slice 3 is 5th of 9. For the cells treated with ML-&, slice 1 is 1st of 6, slice 2 is 3rd of 6 and slice 3 is 5th of 6. The scale bar represents 10 μm.

B) $NHE6_{HA}$ and $MLCK_{gfp}$ were transiently co-transfected in HEK 293 cells. Twenty four (24) hours post-transfection, the cells were treated for 30 min with DMSO vehicle (lane 1) or with 30 μM of ML-7 (lanes 2 and 3). Two 10-cm dishes of confluent cells, per sample, were lysed and used for immunoprecipitation with a polyclonal anti-HA antibody (lanes 1 and 3), or non-specific IgG (lane 2) as a negative control. The protein samples were subjected to SDS-PAGE and transferred to PVDF membranes. The signal was visualized by Western blotting using a monoclonal anti-MLCK (1:5,000). Whole cell lysates show equal amounts of transfected $MLCK_{gfp}$ in each sample.

A)

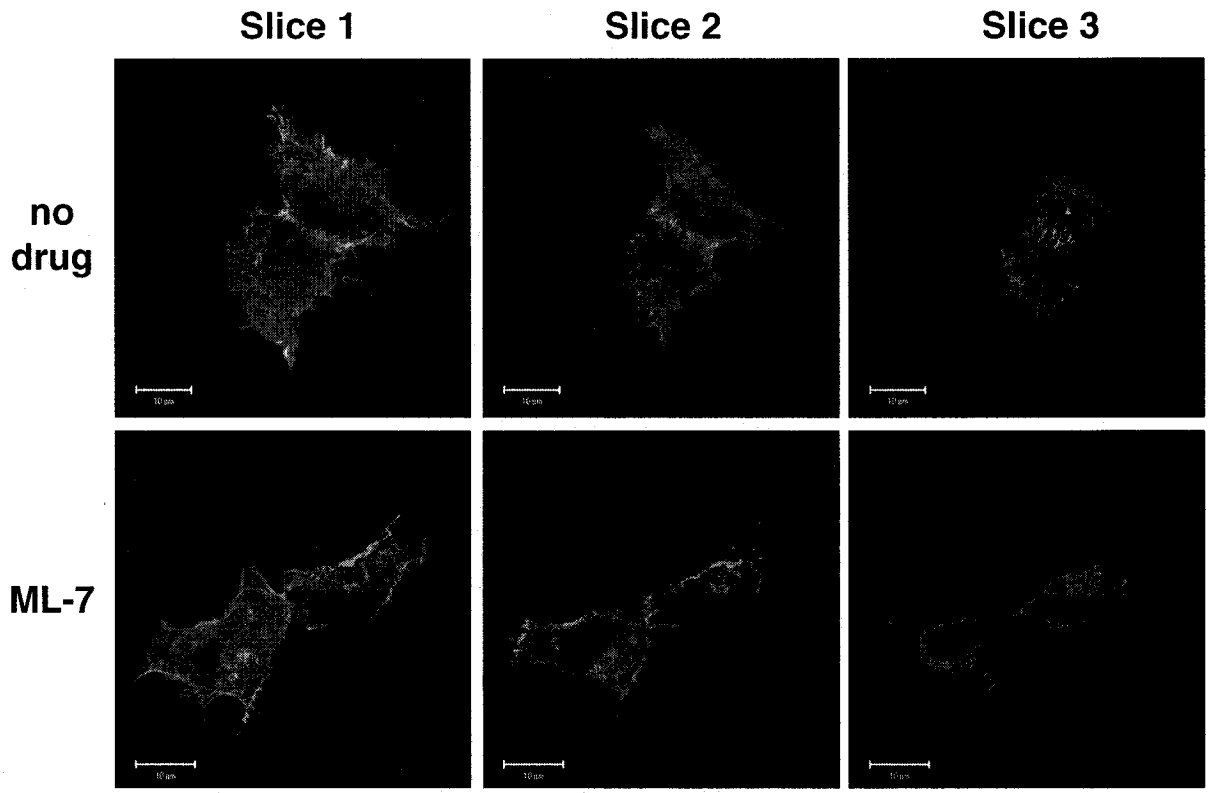
Slice 1
Slice 2
Slice 3
no drug
ML-7

B)

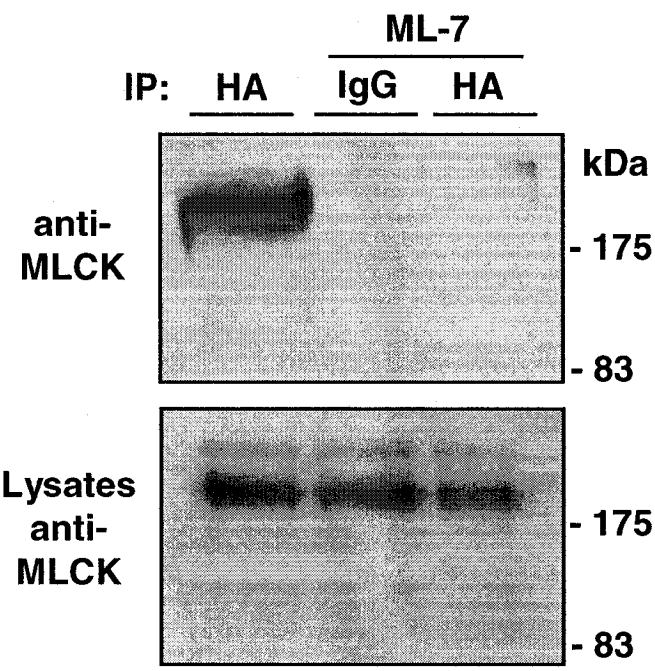
ML-7
IP: HA
IgG
HA
kDa
anti-MLCK
- 175
- 83
Lysates anti-MLCK
- 175
- 83

due to an impediment of myosin/actin – dependent cellular events, such as cytokinesis and vesicle trafficking. We were surprised to see that many cells seemed unaffected by the drug, as they were displaying normal cellular distributions of the two proteins. Nonetheless, we estimated that about 80% of the drug-treated cells had altered $MLCK_{gfp}$ and $NHE6_{HA}$ distributions, versus only about 10% of the untreated cells, by visually comparing eight randomly taken images for each condition (containing 10 to 20 cells each). Representative images for drug treated and untreated cells are shown in Figure 11A. The image selected to represent normal cell morphology is most likely a dividing cell, as it reveals intense $MLCK_{gfp}$ signal between the two cells. This would not be surprising, since the additional actin-binding motifs in the N-terminus of the 210-kDa MLCK likely confer stronger affinity to actin (105), which possibly leads to its targeting it to the cleavage furrow during mitosis (65,157). This is another piece of evidence supporting the idea of cell-cycle regulation of the 210-kDa MLCK. Even thought the cell is most likely dividing, the distribution of $NHE6_{HA}$-containing vesicles is extensively spread throughout the cell. Conversely, in the cells affected by the drug, the distribution of $NHE6_{HA}$ is dramatically altered, as it looks mostly confined to the perinuclear endocytic recycling compartment, while $MLCK_{gfp}$ signal is mostly localized at the cell periphery. Similar distribution was also observed in some cells not treated with ML-7 like previously shown in Figure 10A panel B. This intriguing observation draws a link between the activity of MLCK and the trafficking of $NHE6_{HA}$-containing vesicles, which is supported by preliminary immunoprecipitation data showing a loss of $NHE6_{HA}$-$MLCK_{gfp}$ interaction upon ML-7 treatment (Figure 11B).

Taken together, these results show a connection between the trafficking of $NHE6_{HA}$-containing vesicles and the activity of the non-muscle 210-kDa MLCK. Presumably, by regulating myosin II activity, MLCK controls the movement of NHE6-containing endosomes on actin filaments via a direct or indirect binding with NHE6. Considering that silencing of MLCK has been shown to block Tfn internalization (152) and that myosin VI is essential for clathrin-mediated endocytosis (40), it is entirely possible that MLCK also plays an important role in the endocytosis of NHE6.

SUMMARY AND FUTURE DIRECTIONS

In summary, we succeeded in developing and performing a tandem affinity purification method for the isolation of the integral membrane Na^+/H^+ exchanger isoform 6 and its associated protein complexes. A total of 30 NHE6-interacting proteins were identified by this method, four of which were studied further by co-immunoprecipitation from lysates of transfected cells, co-localization in intact transfected cells by confocal fluorescence microscopy and *in vitro* GST-fusion protein pull-down assays. Among these proteins, the ATP synthase, complex F1, subunit alpha and the myosin light chain kinase showed a positive interaction with NHE6, while ubiquitin and calmodulin showed no association when tested with two or more of the above methods. In addition, the same methods were used to assess the interaction between NHE6 and four of its putative interacting partners identified through a yeast two-hybrid screening of a brain cDNA library. Among these four, only apolipoprotein D exhibited weak and possibly non-specific binding to NHE6, while the data from the remaining three is still preliminary.

The alpha subunit of the mitochondrial ATP synthase showed convincing biochemical interaction with $NHE6_{HA}$ both in *in vitro* and *in vivo* binding assays, but these proteins exhibited little or no overlap when visualized by immunofluorescence microscopy. Our data indicate that the ATP5α binds within the first half of the NHE6 regulatory tail in the region spanning amino acids 499 to 600, and that it possibly acts independently of the ATP synthase complex. Other *in vitro* GST-fusion protein pull down assays are planned to determine the binding site more specifically. In addition, it would be useful to know if ATP5α binds directly to NHE6C tail or via an intermediate. This could be tested by GST-fusion pull-downs with *in vitro* translated ATP5α. Moreover, it would be useful to determine if NHE6 interacts with the shorter ATP5α transcript variant or with the small portions of ATP5α that was present in the membrane fractions. Currently, myc-tagged ATP5α constructs of both the long and short variants are being made for use in fractionation through gravity centrifugation and co-localization by confocal microscopy experiments in transiently transfected cells. Despite the compelling evidence for biochemical interaction between NHE6 and ATP5α, additional

experimental evidence is needed to provide a plausible physiological explanation for this interaction.

In addition to ATP5α, we observed an interaction between $NHE6_{HA}$ and both endogenous MLCK or transfected GFP-tagged MLCK. This interaction was disrupted by the specific MLCK inhibitor ML-7. It is therefore possible that NHE6 participates in the regulation of vesicle trafficking along actin filaments via a direct or indirect interaction with MLCK and its associated proteins. This protein complex, most likely includes actin, myosin light and heavy chains and calmodulin, which were all found in one form or another in the M2P/TAP experiments. Although myosin heavy and light chains were present as a non-specific binding proteins in the control purification experiments, given the presence of MLCK and actin, it is likely that myosin is a true NHE6-interacting protein. This could be verified by doing immunoprecipitation experiments with an endogenous anti-myosin antibody. It would be also interesting to verify if inactivation of MLCK via calmodulin inactivation would have similar effect on NHE6 distribution as the specific MLCK inhibitor ML-7. This could be done by performing the co-immunoprecipitation experiment in the presence of the Ca^{2+} chelator EGTA, which prevents calmodulin activation. Another useful experiment would be to label fixed cells with endogenous antibodies against tubulin, actin and NHE6 to see if and in what parts of the cell NHE6-containing vesicles are associated with each of these cytoskeletal proteins. It wouldn't be surprising to find NHE6 on microtubules, since β-tubulin and kinesin were found in the final eluates of the TAP/M2P experiments.

Finally, considering that the TAP and the traditional Y2H method did not result in the identification of the same NHE6-interacting proteins, it would be useful to try a different approach to search for NHE6-associated proteins, which might have been missed by these two methods. One such method is the dual membrane yeast two-hybrid system, which allows to screen full-length integral membrane proteins and membrane associated proteins in a more natural environment than the conventional Y2H. In addition, it makes possible the indentifiaction of transient or weak protein interactions, which is an advantage over the TAP.

LIST OF REFERENCES

1. **Ackerman, S. H. and A. Tzagoloff**. 2005. Function, structure, and biogenesis of mitochondrial ATP synthase. Prog.Nucleic Acid Res.Mol.Biol. **80**:95-133.

2. **Adams, M. L., I. Ostapiuk, and J. A. Grasso**. 1989. The effects of inhibition of heme synthesis on the intracellular localization of iron in rat reticulocytes. Biochim.Biophys.Acta **1012**:243-253.

3. **Aharonovitz, O., H. C. Zaun, T. Balla, J. D. York, J. Orlowski, and S. Grinstein**. 2000. Intracellular pH regulation by Na(+)/H(+) exchange requires phosphatidylinositol 4,5-bisphosphate. J.Cell Biol. **150**:213-224.

4. **Ahle, S., A. Mann, U. Eichelsbacher, and E. Ungewickell**. 1988. Structural relationships between clathrin assembly proteins from the Golgi and the plasma membrane. EMBO J. **7**:919-929.

5. **Akhter, S., O. Kovbasnjuk, X. Li, M. Cavet, J. Noel, M. Arpin, A. L. Hubbard, and M. Donowitz**. 2002. Na(+)/H(+) exchanger 3 is in large complexes in the center of the apical surface of proximal tubule-derived OK cells. Am.J.Physiol Cell Physiol **283**:C927-C940.

6. **Ali, R., C. L. Brett, S. Mukherjee, and R. Rao**. 2004. Inhibition of sodium/proton exchange by a Rab-GTPase-activating protein regulates endosomal traffic in yeast. J.Biol.Chem. **279**:4498-4506.

7. **Aniento, F., N. Emans, G. Griffiths, and J. Gruenberg**. 1993. Cytoplasmic dynein-dependent vesicular transport from early to late endosomes. J.Cell Biol. **123**:1373-1387.

8. **Apse, M. P., G. S. Aharon, W. A. Snedden, and E. Blumwald**. 1999. Salt tolerance conferred by overexpression of a vacuolar Na+/H+ antiport in Arabidopsis. Science **285**:1256-1258.

9. **Apse, M. P., J. B. Sottosanto, and E. Blumwald**. 2003. Vacuolar cation/H+ exchange, ion homeostasis, and leaf development are altered in a T-DNA insertional mutant of AtNHX1, the Arabidopsis vacuolar Na+/H+ antiporter. Plant J. **36**:229-239.

10. **Aronson, P. S.** 1985. Kinetic properties of the plasma membrane Na+-H+ exchanger. Annu.Rev.Physiol **47**:545-560.

11. **Aspinall, J. O., J. M. Bentel, D. J. Horsfall, D. E. Haagensen, V. R. Marshall, and W. D. Tilley**. 1995. Differential expression of apolipoprotein-D and prostate specific antigen in benign and malignant prostate tissues. J.Urol. **154**:622-628.

12. **Attaphitaya, S., K. Nehrke, and J. E. Melvin**. 2001. Acute inhibition of brain-specific Na(+)/H(+) exchanger isoform 5 by protein kinases A and C and cell shrinkage. Am.J.Physiol Cell Physiol **281**:C1146-C1157.

13. **Attaphitaya, S., K. Park, and J. E. Melvin**. 1999. Molecular cloning and functional expression of a rat Na+/H+ exchanger (NHE5) highly expressed in brain. J.Biol.Chem. **274**:4383-4388.

14. **Ayscough, K. R.** 2000. Endocytosis and the development of cell polarity in yeast require a dynamic F-actin cytoskeleton. Curr.Biol. **10**:1587-1590.

15. **Ayscough, K. R., J. Stryker, N. Pokala, M. Sanders, P. Crews, and D. G. Drubin**. 1997. High rates of actin filament turnover in budding yeast and roles for actin in establishment and maintenance of cell polarity revealed using the actin inhibitor latrunculin-A. J.Cell Biol. **137**:399-416.

16. **Azarani, A., D. Goltzman, and J. Orlowski**. 1995. Parathyroid hormone and parathyroid hormone-related peptide inhibit the apical Na+/H+ exchanger NHE-3 isoform in renal cells (OK) via a dual signaling cascade involving protein kinase A and C. J.Biol.Chem. **270**:20004-20010.

17. **Azarani, A., D. Goltzman, and J. Orlowski**. 1996. Structurally diverse N-terminal peptides of parathyroid hormone (PTH) and PTH-related peptide (PTHRP) inhibit the Na+/H+ exchanger NHE3 isoform by binding to the PTH/PTHRP receptor type I and activating distinct signaling pathways. J.Biol.Chem. **271**:14931-14936.

18. **Bae, T. J., M. S. Kim, J. W. Kim, B. W. Kim, H. J. Choo, J. W. Lee, K. B. Kim, C. S. Lee, J. H. Kim, S. Y. Chang, C. Y. Kang, S. W. Lee, and Y. G. Ko**. 2004. Lipid raft proteome reveals ATP synthase complex in the cell surface. Proteomics. **4**:3536-3548.

19. **Baird, N. R., J. Orlowski, E. Z. Szabo, H. C. Zaun, P. J. Schultheis, A. G. Menon, and G. E. Shull**. 1999. Molecular cloning, genomic organization, and functional expression of Na+/H+ exchanger isoform 5 (NHE5) from human brain. J.Biol.Chem. **274**:4377-4382.

20. **Baker, J. P. and M. A. Titus**. 1998. Myosins: matching functions with motors. Curr.Opin.Cell Biol. **10**:80-86.

21. **Beliveau, R., M. Demeule, and J. Strevey**. 1989. Transport studies with brush border membrane vesicles: choice of experimental parameters. Int.J.Biochem. **21**:955-960.

22. **Bell, S. M., C. M. Schreiner, P. J. Schultheis, M. L. Miller, R. L. Evans, C. V. Vorhees, G. E. Shull, and W. J. Scott**. 1999. Targeted disruption of the murine Nhe1 locus induces ataxia, growth retardation, and seizures. Am.J.Physiol **276**:C788-C795.

23. **Bennett, E. M., S. X. Lin, M. C. Towler, F. R. Maxfield, and F. M. Brodsky**. 2001. Clathrin hub expression affects early endosome distribution with minimal impact on receptor sorting and recycling. Mol.Biol.Cell **12**:2790-2799.

24. **Besson, P., F. Fernandez-Rachubinski, W. Yang, and L. Fliegel**. 1998. Regulation of Na+/H+ exchanger gene expression: mitogenic stimulation increases NHE1 promoter activity. Am.J.Physiol **274**:C831-C839.

25. **Biemesderfer, D., B. DeGray, and P. S. Aronson**. 1998. Membrane topology of NHE3. Epitopes within the carboxyl-terminal hydrophilic domain are exoplasmic. J.Biol.Chem. **273**:12391-12396.

26. **Biemesderfer, D., J. Pizzonia, A. bu-Alfa, M. Exner, R. Reilly, P. Igarashi, and P. S. Aronson**. 1993. NHE3: a Na+/H+ exchanger isoform of renal brush border. Am.J.Physiol **265**:F736-F742.

27. **Biemesderfer, D., R. F. Reilly, M. Exner, P. Igarashi, and P. S. Aronson**. 1992. Immunocytochemical characterization of Na(+)-H+ exchanger isoform NHE-1 in rabbit kidney. Am.J.Physiol **263**:F833-F840.

28. **Biemesderfer, D., P. A. Rutherford, T. Nagy, J. H. Pizzonia, A. K. bu-Alfa, and P. S. Aronson**. 1997. Monoclonal antibodies for high-resolution localization of NHE3 in adult and neonatal rat kidney. Am.J.Physiol **273**:F289-F299.

29. **Birukov, K. G., J. P. Schavocky, V. P. Shirinsky, M. V. Chibalina, L. J. Van Eldik, and D. M. Watterson**. 1998. Organization of the genetic locus for chicken myosin light chain kinase is complex: multiple proteins are encoded and exhibit differential expression and localization. J.Cell Biochem. **70**:402-413.

30. **Bkaily, G., M. Nader, L. Avedanian, D. Jacques, C. Perrault, D. bdel-Samad, P. Orleans-Juste, F. Gobeil, and K. M. Hazzouri**. 2004. Immunofluorescence revealed the presence of NHE-1 in the nuclear membranes of rat cardiomyocytes and isolated nuclei of human, rabbit, and rat aortic and liver tissues. Can.J.Physiol Pharmacol. **82**:805-811.

31. **Blais, Y., K. Sugimoto, M. C. Carriere, D. E. Haagensen, F. Labrie, and J. Simard**. 1994. Potent stimulatory effect of interleukin-1 alpha on apolipoprotein D and gross cystic disease fluid protein-15 expression in human breast-cancer cells. Int.J.Cancer **59**:400-407.

32. **Borghini, I., F. Barja, D. Pometta, and R. W. James**. 1995. Characterization of subpopulations of lipoprotein particles isolated from human cerebrospinal fluid. Biochim.Biophys.Acta **1255**:192-200.

33. **Boron, W. F. and E. L. Boulpaep**. 1983. Intracellular pH regulation in the renal proximal tubule of the salamander. Na-H exchange. J.Gen.Physiol **81**:29-52.

34. **Bowers, K., B. P. Levi, F. I. Patel, and T. H. Stevens**. 2000. The sodium/proton exchanger Nhx1p is required for endosomal protein trafficking in the yeast Saccharomyces cerevisiae. Mol.Biol.Cell **11**:4277-4294.

35. **Boyles, J. K., L. M. Notterpek, and L. J. Anderson**. 1990. Accumulation of apolipoproteins in the regenerating and remyelinating mammalian peripheral nerve. Identification of apolipoprotein D, apolipoprotein A-IV, apolipoprotein E, and apolipoprotein A-I. J.Biol.Chem. **265**:17805-17815.

36. **Brett, C. L., M. Donowitz, and R. Rao**. 2005. Evolutionary origins of eukaryotic sodium/proton exchangers. Am.J.Physiol Cell Physiol **288**:C223-C239.

37. **Brett, C. L., D. N. Tukaye, S. Mukherjee, and R. Rao**. 2005. The yeast endosomal Na+K+/H+ exchanger Nhx1 regulates cellular pH to control vesicle trafficking. Mol.Biol.Cell **16**:1396-1405.

38. **Brett, C. L., Y. Wei, M. Donowitz, and R. Rao**. 2002. Human Na(+)/H(+) exchanger isoform 6 is found in recycling endosomes of cells, not in mitochondria. Am.J.Physiol Cell Physiol **282**:C1031-C1041.

39. **Brini, M. and E. Carafoli**. 2000. Calcium signalling: a historical account, recent developments and future perspectives. Cell Mol.Life Sci. **57**:354-370.

40. **Buss, F., J. P. Luzio, and J. Kendrick-Jones**. 2002. Myosin VI, an actin motor for membrane traffic and cell migration. Traffic. **3**:851-858.

41. **Chambrey, R., J. P. St, D. Eladari, F. Quentin, D. G. Warnock, D. R. Abrahamson, R. A. Podevin, and M. Paillard**. 2001. Localization and functional characterization of Na+/H+ exchanger isoform NHE4 in rat thick ascending limbs. Am.J.Physiol Renal Physiol **281**:F707-F717.

42. **Chang, M. P., W. G. Mallet, K. E. Mostov, and F. M. Brodsky**. 1993. Adaptor self-aggregation, adaptor-receptor recognition and binding of alpha-adaptin subunits to the plasma membrane contribute to recruitment of adaptor (AP2) components of clathrin-coated pits. EMBO J. **12**:2169-2180.

43. **Chen, W., Y. Feng, D. Chen, and A. Wandinger-Ness**. 1998. Rab11 is required for trans-golgi network-to-plasma membrane transport and a preferential target for GDP dissociation inhibitor. Mol.Biol.Cell **9**:3241-3257.

44. **Chow, C. W.** 1999. Regulation and intracellular localization of the epithelial isoforms of the Na+/H+ exchangers NHE2 and NHE3. Clin.Invest Med. **22**:195-206.

45. **Cope, M. J., J. Whisstock, I. Rayment, and J. Kendrick-Jones**. 1996. Conservation within the myosin motor domain: implications for structure and function. Structure. **4**:969-987.

46. **Counillon, L., A. Franchi, and J. Pouyssegur**. 1993. A point mutation of the Na+/H+ exchanger gene (NHE1) and amplification of the mutated allele confer amiloride resistance upon chronic acidosis. Proc.Natl.Acad.Sci.U.S.A **90**:4508-4512.

47. **Counillon, L., J. Noel, R. A. Reithmeier, and J. Pouyssegur**. 1997. Random mutagenesis reveals a novel site involved in inhibitor interaction within the fourth transmembrane segment of the Na+/H+ exchanger-1. Biochemistry **36**:2951-2959.

48. **Counillon, L. and J. Pouyssegur**. 2000. The expanding family of eucaryotic Na(+)/H(+) exchangers. J.Biol.Chem. **275**:1-4.

49. **Counillon, L., J. Pouyssegur, and R. A. Reithmeier**. 1994. The Na+/H+ exchanger NHE-1 possesses N- and O-linked glycosylation restricted to the first N-terminal extracellular domain. Biochemistry **33**:10463-10469.

50. **Counillon, L., W. Scholz, H. J. Lang, and J. Pouyssegur**. 1993. Pharmacological characterization of stably transfected Na+/H+ antiporter isoforms using amiloride analogs and a new inhibitor exhibiting anti-ischemic properties. Mol.Pharmacol. **44**:1041-1045.

51. **D'Souza, S., A. Garcia-Cabado, F. Yu, K. Teter, G. Lukacs, K. Skorecki, H. P. Moore, J. Orlowski, and S. Grinstein**. 1998. The epithelial sodium-hydrogen antiporter Na+/H+ exchanger 3 accumulates and is functional in recycling endosomes. J.Biol.Chem. **273**:2035-2043.

52. **Darley, C. P., O. C. van Wuytswinkel, W. K. van der, W. H. Mager, and A. H. de Boer**. 2000. Arabidopsis thaliana and Saccharomyces cerevisiae NHX1 genes encode amiloride sensitive electroneutral Na+/H+ exchangers. Biochem.J. **351**:241-249.

53. **Daro, E., S. P. van der, T. Galli, and I. Mellman**. 1996. Rab4 and cellubrevin define different early endosome populations on the pathway of transferrin receptor recycling. Proc.Natl.Acad.Sci.U.S.A **93**:9559-9564.

54. **de Silva, M. G., K. Elliott, H. H. Dahl, E. Fitzpatrick, S. Wilcox, M. Delatycki, R. Williamson, D. Efron, M. Lynch, and S. Forrest**. 2003. Disruption of a novel member of a sodium/hydrogen exchanger family and DOCK3 is associated with an attention deficit hyperactivity disorder-like phenotype. J.Med.Genet. **40**:733-740.

55. **Demaurex, N.** 2002. pH Homeostasis of cellular organelles. News Physiol Sci. **17**:1-5.

56. **Demaurex, N., W. Furuya, S. D'Souza, J. S. Bonifacino, and S. Grinstein**. 1998. Mechanism of acidification of the trans-Golgi network (TGN). In situ measurements of pH using retrieval of TGN38 and furin from the cell surface. J.Biol.Chem. **273**:2044-2051.

57. **Denker, S. P. and D. L. Barber**. 2002. Cell migration requires both ion translocation and cytoskeletal anchoring by the Na-H exchanger NHE1. J.Cell Biol. **159**:1087-1096.

58. **Denker, S. P. and D. L. Barber**. 2002. Ion transport proteins anchor and regulate the cytoskeleton. Curr.Opin.Cell Biol. **14**:214-220.

59. **Denker, S. P., D. C. Huang, J. Orlowski, H. Furthmayr, and D. L. Barber**. 2000. Direct binding of the Na--H exchanger NHE1 to ERM proteins regulates the cortical cytoskeleton and cell shape independently of H(+) translocation. Mol.Cell **6**:1425-1436.

60. **Do, C. S., D. Seguin, R. Milne, and E. Rassart**. 2002. Modulation of apolipoprotein D and apolipoprotein E mRNA expression by growth arrest and identification of key elements in the promoter. J.Biol.Chem. **277**:5514-5523.

61. **Dominguez, R., Y. Freyzon, K. M. Trybus, and C. Cohen**. 1998. Crystal structure of a vertebrate smooth muscle myosin motor domain and its complex with the essential light chain: visualization of the pre-power stroke state. Cell **94**:559-571.

62. **Dransfield, D. T., A. J. Bradford, J. Smith, M. Martin, C. Roy, P. H. Mangeat, and J. R. Goldenring**. 1997. Ezrin is a cyclic AMP-dependent protein kinase anchoring protein. EMBO J. **16**:35-43.

63. **Drayna, D., C. Fielding, J. McLean, B. Baer, G. Castro, E. Chen, L. Comstock, W. Henzel, W. Kohr, L. Rhee, and .** 1986. Cloning and expression of human apolipoprotein D cDNA. J.Biol.Chem. **261**:16535-16539.

64. **Dulyaninova, N. G. and A. R. Bresnick**. 2004. The long myosin light chain kinase is differentially phosphorylated during interphase and mitosis. Exp.Cell Res. **299**:303-314.

65. **Dulyaninova, N. G., Y. V. Patskovsky, and A. R. Bresnick**. 2004. The N-terminus of the long MLCK induces a disruption in normal spindle morphology and metaphase arrest. J.Cell Sci. **117**:1481-1493.

66. **Dumas, J. J., E. Merithew, E. Sudharshan, D. Rajamani, S. Hayes, D. Lawe, S. Corvera, and D. G. Lambright**. 2001. Multivalent endosome targeting by homodimeric EEA1. Mol.Cell **8**:947-958.

67. **Dunn, K. W., T. E. McGraw, and F. R. Maxfield**. 1989. Iterative fractionation of recycling receptors from lysosomally destined ligands in an early sorting endosome. J.Cell Biol. **109**:3303-3314.

68. **Dziembowski, A. and B. Seraphin**. 2004. Recent developments in the analysis of protein complexes. FEBS Lett. **556**:1-6.

69. **Fafournoux, P., J. Noel, and J. Pouyssegur**. 1994. Evidence that Na+/H+ exchanger isoforms NHE1 and NHE3 exist as stable dimers in membranes with a high degree of specificity for homodimers. J.Biol.Chem. **269**:2589-2596.

70. **Farinas, J. and A. S. Verkman**. 1999. Receptor-mediated targeting of fluorescent probes in living cells. J.Biol.Chem. **274**:7603-7606.

71. **Fisher, S. A. and M. Ikebe**. 1995. Developmental and tissue distribution of expression of nonmuscle and smooth muscle isoforms of myosin light chain kinase. Biochem.Biophys.Res.Commun. **217**:696-703.

72. **Fliegel, L., R. Murtazina, P. Dibrov, C. Harris, A. Moor, and F. A. Fernandez-Rachubinski**. 1998. Regulation and characterization of the Na+/H+ exchanger. Biochem.Cell Biol. **76**:735-741.

73. **Flores, A. I. and J. M. Cuezva**. 1997. Identification of sequence similarity between 60 kDa and 70 kDa molecular chaperones: evidence for a common evolutionary background? Biochem.J. **322 (Pt 2)**:641-647.

74. **Gagescu, R., N. Demaurex, R. G. Parton, W. Hunziker, L. A. Huber, and J. Gruenberg**. 2000. The recycling endosome of Madin-Darby canine kidney cells is a mildly acidic compartment rich in raft components. Mol.Biol.Cell **11**:2775-2791.

75. **Gekle, M., K. Drumm, S. Mildenberger, R. Freudinger, B. Gassner, and S. Silbernagl**. 1999. Inhibition of Na+-H+ exchange impairs receptor-mediated albumin endocytosis in renal proximal tubule-derived epithelial cells from opossum. J.Physiol **520 Pt 3**:709-721.

76. **Gingras, A. C., M. Caballero, M. Zarske, A. Sanchez, T. R. Hazbun, S. Fields, N. Sonenberg, E. Hafen, B. Raught, and R. Aebersold**. 2005. A novel, evolutionarily conserved protein phosphatase complex involved in cisplatin sensitivity. Mol.Cell Proteomics. **4**:1725-1740.

77. **Gottlieb, T. A., I. E. Ivanov, M. Adesnik, and D. D. Sabatini**. 1993. Actin microfilaments play a critical role in endocytosis at the apical but not the basolateral surface of polarized epithelial cells. J.Cell Biol. **120**:695-710.

78. **Goyal, S., S. Mentone, and P. S. Aronson**. 2005. Immunolocalization of NHE8 in rat kidney. Am.J.Physiol Renal Physiol **288**:F530-F538.

79. **Goyal, S., H. G. Vanden, and P. S. Aronson**. 2003. Renal expression of novel Na+/H+ exchanger isoform NHE8. Am.J.Physiol Renal Physiol **284**:F467-F473.

80. **Grabe, M. and G. Oster**. 2001. Regulation of organelle acidity. J.Gen.Physiol **117**:329-344.

81. **Grinstein, S., C. A. Clarke, and A. Rothstein**. 1983. Activation of Na+/H+ exchange in lymphocytes by osmotically induced volume changes and by cytoplasmic acidification. J.Gen.Physiol **82**:619-638.

82. **Grinstein, S., D. Rotin, and M. J. Mason**. 1989. Na+/H+ exchange and growth factor-induced cytosolic pH changes. Role in cellular proliferation. Biochim.Biophys.Acta **988**:73-97.

83. **Grinstein, S., M. Woodside, T. K. Waddell, G. P. Downey, J. Orlowski, J. Pouyssegur, D. C. Wong, and J. K. Foskett**. 1993. Focal localization of the NHE-1 isoform of the Na+/H+ antiport: assessment of effects on intracellular pH. EMBO J. **12**:5209-5218.

84. **Gruwel, M. L., V. L. Rauw, M. Loewen, and S. R. Abrams**. 2001. Effects of Sodium Chloride on plant cells; a 31P and 23Na NMR system to study salt tolerance. Plant Sci. **160**:785-794.

85. **Gu, X. Q., H. Yao, and G. G. Haddad**. 2001. Increased neuronal excitability and seizures in the Na(+)/H(+) exchanger null mutant mouse. Am.J.Physiol Cell Physiol **281**:C496-C503.

86. **Haagensen, D. E. and G. Mazoujian**. 1986. Biochemistry and immunohistochemistry of fluid proteins of the breast in gross cystic disease, p. 474. *In* Diseases of the Breast. Philadelphia.

87. **Harper, J. F., B. Hong, I. Hwang, H. Q. Guo, R. Stoddard, J. F. Huang, M. G. Palmgren, and H. Sze**. 1998. A novel calmodulin-regulated Ca2+-ATPase (ACA2) from Arabidopsis with an N-terminal autoinhibitory domain. J.Biol.Chem. **273**:1099-1106.

88. **Haworth, R. S., O. Frohlich, and L. Fliegel**. 1993. Multiple carbohydrate moieties on the Na+/H+ exchanger. Biochem.J. **289 (Pt 3)**:637-640.

89. **Hayashi, H., K. Szaszi, N. Coady-Osberg, W. Furuya, A. P. Bretscher, J. Orlowski, and S. Grinstein**. 2004. Inhibition and redistribution of NHE3, the apical Na+/H+ exchanger, by Clostridium difficile toxin B. J.Gen.Physiol **123**:491-504.

90. **Herring, B. P., S. Dixon, and P. J. Gallagher**. 2000. Smooth muscle myosin light chain kinase expression in cardiac and skeletal muscle. Am.J.Physiol Cell Physiol **279**:C1656-C1664.

91. **Hisamitsu, T., T. Pang, M. Shigekawa, and S. Wakabayashi**. 2004. Dimeric interaction between the cytoplasmic domains of the Na+/H+ exchanger NHE1 revealed by symmetrical intermolecular cross-linking and selective co-immunoprecipitation. Biochemistry **43**:11135-11143.

92. **Hodge, T. and M. J. Cope**. 2000. A myosin family tree. J.Cell Sci. **113 Pt 19**:3353-3354.

93. **Hoogerwerf, W. A., S. C. Tsao, O. Devuyst, S. A. Levine, C. H. Yun, J. W. Yip, M. E. Cohen, P. D. Wilson, A. J. Lazenby, C. M. Tse, and M. Donowitz**. 1996. NHE2 and NHE3 are human and rabbit intestinal brush-border proteins. Am.J.Physiol **270**:G29-G41.

94. **Hopkins, C. R.** 1983. Intracellular routing of transferrin and transferrin receptors in epidermoid carcinoma A431 cells. Cell **35**:321-330.

95. **Hu, M. C., L. Fan, L. A. Crowder, Z. Karim-Jimenez, H. Murer, and O. W. Moe**. 2001. Dopamine acutely stimulates Na+/H+ exchanger (NHE3) endocytosis via clathrin-coated vesicles: dependence on protein kinase A-mediated NHE3 phosphorylation. J.Biol.Chem. **276**:26906-26915.

96. **Ikebe, M. and D. J. Hartshorne**. 1985. Phosphorylation of smooth muscle myosin at two distinct sites by myosin light chain kinase. J.Biol.Chem. **260**:10027-10031.

97. **Johnson, L. S., K. W. Dunn, B. Pytowski, and T. E. McGraw**. 1993. Endosome acidification and receptor trafficking: bafilomycin A1 slows receptor externalization by a mechanism involving the receptor's internalization motif. Mol.Biol.Cell **4**:1251-1266.

98. **Kaksonen, M., C. P. Toret, and D. G. Drubin**. 2006. Harnessing actin dynamics for clathrin-mediated endocytosis. Nat.Rev.Mol.Cell Biol. **7**:404-414.

99. **Kamm, K. E. and J. T. Stull**. 1985. The function of myosin and myosin light chain kinase phosphorylation in smooth muscle. Annu.Rev.Pharmacol.Toxicol. **25**:593-620.

100. **Kamm, K. E. and J. T. Stull**. 2001. Dedicated myosin light chain kinases with diverse cellular functions. J.Biol.Chem. **276**:4527-4530.

101. **Khadilkar, A., P. Iannuzzi, and J. Orlowski**. 2001. Identification of sites in the second exomembrane loop and ninth transmembrane helix of the mammalian Na+/H+ exchanger important for drug recognition and cation translocation. J.Biol.Chem. **276**:43792-43800.

102. **Khan, I.** 2001. Topology of the C-terminus of sodium hydrogen exchanger isoform-1: presence of an extracellular epitope. Arch.Biochem.Biophys. **391**:25-29.

103. **Kim, J. H., L. Johannes, B. Goud, C. Antony, C. A. Lingwood, R. Daneman, and S. Grinstein**. 1998. Noninvasive measurement of the pH of the endoplasmic reticulum at rest and during calcium release. Proc.Natl.Acad.Sci.U.S.A **95**:2997-3002.

104. **Kornfeld, S. and I. Mellman**. 1989. The biogenesis of lysosomes. Annu.Rev.Cell Biol. **5**:483-525.

105. **Kudryashov, D. S., M. V. Chibalina, K. G. Birukov, T. J. Lukas, J. R. Sellers, L. J. Van Eldik, D. M. Watterson, and V. P. Shirinsky**. 1999. Unique sequence of a high molecular weight myosin light chain kinase is involved in interaction with actin cytoskeleton. FEBS Lett. **463**:67-71.

106. **Kurashima, K., E. Z. Szabo, G. Lukacs, J. Orlowski, and S. Grinstein**. 1998. Endosomal recycling of the Na+/H+ exchanger NHE3 isoform is regulated by the phosphatidylinositol 3-kinase pathway. J.Biol.Chem. **273**:20828-20836.

107. **Lakadamyali, M., M. J. Rust, and X. Zhuang**. 2006. Ligands for clathrin-mediated endocytosis are differentially sorted into distinct populations of early endosomes. Cell **124**:997-1009.

108. **Lamaze, C., L. M. Fujimoto, H. L. Yin, and S. L. Schmid**. 1997. The actin cytoskeleton is required for receptor-mediated endocytosis in mammalian cells. J.Biol.Chem. **272**:20332-20335.

109. **Lawe, D. C., A. Chawla, E. Merithew, J. Dumas, W. Carrington, K. Fogarty, L. Lifshitz, R. Tuft, D. Lambright, and S. Corvera**. 2002. Sequential roles for phosphatidylinositol 3-phosphate and Rab5 in tethering and fusion of early endosomes via their interaction with EEA1. J.Biol.Chem. **277**:8611-8617.

110. **Lazar, V. and J. G. Garcia**. 1999. A single human myosin light chain kinase gene (MLCK; MYLK). Genomics **57**:256-267.

111. **Lehoux, S., J. Abe, J. A. Florian, and B. C. Berk**. 2001. 14-3-3 Binding to Na+/H+ exchanger isoform-1 is associated with serum-dependent activation of Na+/H+ exchange. J.Biol.Chem. **276**:15794-15800.

112. **Li, Q., X. Q. Dai, P. Y. Shen, H. F. Cantiello, E. Karpinski, and X. Z. Chen**. 2004. A modified mammalian tandem affinity purification procedure to prepare functional polycystin-2 channel. FEBS Lett. **576**:231-236.

113. **Lin, P. J., W. P. Williams, Y. Luu, R. S. Molday, J. Orlowski, and M. Numata**. 2005. Secretory carrier membrane proteins interact and regulate trafficking of the organellar (Na+,K+)/H+ exchanger NHE7. J.Cell Sci. **118**:1885-1897.

114. **Llopis, J., J. M. McCaffery, A. Miyawaki, M. G. Farquhar, and R. Y. Tsien.** 1998. Measurement of cytosolic, mitochondrial, and Golgi pH in single living cells with green fluorescent proteins. Proc.Natl.Acad.Sci.U.S.A **95**:6803-6808.

115. **Martinez, L. O., S. Jacquet, J. P. Esteve, C. Rolland, E. Cabezon, E. Champagne, T. Pineau, V. Georgeaud, J. E. Walker, F. Terce, X. Collet, B. Perret, and R. Barbaras.** 2003. Ectopic beta-chain of ATP synthase is an apolipoprotein A-I receptor in hepatic HDL endocytosis. Nature **421**:75-79.

116. **Maxfield, F. R. and T. E. McGraw.** 2004. Endocytic recycling. Nat.Rev.Mol.Cell Biol. **5**:121-132.

117. **Mayor, S., J. F. Presley, and F. R. Maxfield.** 1993. Sorting of membrane components from endosomes and subsequent recycling to the cell surface occurs by a bulk flow process. J.Cell Biol. **121**:1257-1269.

118. **McBride, H. M., V. Rybin, C. Murphy, A. Giner, R. Teasdale, and M. Zerial.** 1999. Oligomeric complexes link Rab5 effectors with NSF and drive membrane fusion via interactions between EEA1 and syntaxin 13. Cell **98**:377-386.

119. **McCartney, R. R. and M. C. Schmidt.** 2001. Regulation of Snf1 kinase. Activation requires phosphorylation of threonine 210 by an upstream kinase as well as a distinct step mediated by the Snf4 subunit. J.Biol.Chem. **276**:36460-36466.

120. **McConathy, W. J. and P. Alaupovic.** 1973. Isolation and partial characterization of apolipoprotein D: a new protein moiety of the human plasma lipoprotein system. FEBS Lett. **37**:178-182.

121. **McGraw, T. E., K. W. Dunn, and F. R. Maxfield.** 1993. Isolation of a temperature-sensitive variant Chinese hamster ovary cell line with a morphologically altered endocytic recycling compartment. J.Cell Physiol **155**:579-594.

122. **McPherson, P. S., B. K. Kay, and N. K. Hussain.** 2001. Signaling on the endocytic pathway. Traffic. **2**:375-384.

123. **Mellman, I.** 1996. Endocytosis and molecular sorting. Annu.Rev.Cell Dev.Biol. **12**:575-625.

124. **Mermall, V., P. L. Post, and M. S. Mooseker.** 1998. Unconventional myosins in cell movement, membrane traffic, and signal transduction. Science **279**:527-533.

125. **Miyazaki, E., M. Sakaguchi, S. Wakabayashi, M. Shigekawa, and K. Mihara.** 2001. NHE6 protein possesses a signal peptide destined for endoplasmic

reticulum membrane and localizes in secretory organelles of the cell. J.Biol.Chem. **276**:49221-49227.

126. **Moe, O. W., M. Amemiya, and Y. Yamaji**. 1995. Activation of protein kinase A acutely inhibits and phosphorylates Na/H exchanger NHE-3. J.Clin.Invest **96**:2187-2194.

127. **Morais Cabral, J. H., G. L. Atkins, L. M. Sanchez, Y. S. Lopez-Boado, C. Lopez-Otin, and L. Sawyer**. 1995. Arachidonic acid binds to apolipoprotein D: implications for the protein's function. FEBS Lett. **366**:53-56.

128. **Moser, T. L., D. J. Kenan, T. A. Ashley, J. A. Roy, M. D. Goodman, U. K. Misra, D. J. Cheek, and S. V. Pizzo**. 2001. Endothelial cell surface F1-F0 ATP synthase is active in ATP synthesis and is inhibited by angiostatin. Proc.Natl.Acad.Sci.U.S.A **98**:6656-6661.

129. **Mukherjee, S., L. Kallay, C. L. Brett, and R. Rao**. 2006. Mutational analysis of the intramembranous H10 loop of yeast Nhx1 reveals a critical role in ion homoeostasis and vesicle trafficking. Biochem.J. **398**:97-105.

130. **Nakamura, N., S. Tanaka, Y. Teko, K. Mitsui, and H. Kanazawa**. 2005. Four Na+/H+ exchanger isoforms are distributed to Golgi and post-Golgi compartments and are involved in organelle pH regulation. J.Biol.Chem. **280**:1561-1572.

131. **Nass, R. and R. Rao**. 1999. The yeast endosomal Na+/H+ exchanger, Nhx1, confers osmotolerance following acute hypertonic shock. Microbiology **145 (Pt 11)**:3221-3228.

132. **Navarro, A., V. E. Del, and J. Tolivia**. 2004. Differential expression of apolipoprotein d in human astroglial and oligodendroglial cells. J.Histochem.Cytochem. **52**:1031-1036.

133. **Numata, M. and J. Orlowski**. 2001. Molecular cloning and characterization of a novel (Na+,K+)/H+ exchanger localized to the trans-Golgi network. J.Biol.Chem. **276**:17387-17394.

134. **Numata, M., K. Petrecca, N. Lake, and J. Orlowski**. 1998. Identification of a mitochondrial Na+/H+ exchanger. J.Biol.Chem. **273**:6951-6959.

135. **Nunnally, M. H. and J. T. Stull**. 1984. Mammalian skeletal muscle myosin light chain kinases. A comparison by antiserum cross-reactivity. J.Biol.Chem. **259**:1776-1780.

136. **Okamura, H., J. C. Yasuhara, D. M. Fambrough, and K. Takeyasu**. 2003. P-type ATPases in Caenorhabditis and Drosophila: implications for evolution of the P-type ATPase subunit families with special reference to the Na,K-ATPase and H,K-ATPase subgroup. J.Membr.Biol. **191**:13-24.

137. **Orlowski, J.** 1993. Heterologous expression and functional properties of amiloride high affinity (NHE-1) and low affinity (NHE-3) isoforms of the rat Na/H exchanger. J.Biol.Chem. **268**:16369-16377.

138. **Orlowski, J. and S. Grinstein**. 2004. Diversity of the mammalian sodium/proton exchanger SLC9 gene family. Pflugers Arch. **447**:549-565.

139. **Orlowski, J. and S. Grinstein**. 1997. Na+/H+ exchangers of mammalian cells. J.Biol.Chem. **272**:22373-22376.

140. **Otsu, K., J. L. Kinsella, P. Heller, and J. P. Froehlich**. 1993. Sodium dependence of the Na(+)-H+ exchanger in the pre-steady state. Implications for the exchange mechanism. J.Biol.Chem. **268**:3184-3193.

141. **Otsu, K., J. L. Kinsella, E. Koh, and J. P. Froehlich**. 1992. Proton dependence of the partial reactions of the sodium-proton exchanger in renal brush border membranes. J.Biol.Chem. **267**:8089-8096.

142. **Pang, T., X. Su, S. Wakabayashi, and M. Shigekawa**. 2001. Calcineurin homologous protein as an essential cofactor for Na+/H+ exchangers. J.Biol.Chem. **276**:17367-17372.

143. **Pang, T., S. Wakabayashi, and M. Shigekawa**. 2002. Expression of calcineurin B homologous protein 2 protects serum deprivation-induced cell death by serum-independent activation of Na+/H+ exchanger. J.Biol.Chem. **277**:43771-43777.

144. **Pardo, J. M., B. Cubero, E. O. Leidi, and F. J. Quintero**. 2006. Alkali cation exchangers: roles in cellular homeostasis and stress tolerance. J.Exp.Bot. **57**:1181-1199.

145. **Park, M., L. Lin, S. Thomas, H. D. Braymer, P. M. Smith, D. H. Harrison, and D. A. York**. 2004. The F1-ATPase beta-subunit is the putative enterostatin receptor. Peptides **25**:2127-2133.

146. **Paroutis, P., N. Touret, and S. Grinstein**. 2004. The pH of the secretory pathway: measurement, determinants, and regulation. Physiology.(Bethesda.) **19**:207-215.

147. **Patel, R. C., D. Lange, W. J. McConathy, Y. C. Patel, and S. C. Patel**. 1997. Probing the structure of the ligand binding cavity of lipocalins by fluorescence spectroscopy. Protein Eng **10**:621-625.

148. **Pearlman, W. H., J. L. Gueriguian, and M. E. Sawyer**. 1973. A specific progesterone-binding component of human breast cyst fluid. J.Biol.Chem. **248**:5736-5741.

149. **Pearse, B. M. and R. A. Crowther**. 1987. Structure and assembly of coated vesicles. Annu.Rev.Biophys.Biophys.Chem. **16**:49-68.

150. **Peitsch, M. C. and M. S. Boguski**. 1989. Is apolipoprotein D a mammalian bilin-binding protein? New Biol. **2**:197-206.

151. **Pelkmans, L.** 2005. Secrets of caveolae- and lipid raft-mediated endocytosis revealed by mammalian viruses. Biochim.Biophys.Acta **1746**:295-304.

152. **Pelkmans, L., E. Fava, H. Grabner, M. Hannus, B. Habermann, E. Krausz, and M. Zerial**. 2005. Genome-wide analysis of human kinases in clathrin- and caveolae/raft-mediated endocytosis. Nature **436**:78-86.

153. **Peti-Peterdi, J., R. Chambrey, Z. Bebok, D. Biemesderfer, P. L. St John, D. R. Abrahamson, D. G. Warnock, and P. D. Bell**. 2000. Macula densa Na(+)/H(+) exchange activities mediated by apical NHE2 and basolateral NHE4 isoforms. Am.J.Physiol Renal Physiol **278**:F452-F463.

154. **Petrecca, K., R. Atanasiu, S. Grinstein, J. Orlowski, and A. Shrier**. 1999. Subcellular localization of the Na+/H+ exchanger NHE1 in rat myocardium. Am.J.Physiol **276**:H709-H717.

155. **Pizzonia, J. H., D. Biemesderfer, A. K. bu-Alfa, M. S. Wu, M. Exner, P. Isenring, P. Igarashi, and P. S. Aronson**. 1998. Immunochemical characterization of Na+/H+ exchanger isoform NHE4. Am.J.Physiol **275**:F510-F517.

156. **Ponka, P., A. Wilczynska, and H. M. Schulman**. 1982. Iron utilization in rabbit reticulocytes. A study using succinylacetone as an inhibitor or heme synthesis. Biochim.Biophys.Acta **720**:96-105.

157. **Poperechnaya, A., O. Varlamova, P. J. Lin, J. T. Stull, and A. R. Bresnick**. 2000. Localization and activity of myosin light chain kinase isoforms during the cell cycle. J.Cell Biol. **151**:697-708.

158. **Presley, J. F., S. Mayor, T. E. McGraw, K. W. Dunn, and F. R. Maxfield**. 1997. Bafilomycin A1 treatment retards transferrin receptor recycling more than bulk membrane recycling. J.Biol.Chem. **272**:13929-13936.

159. **Provost, P. R., Y. L. Marcel, R. W. Milne, P. K. Weech, and E. Rassart**. 1991. Apolipoprotein D transcription occurs specifically in nonproliferating quiescent and senescent fibroblast cultures. FEBS Lett. **290**:139-141.

160. **Rayment, I., H. M. Holden, M. Whittaker, C. B. Yohn, M. Lorenz, K. C. Holmes, and R. A. Milligan**. 1993. Structure of the actin-myosin complex and its implications for muscle contraction. Science **261**:58-65.

161. **Reczek, D., M. Berryman, and A. Bretscher**. 1997. Identification of EBP50: A PDZ-containing phosphoprotein that associates with members of the ezrin-radixin-moesin family. J.Cell Biol. **139**:169-179.

162. **Ren, M., G. Xu, J. Zeng, C. De Lemos-Chiarandini, M. Adesnik, and D. D. Sabatini**. 1998. Hydrolysis of GTP on rab11 is required for the direct delivery of transferrin from the pericentriolar recycling compartment to the cell surface but not from sorting endosomes. Proc.Natl.Acad.Sci.U.S.A **95**:6187-6192.

163. **Richardson, D. R., P. Ponka, and D. Vyoral**. 1996. Distribution of iron in reticulocytes after inhibition of heme synthesis with succinylacetone: examination of the intermediates involved in iron metabolism. Blood **87**:3477-3488.

164. **Rigaut, G., A. Shevchenko, B. Rutz, M. Wilm, M. Mann, and B. Seraphin**. 1999. A generic protein purification method for protein complex characterization and proteome exploration. Nat.Biotechnol. **17**:1030-1032.

165. **Robinson, M. S.** 2004. Adaptable adaptors for coated vesicles. Trends Cell Biol. **14**:167-174.

166. **Robinson, M. S.** 1994. The role of clathrin, adaptors and dynamin in endocytosis. Curr.Opin.Cell Biol. **6**:538-544.

167. **Robinson, M. S. and B. M. Pearse**. 1986. Immunofluorescent localization of 100K coated vesicle proteins. J.Cell Biol. **102**:48-54.

168. **Rothman, J. E.** 1994. Intracellular membrane fusion. Adv.Second Messenger Phosphoprotein Res. **29**:81-96.

169. **Rothman, J. E.** 1994. Intracellular membrane fusion. Adv.Second Messenger Phosphoprotein Res. **29**:81-96.

170. **Sardet, C., A. Franchi, and J. Pouyssegur**. 1989. Molecular cloning, primary structure, and expression of the human growth factor-activatable Na+/H+ antiporter. Cell **56**:271-280.

171. **Sato, Y., N. Ariyoshi, K. Mihara, and M. Sakaguchi**. 2004. Topogenesis of NHE1: direct insertion of the membrane loop and sequestration of cryptic glycosylation and processing sites just after TM9. Biochem.Biophys.Res.Commun. **324**:281-287.

172. **Schapiro, F. B. and S. Grinstein**. 2000. Determinants of the pH of the Golgi complex. J.Biol.Chem. **275**:21025-21032.

173. **Schmid, S. L.** 1997. Clathrin-coated vesicle formation and protein sorting: an integrated process. Annu.Rev.Biochem. **66**:511-548.

174. **Schmid, S. L., R. Fuchs, P. Male, and I. Mellman**. 1988. Two distinct subpopulations of endosomes involved in membrane recycling and transport to lysosomes. Cell **52**:73-83.

175. **Scholz, W., U. Albus, L. Counillon, H. Gogelein, H. J. Lang, W. Linz, A. Weichert, and B. A. Scholkens**. 1995. Protective effects of HOE642, a selective sodium-hydrogen exchange subtype 1 inhibitor, on cardiac ischaemia and reperfusion. Cardiovasc.Res. **29**:260-268.

176. **Sellers, J. R.** 2000. Myosins: a diverse superfamily. Biochim.Biophys.Acta **1496**:3-22.

177. **Sergeant, N., A. Wattez, M. Galvan-valencia, A. Ghestem, J. P. David, J. Lemoine, P. E. Sautiere, J. Dachary, J. P. Mazat, J. C. Michalski, J. Velours, R. Mena-Lopez, and A. Delacourte**. 2003. Association of ATP synthase alpha-chain with neurofibrillary degeneration in Alzheimer's disease. Neuroscience **117**:293-303.

178. **Simard, J., L. Y. de, D. E. Haagensen, and F. Labrie**. 1992. Additive stimulatory action of glucocorticoids and androgens on basal and estrogen-repressed apolipoprotein-D messenger ribonucleic acid levels and secretion in human breast cancer cells. Endocrinology **130**:1115-1121.

179. **Simpson, F., A. A. Peden, L. Christopoulou, and M. S. Robinson**. 1997. Characterization of the adaptor-related protein complex, AP-3. J.Cell Biol. **137**:835-845.

180. **Smith, K. M., R. M. Lawn, and J. N. Wilcox**. 1990. Cellular localization of apolipoprotein D and lecithin:cholesterol acyltransferase mRNA in rhesus monkey tissues by in situ hybridization. J.Lipid Res. **31**:995-1004.

181. **Snedden, W. A. and H. Fromm**. 2001. New Phytol. **151**:35-66.

182. **Sorkin, A.** 2004. Cargo recognition during clathrin-mediated endocytosis: a team effort. Curr.Opin.Cell Biol. **16**:392-399.

183. **Spreyer, P., H. Schaal, G. Kuhn, T. Rothe, A. Unterbeck, K. Olek, and H. W. Muller**. 1990. Regeneration-associated high level expression of apolipoprotein D mRNA in endoneurial fibroblasts of peripheral nerve. EMBO J. **9**:2479-2484.

184. **Steinman, R. M., I. S. Mellman, W. A. Muller, and Z. A. Cohn**. 1983. Endocytosis and the recycling of plasma membrane. J.Cell Biol. **96**:1-27.

185. **Stoorvogel, W., V. Oorschot, and H. J. Geuze**. 1996. A novel class of clathrin-coated vesicles budding from endosomes. J.Cell Biol. **132**:21-33.

186. **Stull, J. T., P. J. Lin, J. K. Krueger, J. Trewhella, and G. Zhi**. 1998. Myosin light chain kinase: functional domains and structural motifs. Acta Physiol Scand. **164**:471-482.

187. **Szabo, E. Z., M. Numata, V. Lukashova, P. Iannuzzi, and J. Orlowski**. 2005. beta-Arrestins bind and decrease cell-surface abundance of the Na+/H+ exchanger NHE5 isoform. Proc.Natl.Acad.Sci.U.S.A **102**:2790-2795.

188. **Szabo, E. Z., M. Numata, G. E. Shull, and J. Orlowski**. 2000. Kinetic and pharmacological properties of human brain Na(+)/H(+) exchanger isoform 5 stably expressed in Chinese hamster ovary cells. J.Biol.Chem. **275**:6302-6307.

189. **Szaszi, K., A. Paulsen, E. Z. Szabo, M. Numata, S. Grinstein, and J. Orlowski**. 2002. Clathrin-mediated endocytosis and recycling of the neuron-specific Na+/H+ exchanger NHE5 isoform. Regulation by phosphatidylinositol 3'-kinase and the actin cytoskeleton. J.Biol.Chem. **277**:42623-42632.

190. **Takahashi, E., J. Abe, B. Gallis, R. Aebersold, D. J. Spring, E. G. Krebs, and B. C. Berk**. 1999. p90(RSK) is a serum-stimulated Na+/H+ exchanger isoform-1 kinase. Regulatory phosphorylation of serine 703 of Na+/H+ exchanger isoform-1. J.Biol.Chem. **274**:20206-20214.

191. **Terrisse, L., J. Poirier, P. Bertrand, A. Merched, S. Visvikis, G. Siest, R. Milne, and E. Rassart**. 1998. Increased levels of apolipoprotein D in cerebrospinal fluid and hippocampus of Alzheimer's patients. J.Neurochem. **71**:1643-1650.

192. **Tominaga, T. and D. L. Barber**. 1998. Na-H exchange acts downstream of RhoA to regulate integrin-induced cell adhesion and spreading. Mol.Biol.Cell **9**:2287-2303.

193. **Tominaga, T., T. Ishizaki, S. Narumiya, and D. L. Barber**. 1998. p160ROCK mediates RhoA activation of Na-H exchange. EMBO J. **17**:4712-4722.

194. **Traub, L. M.** 2003. Sorting it out: AP-2 and alternate clathrin adaptors in endocytic cargo selection. J.Cell Biol. **163**:203-208.

195. **Traub, L. M., S. Kornfeld, and E. Ungewickell**. 1995. Different domains of the AP-1 adaptor complex are required for Golgi membrane binding and clathrin recruitment. J.Biol.Chem. **270**:4933-4942.

196. **Tse, C. M., S. A. Levine, C. H. Yun, S. Khurana, and M. Donowitz**. 1994. Na+/H+ exchanger-2 is an O-linked but not an N-linked sialoglycoprotein. Biochemistry **33**:12954-12961.

197. **van Dam, E. M. and W. Stoorvogel**. 2002. Dynamin-dependent transferrin receptor recycling by endosome-derived clathrin-coated vesicles. Mol.Biol.Cell **13**:169-182.

198. **van der, S. P., M. Hull, P. Webster, P. Male, B. Goud, and I. Mellman**. 1992. The small GTP-binding protein rab4 controls an early sorting event on the endocytic pathway. Cell **70**:729-740.

199. **Venema, K., F. J. Quintero, J. M. Pardo, and J. P. Donaire**. 2002. The arabidopsis Na+/H+ exchanger AtNHX1 catalyzes low affinity Na+ and K+ transport in reconstituted liposomes. J.Biol.Chem. **277**:2413-2418.

200. **Verin, A. D., V. Lazar, R. J. Torry, C. A. Labarrere, C. E. Patterson, and J. G. Garcia**. 1998. Expression of a novel high molecular-weight myosin light chain kinase in endothelium. Am.J.Respir.Cell Mol.Biol. **19**:758-766.

201. **Wade, J. B., P. A. Welling, M. Donowitz, S. Shenolikar, and E. J. Weinman**. 2001. Differential renal distribution of NHERF isoforms and their colocalization with NHE3, ezrin, and ROMK. Am.J.Physiol Cell Physiol **280**:C192-C198.

202. **Wakabayashi, S., B. Bertrand, T. Ikeda, J. Pouyssegur, and M. Shigekawa**. 1994. Mutation of calmodulin-binding site renders the Na+/H+ exchanger (NHE1) highly H(+)-sensitive and Ca2+ regulation-defective. J.Biol.Chem. **269**:13710-13715.

203. **Wakabayashi, S., T. Ikeda, T. Iwamoto, J. Pouyssegur, and M. Shigekawa**. 1997. Calmodulin-binding autoinhibitory domain controls "pH-sensing" in the Na+/H+ exchanger NHE1 through sequence-specific interaction. Biochemistry **36**:12854-12861.

204. **Wakabayashi, S., T. Pang, X. Su, and M. Shigekawa**. 2000. A novel topology model of the human Na(+)/H(+) exchanger isoform 1. J.Biol.Chem. **275**:7942-7949.

205. **Wakabayashi, S., C. Sardet, P. Fafournoux, L. Counillon, S. Meloche, G. Pages, and J. Pouyssegur**. 1992. Structure function of the growth factor-activatable Na+/H+ exchanger (NHE1). Rev.Physiol Biochem.Pharmacol. **119**:157-186.

206. **Watterson, D. M., M. Collinge, T. J. Lukas, L. J. Van Eldik, K. G. Birukov, O. V. Stepanova, and V. P. Shirinsky**. 1995. Multiple gene products are produced from a novel protein kinase transcription region. FEBS Lett. **373**:217-220.

207. **Weinman, E. J., C. Minkoff, and S. Shenolikar**. 2000. Signal complex regulation of renal transport proteins: NHERF and regulation of NHE3 by PKA. Am.J.Physiol Renal Physiol **279**:F393-F399.

208. **Weinman, E. J., D. Steplock, M. Donowitz, and S. Shenolikar**. 2000. NHERF associations with sodium-hydrogen exchanger isoform 3 (NHE3) and ezrin are essential for cAMP-mediated phosphorylation and inhibition of NHE3. Biochemistry **39**:6123-6129.

209. **Weinman, E. J., D. Steplock, and S. Shenolikar**. 2001. Acute regulation of NHE3 by protein kinase A requires a multiprotein signal complex. Kidney Int. **60**:450-454.

210. **Weinman, E. J., D. Steplock, J. B. Wade, and S. Shenolikar**. 2001. Ezrin binding domain-deficient NHERF attenuates cAMP-mediated inhibition of Na(+)/H(+) exchange in OK cells. Am.J.Physiol Renal Physiol **281**:F374-F380.

211. **Wells, K. M. and R. Rao**. 2001. The yeast Na+/H+ exchanger Nhx1 is an N-linked glycoprotein. Topological implications. J.Biol.Chem. **276**:3401-3407.

212. **White, R. A., L. A. Boydston, T. R. Brookshier, S. G. McNulty, N. N. Nsumu, B. P. Brewer, and K. Blackmore**. 2005. Iron metabolism mutant hbd mice have a deletion in Sec1511, which has homology to a yeast gene for vesicle docking. Genomics **86**:668-673.

213. **Whitney, J. A., M. Gomez, D. Sheff, T. E. Kreis, and I. Mellman**. 1995. Cytoplasmic coat proteins involved in endosome function. Cell **83**:703-713.

214. **Wiederkehr, M. R., S. F. Di, R. Collazo, H. Quinones, L. Fan, H. Murer, C. Helmle-Kolb, and O. W. Moe**. 2001. Characterization of acute inhibition of Na/H exchanger NHE-3 by dopamine in opossum kidney cells. Kidney Int. **59**:197-209.

215. **Wiederkehr, M. R., H. Zhao, and O. W. Moe**. 1999. Acute regulation of Na/H exchanger NHE3 activity by protein kinase C: role of NHE3 phosphorylation. Am.J.Physiol **276**:C1205-C1217.

216. **Williams, K. A.** 2000. Three-dimensional structure of the ion-coupled transport protein NhaA. Nature **403**:112-115.

217. **Xu, H., R. Chen, and F. K. Ghishan**. 2005. Subcloning, localization, and expression of the rat intestinal sodium-hydrogen exchanger isoform 8. Am.J.Physiol Gastrointest.Liver Physiol **289**:G36-G41.

218. **Yamaguchi, T., G. S. Aharon, J. B. Sottosanto, and E. Blumwald**. 2005. Vacuolar Na+/H+ antiporter cation selectivity is regulated by calmodulin from within the vacuole in a Ca2+- and pH-dependent manner. Proc.Natl.Acad.Sci.U.S.A **102**:16107-16112.

219. **Yamaguchi, T., M. P. Apse, H. Shi, and E. Blumwald**. 2003. Topological analysis of a plant vacuolar Na+/H+ antiporter reveals a luminal C terminus

that regulates antiporter cation selectivity. Proc.Natl.Acad.Sci.U.S.A **100**:12510-12515.

220. **Yamaguchi, T., S. Fukada-Tanaka, Y. Inagaki, N. Saito, K. Yonekura-Sakakibara, Y. Tanaka, T. Kusumi, and S. Iida**. 2001. Genes encoding the vacuolar Na+/H+ exchanger and flower coloration. Plant Cell Physiol **42**:451-461.

221. **Yamashiro, D. J. and F. R. Maxfield**. 1984. Acidification of endocytic compartments and the intracellular pathways of ligands and receptors. J.Cell Biochem. **26**:231-246.

222. **Yamashiro, D. J., B. Tycko, S. R. Fluss, and F. R. Maxfield**. 1984. Segregation of transferrin to a mildly acidic (pH 6.5) para-Golgi compartment in the recycling pathway. Cell **37**:789-800.

223. **Yan, W., K. Nehrke, J. Choi, and D. L. Barber**. 2001. The Nck-interacting kinase (NIK) phosphorylates the Na+-H+ exchanger NHE1 and regulates NHE1 activation by platelet-derived growth factor. J.Biol.Chem. **276**:31349-31356.

224. **Yonemura, S., S. Tsukita, and S. Tsukita**. 1999. Direct involvement of ezrin/radixin/moesin (ERM)-binding membrane proteins in the organization of microvilli in collaboration with activated ERM proteins. J.Cell Biol. **145**:1497-1509.

225. **Yu, F. H., G. E. Shull, and J. Orlowski**. 1993. Functional properties of the rat Na/H exchanger NHE-2 isoform expressed in Na/H exchanger-deficient Chinese hamster ovary cells. J.Biol.Chem. **268**:25536-25541.

226. **Yun, C. H., G. Lamprecht, D. V. Forster, and A. Sidor**. 1998. NHE3 kinase A regulatory protein E3KARP binds the epithelial brush border Na+/H+ exchanger NHE3 and the cytoskeletal protein ezrin. J.Biol.Chem. **273**:25856-25863.

227. **Yun, C. H., P. J. Little, S. K. Nath, S. A. Levine, J. Pouyssegur, C. M. Tse, and M. Donowitz**. 1993. Leu143 in the putative fourth membrane spanning domain is critical for amiloride inhibition of an epithelial Na+/H+ exchanger isoform (NHE-2). Biochem.Biophys.Res.Commun. **193**:532-539.

228. **Yun, C. H., S. Oh, M. Zizak, D. Steplock, S. Tsao, C. M. Tse, E. J. Weinman, and M. Donowitz**. 1997. cAMP-mediated inhibition of the epithelial brush border Na+/H+ exchanger, NHE3, requires an associated regulatory protein. Proc.Natl.Acad.Sci.U.S.A **94**:3010-3015.

229. **Zhang, A. S., A. D. Sheftel, and P. Ponka**. 2005. Intracellular kinetics of iron in reticulocytes: evidence for endosome involvement in iron targeting to mitochondria. Blood **105**:368-375.

230. **Zhang, H. X., J. N. Hodson, J. P. Williams, and E. Blumwald**. 2001. Engineering salt-tolerant Brassica plants: characterization of yield and seed oil quality in transgenic plants with increased vacuolar sodium accumulation. Proc.Natl.Acad.Sci.U.S.A **98**:12832-12836.

231. **Zhang, Y., J. M. Norian, C. E. Magyar, N. H. Holstein-Rathlou, A. K. Mircheff, and A. A. McDonough**. 1999. In vivo PTH provokes apical NHE3 and NaPi2 redistribution and Na-K-ATPase inhibition. Am.J.Physiol **276**:F711-F719.

232. **Zhao, H., M. R. Wiederkehr, L. Fan, R. L. Collazo, L. A. Crowder, and O. W. Moe**. 1999. Acute inhibition of Na/H exchanger NHE-3 by cAMP. Role of protein kinase a and NHE-3 phosphoserines 552 and 605. J.Biol.Chem. **274**:3978-3987.

233. **Zhi, G., J. W. Ryder, J. Huang, P. Ding, Y. Chen, Y. Zhao, K. E. Kamm, and J. T. Stull**. 2005. Myosin light chain kinase and myosin phosphorylation effect frequency-dependent potentiation of skeletal muscle contraction. Proc.Natl.Acad.Sci.U.S.A **102**:17519-17524.

234. **Zielinsky, R. E.** 1998. Annu.Rev.Plant Physiol.Plant Mol.Biol. **49**:697-725.

APPENDIX A

Primers used for making DNA constructs

Oligo No.	Sequence	Description
JO-1290	-CCG CGT **GGA TCC** AAC ACT GAA CCG GCC ACA	NHE6 / N608 S (BamHI)
JO-1294	-GTC ACG ATG **AAT TC**G GCT GGA CCA TGT CTC	NHE6 / A669 AS (EcoRI)
JO-1294	-GTC ACG ATG **AAT TC**G GCT GGA CCA TGT CTC	NHE6 / A669 AS (EcoRI)
JO-1340	-CTC GAG **AAT TC**A TGG CTC GGC GCG GCT GG	NHE6 / SM1 (EcoRI)
JO-1341	-GTC GAC **TCT AGA** GGA TGC ATA GTC CGG GAC	NHE6 / AS-S679 (XbaI)
JO-1364	-CCG CGT GGA TCC GCA ATG CTG TCA TGC TTG	NHE6 / A499-GST-S
JO-1367	-ATG GCG GTC TCC ACA GGA G	UBE2V2 / 5'
JO-1368	-TCC ACT AAA ATT AAT TGT TGT ATG	UBE2V2 / 3'
JO-1371	-ATG GCT GAA GAA CAA CCG CAG	CLIC1 / 5'
JO-1372	-GGC TTA TTT GAG GGC CTT TGC	CLIC1 / 3'
JO-1379	-CCG CCG ATC CGC TAC TCA TCA CAC GCT G	PTGDS / 5' (BamHI)
JO-1380	-CCC GGA ATT CCT ATT GTT CCG TCA TGC ACT TAT CG	PTGDS / 3' (EcoRI)
JO-1384	-CCG CGG ATC CGC TGA AGA ACA ACC GCA G	CLIC1 / 5' (BamHI)
JO-1385	-CCC CCG CTC GAG TTA TTT GAG GGC CTT TGC CAC	CLIC1 / 3' (XhoI)
JO-1386	-CCG CGG ATC CGC GGT CTC CAC AGG AG	UBE2V2 / 5' (BamHI)
JO-1387	-CCC GGA ATT CTT AAT TGT TGT ATG TTT GTC C	UVE2V2 / 3' (EcoRI)
JO-1394	-CCC GGA ATT CGT GAT GCT GCT GCT GCT TTC C	APOD / 5' (EcoRI)
JO-1395	-CCC AAG CTT TTA CGA GAG CTT GGG GCA G	APOD / 3' (HindIII)
JO-1424	-CCC GGA ATT CCT ACC AGC AGG CAG GGA GTG TTG	NHE6 / C GST / EcoRI (554)3'
JO-1425	-CCC GGA ATT CCT AGA TGT CAC CAT CAT TGA G	NHE6 / C GST / EcoRI (598)3'
JO-1426	-CCC GGA ATT CCT ATT CAG GAA CAC CCA AGT GTT C	NHE6 / C GST / EcoRI (520) 3'
JO-1427	-CCC GGA ATT CCT ACA TAA ATC TCC TTG GGG C	NHE6 / C GST / EcoRI (621)3'

APPENDIX B

No.	Protein Identifier(s)	Sequence identifier	Protein Description	Peptides	Query Counts			GO biological process from GOA and InterProScan	GO molecular function from GOA and InterProScan	GO cellular component from GOA and InterProScan	InterProScan Predictions
					Unique	Shared	Total Pro-Rated				
0	nrdb|14670356 nrdb|47122603 nrdb|14670354 nrdb|14670352	54635 22420 54634 54633	general transcription factor II, i isoform 4 [Homo sapiens] General transcription factor II, i, isoform 4 [Homo sapiens] general transcription factor II, i isoform 3 [Homo sapiens] general transcription factor II, i isoform 2 [Homo sapiens]	AKGPVTIPYPLFQSHVEDLYVEGLPEGIPFR from job(s) **241906** ANELPQPPVPEPANAGK from job(s) **241906, 240412** ANELPQPPVPEPANAGKR from job(s) **249008, 249007, 249006** DQSAVVVQGLPEGVAFK from job(s) **241906** FEAHPNDLYVEGLPENIPFR from job(s) **241906, 241905, 241039** FTVIRPFPGLVINNQLVDQSESEGPVIQESAEPSQLEVPATEEIK from job(s) **240412** GPVTIPYPLFQSHVEDLYVEGLPEGIPFR from job(s) **241906, 241905, 241039** ITINPGCVVVDGMPPGVSFK from job(s) **241039** KINSSPNVNTTASGVEDLNIIQVTIPDDDNER from job(s) **240412** SILSPGGSCGPIKVK from job(s) **249007** TPTQTNGSNVPFKPR from job(s) **249007, 249006** VMVTDADRSILSPGGSCGPIK from job(s) **249006** VPEIEVTVEGPNNNNPQTSAVR from job(s) **241905, 241039, 240412** VPFALFESFPEDFYVEGLPEGVPFR from job **241906, 241905, 240412** VPYPVFESNPEFLYVEGLPEGIPFR from job(s) **241906, 241905, 241039, 240412**	36	0	36				PR004212 (R) GTF2I-like repeat
1	nrdb|1346640 nrdb|41406064	74738 722413	Myosin-10 (Myosin heavy chain, nonmuscle IIb) (Nonmuscle myosin heavy chain IIb) (NMMHC II-b) (NMMHC-IIB) (Cellular myosin heavy chain, type B) (Nonmuscle myosin heavy chain-B) (NMMHC-B) myosin, heavy polypeptide 10, non-muscle [Homo sapiens]	AGVLAHLEEER from job(s) **241906** ALEEETKNHEAQIQDMR from job(s) **249007** ALELDPNLYR from job(s) **241906, 240412** AVIYNPATQADWTAK from job(s) **241906** DAASLESQLQDTQELLQEETR from job(s) **241906, 240412** ELEAELEDER from job(s) **241906** ELQAQIAELQEDFESEK from job(s) **240412** HAEQERDELADEITNSASGK from job(s) **249007, 241906, 240412** HATALEELSEQLEQAK from job(s) **241906, 240412** HATALEELSEQLEQAKR from job(s) **241906** IGQLEEQLEQEAK from job(s) **240412** KLDGETTDLQDQIAELQAQIDELK from job **241906, 241905, 240412** KQELEEILHDLESR from job(s) **240412** LQNELDNVSTLLEEAEKK from job(s) **241906** LQQELDDLTVDLDHQR from job(s) **249007, 241906** QLLQANPILESFGNAK from job(s) **249007, 241906, 240412** SLEAEILQLQEELASSER from job(s) **241906, 241905, 241039** TQLEELEDELQATEDAK from job(s) **241906, 240412**	31	5	36	GO:0008360 regulation of cell shape #IEA#	GO:0000166 nucleotide binding #IEA# GO:0003774 motor activity #IEA# GO:0003779 actin binding #NAS# GO:0005516 calmodulin binding #IEA# GO:0005524 ATP binding #NAS#	GO:0016459 myosin #NAS#	IPR000048 (D) IQ calmodulin-binding region IPR001609 (D) Myosin head (motor domain) IPR002017 (R) Spectrin repeat IPR002928 (D) Myosin tail PR003345 (R) M protein repeat IPR004009 (D) Myosin N-terminal SH3-like domain
2	nrdb|57162568	1907230	solute carrier family 9 (sodium/hydrogen exchanger), isoform 6 [Homo sapiens]	AANIYPLSLLLNLGR from job(s) **241905, 241039** ELAFGDHELVIR from job(s) **249008, 241907, 241905, 241040, 241039** LVLPMDDSEPPLNLLDNTR from job(s) **249008, 241907, 241905, 241040, 241039** MDEEIVSEK from job(s) **249008** RFMGNSSEDALDR from job(s) **249008** VGVDSDQEHLGVPENER from job(s) **249008, 241907, 241040** VGVDSDQEHLGVPENERR from job(s) **249008**	31	0	31	GO:0006811 ion transport #IEA# GO:0006814 sodium ion transport #IEA# GO:0006885 regulation of pH #IEA#	GO:0015297 antiporter activity #IEA# GO:0015299 solute:hydrogen antiporter activity #IEA#	GO:0016021 integral to membrane #IEA#	

3	nrdb|62897409 nrdb|15277503 nrdb|62897671 nrdb|16924319 nrdb|14250401	2763797 59780 2763903 140656 82251	beta actin variant [Homo sapiens] ACTB protein [Homo sapiens] Unknown (protein for IMAGE:3538275) [Homo sapiens] actin, beta [Homo sapiens]	AGFAGDDAPR from job(s) 249008, 249007 AVFPSIVGRPR from job(s) 249007 DLYANTVLSGGTTMYPGIADR from job(s) 241039 DSYVGDEAQSKR from job(s) 249008 EITALAPSTMK from job(s) 249008 HQGVMVGMGQK from job(s) 249008, 249007 HQGVMVGMGQKDSYVGDEAQSK from job(s) 249007 IWHHTFYNELR from job(s) 241906, 240412 LCYVALDFEQEMATAASSSSLEK from job(s) 241039 MQKEITALAPSTMK from job(s) 249007 SYELPDGQVITIGNER from job(s) 249008, 249007, 241907, 241906, 241905, 241040, 241039 VAPEEHPVLLTEAPLNPK from job(s) 249008, 249006, 241907, 241906, 241040, 241039	7	22	29		GO:0003774 motor activity #IEA# GO:0005200 structural constituent of cytoskeleton #IEA# GO:0005515 protein binding #IEA#	GO:0005884 actin filament #IEA#	IPR004000 (F) Actin/actin-like PR004001 (F) Actin
4	nrdb|62896697 nrdb|16741043 nrdb|21728376	2763485 120568 88823	myosin regulatory light chain MRCL3 variant [Homo sapiens] MRCL3 [Homo sapiens] myosin regulatory light chain-like [Mus musculus]	ATSNVFAMFDQSQIQEFK from job(s) 240412 FTDEEVDELYR from job(s) 241906, 241905, 241039, 240412 GNFNYIEFTR from job(s) 249008, 249007, 240412 LNGTDPEDVIR from job(s) 241906 NAFACFDEEATGTIQEDYLR from job(s) 241906, 240412	22	0	22		GO:0005509 calcium ion binding #IEA#		IPR002048 (D) Calcium-binding EF-hand
5	nrdb|18088719	67493	Tubulin, beta polypeptide [Homo sapiens]	AILVDLEPGTMDSVR from job(s) 249008, 249006, 241905 ALTVPELTQQVFDAK from job(s) 249008, 241907, 241040 EIVHIQAGQCGNQIGAK from job(s) 249008, 241905, 241040, 241039 GHYTEGAELVDSVLDVVR from job(s) 241905, 241039 IMNTFSVVPSPK from job(s) 241040 ISVYYNEATGGK from job(s) 249008, 241907, 241039 LTTPTYGDLNHLVSATMSGVTTCLRFPGQLNADLR from 241039 MREIVHIQAGQCGNQIGAK from job(s) 249007 SGPFGQIFRPDNFVFGQSGAGNNWAK from job(s) 241905, 241039	9	12	21				IPR000217 (F) Tubulin family IPR002453 (F) Beta tubulin IPR003008 (D) Tubulin/FtsZ, GTPase IPR008280 (D) Tubulin/FtsZ, C-terminal
6	nrdb|13436317 nrdb|340021 nrdb|37492 nrdb|18204869 nrdb|62897609	82928 36248 31425 111316 2763875	Tubulin alpha 6 [Homo sapiens] alpha-tubulin alpha-tubulin [Homo sapiens] K-ALPHA-1 protein [Homo sapiens] tubulin alpha 6 variant [Homo sapiens]	AVFVDLEPTVIDEVR from job(s) 249008, 249007, 249006, 241907, 241905, 241040 IHFPLATYAPVISAEK from job(s) 249007, 241905, 241039 QLFHPEQLITGKEDAANNYAR from job(s) 249007 TIGGGDDSFNTFFSETGAGK from job(s) 241907, 241040, 241039 VGINYQPPTVVPGGDLAK from job(s) 241907, 241039	18	0	18	GO:0007018 microtubule-based movement #IEA#	GO:0000166 nucleotide binding #IEA# GO:0003924 GTPase activity #IEA# GO:0005198 structural molecule activity #IEA# GO:0005525 GTP binding #IEA#	GO:0005874 microtubule #IEA#	IPR000217 (F) Tubulin family IPR003008 (D) Tubulin/FtsZ, GTPase IPR008280 (D) Tubulin/FtsZ, C-terminal IPR002452 (F) Alpha tubulin
7	nrdb|33438760	185807	myosin heavy chain [Homo sapiens]	AEAELCAEAEETR from job(s) 240412 AQAELENVSGALNEAESK from job(s) 240412 AQVTELEDELTAAEDAK from job(s) 241906, 240412 DLGEELEALRGELEDTLDSTNAQQELR from job(s) 240412 EAQAALAEAQEDLESER from job(s) 241906 ELSSTEAQLHDAQELLQEETR from job(s) 241906 HEVPPHVYAVTEGAYR from job(s) 240412 LAQAEEQLEQETR from job(s) 241906	3	13	13.75	GO:0008360 regulation of cell shape #IEA#	GO:0000166 nucleotide binding #IEA# GO:0003774 motor activity #IEA# GO:0003779 actin binding	GO:0016459 myosin #IEA#	IPR000048 (D) IQ calmodulin-binding region IPR001609 (D) Myosin head (motor domain) IPR002928 (D) Myosin tail

APPENDIX C

Protein name	18-août-05			02-sept-05			08-nov-05			No. peptides		Function
	1	2	3	1	2	3	1	2	3	Total	Distinct	
Integral to membrane (organelles non-specified)												
NHE6		3	3		3	3			6	**18**	**6**	Na/H antiporter activity
ATPase, Ca++ transporting, cardiac muscle, slow twitch 2			1		1	2				**4**	**2**	calcium/proton transport, sarcoplasmic reticulum
cytoskeleton-associated protein 4 (CKAP4)		1			1			1		**3**	**3**	
VAMP (vesicle-associated membrane protein)-associated protein A							1	1		**2**	**2**	protein complex assembly, exocytosis, protein trafficking
ATPase, Ca++ transporting, plasma membrane 4			1			1				**2**	**2**	calcium ion transport, metabolism
phosphatidylserine synthase 2						1				**1**		phospholipid biosynthesis
brain-selective and closely mapped on the counter allele of CMAP in cystatin cluster		1								**1**		biosythesis
transmembrane protein 41B (KIAA0033)								1		**1**		phosophoenolpyruvate-dependent sugar phosphotransferase system
microsomal glutathione S-transferase 1 (MGST1)		1								**1**		microsome, GST activity
monocarboxylate transporter 1 (MCT1)						1				**1**		organic ion transport
Acyl-CoA synthetase		1								**1**		lipid metabolism
basigin, EMMPRIN, CD147					1					**1**		cell surface receptor linked to signal transduction
neutral amino acid transporter		1								**1**		dicarboxylic acid transport
RAP1B, member of RAS oncogene family					1					**1**		protein transport, cell cycle regulation, signal transduction, immunoglobuin family
Endoplasmic Reticulum												
BiP protein		1	3		1	1	1		1	**8**	**6**	chaperone, lumen
ribophorin II precursor (RPN2)		3			3					**6**	**4**	N-linked glycosylation via asparagine
aldehyde dehydrogenase 3A2		2	2		1	1				**6**	**4**	membrane, lipid metabolism
ribophorin I		2			2					**4**	**2**	membrane, protein amino acid glycosylation
signal sequence receptor, delta (translocon-associated protein delta)		2			1					**3**	**3**	membrane, intracellular protein transport, Ca binding
calnexin			1			1			1	**3**	**2**	lumen, chaperone
translocating chain-associating membrane protein (TRAM1)		1							1	**2**	**1**	translocation of secretory proteins
delta7-sterol reductase (D7SR); 7-dehyrocholesterol reductase (DHCR7)						1				**1**		membrane, cholesterol biosynthesis
oligosaccharyltransferase		1								**1**		membrane, N-linked glycosylation via asparagine
zinc metalloproteinase STE24 homolog								1		**1**		membrane ER, Golgi, proteolysis and peptidolysis
SURF-4 isoform, surfeit 4					1					**1**		membrane, unknown function

Protein name	18-août-05			02-sept-05			08-nov-05			No. peptides		Function
	1	2	3	1	2	3	1	2	3	Total	Distinct	
Mitochondria												
voltage-dependent anion channel 2 (porin)		1			4					**5**	**4**	outer membrane, anion transport
ATP synthase, H+ transporting, mitochondrial F1 complex, α subunit (ATP5A1)					1				1	**2**	**2**	inner membrane
tricarboxylate carrier protein		1			1					**2**	**1**	tricarboxylate/iron carrier
translocase of outer mitochondrial membrane 70 homolog A		1			1					**2**	**1**	integral to membrane, protein binding
leucine-rich PPR motif-containing protein		1								**1**		protein/RNA/DNA binding
B-cell receptor associated protein		1								**1**		inner membrane, regulation of transcription
prohibitin								1		**1**		inner membrane, DNA replication, regulation of cell
chaperonin (HSP60)		1								**1**		matrix, protein folding
transmembrane protein, motor protein, mitofilin		1								**1**		inner membrane, unknown function
heat shock 70kD protein 9B		1								**1**		protein folding
peripheral benzodiazepine receptor		1								**1**		outer membrane, signal transduction, protein-mitochondrial targeting, also at plasma membrane
Nucleus												
heat shock 70kDa protein 1A			3		2	2			2	**9**	**5**	protein folding
ubiquitin		1	1			1				**3**	**1**	protein modification, cell cycle
HNRPH1		1			1				1	**3**	**2**	RNA binding
thymopoietin isoform β		2						1		**3**	**3**	lamino-associated polypeptide 2 / emerin
leucine-rich PPR motif-containing protein		1								**1**		protein/RNA/DNA binding
B-cell receptor associated protein		1								**1**		inner membrane, regulation of transcription
BCL2-associated transcription factor 1								1		**1**		regulation of transcription
lamin B receptor					1					**1**		integral to nuclear membrane, DNA binding
Cytoskeleton												
actin-β	1	4	2	3	1	2	1	6	6	**26**	**11**	
β-tubulin		5	3		4	2	1	1	4	**20**	**9**	
α-tubulin		3	2		2	2	1	4	1	**15**	**5**	
tropomodulin 3								1		**1**		actin capping protein complex
Cytosol												
heat shock 70kDa protein 1A			3		2	2			2	**9**	**5**	protein folding
skeletal myosin light chain kinase (MLCK)		2	1		1				1	**5**	**2**	serine/threonine protein kinase
protein phosphatase 1B1 43 kDa isoform	1	2			1					**4**	**3**	protein amino acid dephosphorylation
calmodulin		2	1						1	**4**	**3**	Ca2+ binding, cell cycle
B-ind1 protein		1			1	1				**3**	**1**	small GTPase mediated signal transduction
ubiquitin		1	1			1				**3**	**1**	protein modification, cell cycle

Protein name	18-août-05			02-sept-05			08-nov-05			No. peptides		Function
	1	2	3	1	2	3	1	2	3	Total	Distinct	
Cytosol (continued)												
chain A, crystal structure of human carbonyl reductase 1 (Cbr1) in complex with hydroxy-Pp	1							2		**3**	**3**	short-chain dehydrogenase-reducatase, metabolism
small GTP binding protein Rab7					1			1		**2**	**1**	Golgi, protein transport, endocytosis
ancient ubiquitous protein 1(AUP1)					1					**1**		integrin signalling
RAB2B		1								**1**		ER, Golgi, intracellular protein transport
RAB1B		1								**1**		intracellular protein transport
kinesin-related protein		1								**1**		microtubule associated complex, microtubule-based movement
ribosomal protein S3		1	2						1	**4**	**2**	protein synthesis
ribosomal protein S18			1						2	**3**	**2**	protein synthesis
ribosomal protein L11			1			1				**2**	**1**	protein synthesis
PREDICTED: similar to 40S ribosomal protein S17			1						1	**2**	**2**	protein synthesis
similar to ribosomal protein L23 (RPL23)		1				1				**2**	**1**	protein synthesis
similar to ribosomal protein S14									1	**1**		protein synthesis
ribosomal protein L13 (RPL13)					1					**1**		protein synthesis
PREDICTED: similar to ribosomal protein S27									1	**1**		protein synthesis
Unknown function and/or location												
CHCHD2 protein		2			2		1			**5**	**2**	
DNA dependent protein kinase catalytic subunit			2			1			1	**4**	**3**	DNA repair
STMF151		1			1					**2**	**1**	
KIAA0090		1			1					**2**	**1**	
transmembrane protein, uncharacterized hypothalamus protein HTMP			1			1				**2**	**1**	
hypothetical protein LOC55379					1					**1**		leucine-rich repeat
MBC3205		1								**1**		
UNQ501 protein								1		**1**		
KIAA0887 protein					1					**1**		
PREDICTED: similar to Enhancer of rudimentary homolog		1			1					**2**	**1**	regulation of cell cycle

Total number of proteins (all TAP and M2P combined)				**77**
Total number of proteins (all TAP combined)				**29**
Total number of proteins in each TAP run	**20**	**20**	**18**	
Number of common proteins between TAP runs (18 Aug. AND 2 Sept.)				**15**
Number of common proteins between TAP runs (18 Aug. OR 2 Sept. AND 8 Nov.)				**14**
Number of common proteins between ALL TAP runs (18 Aug. AND 2 Sept. AND 8 Nov.)				**9**

1 = control experiment of single affinity purification
2 = single affinity purification
3 = tandem affinity purification

APPENDIX D

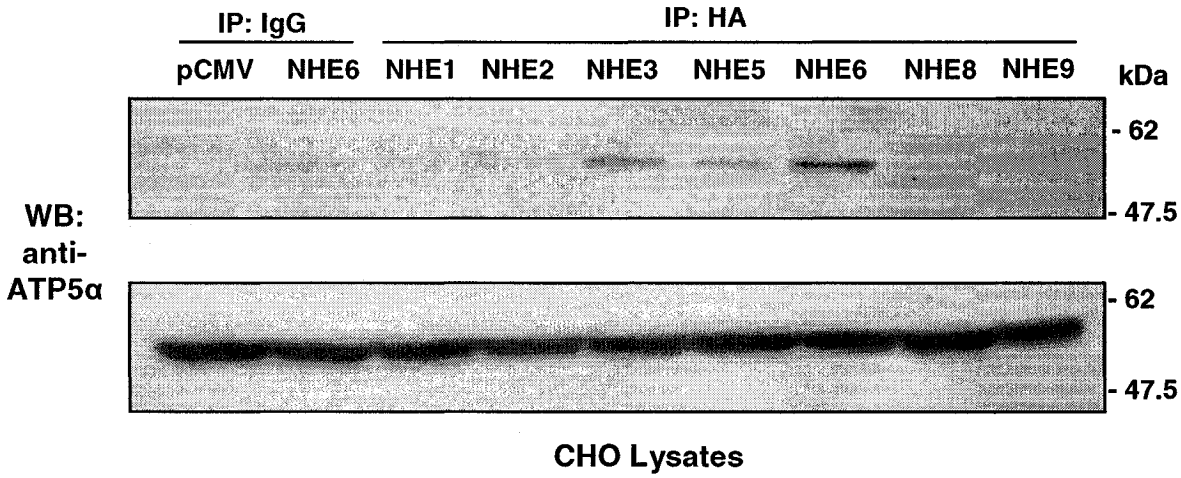

Interaction between endogenous ATP5α and transfected HA-tagged NHEs in CHO cells

HA-tagged NHEs were immunoprecipitated by adding a polyclonal anti-HA antibody to lysates from CHO transfected cells and incubating overnight. As a control, pCMV and $NHE6_{HA}$ transfected lysates were incubated with a non-specific IgG antibody. The endogenous α subunit of the mitochondrial ATP synthase, which precipitated along with some HA-tagged NHEs was visualized by western blotting with a mouse monoclonal anti-ATP5α antibody (1:6,000).

APPENDIX E

4. RESEARCH PERSONNEL: (attach additional sheets if preferred)

Name	Department	Check appropriate classification				
		Investigator	Technician & Research Assistant	Student		Fellow
				Undergraduate	Graduate	
John Orlowski	Physiology	X				
Annie Boucher	Physiology		X			

5. EMERGENCY: Person(s) designated to handle emergencies

Name: John Orlowski Phone No: work: 398-8335 home: 631-0871

Name: Phone No: work: home:

6. Briefly describe:

i) the biohazardous material involved & designated biosafety risk group:

Mammalian Cell Culture (Location: Rm. 1141)

Mammalian cell lines (including rodent and human cells) will be maintained in this room. None of the cell lines used contain infectious agents that may pose a health hazard to humans. However, all investigators using this facility will follow the laboratory protocol for cell culture listed below.

Bacterial Cell Culture (Location: Rm. 1114 and 1151)

All bacteria used are *E. coli.* Strain derivatives that have been approved by CIHR for recombinant DNA procedures and do not pose any risk to human health. All investigators using bacteria will follow standard laboratory procedures for use of bacteria.

ii) the procedures to be conducted:

1. All investigators will wear disposable rubber gloves.
2. The interior surfaces of the biological containment, laminar flow hood will be sprayed or swabbed with appropriate disinfectants, such as 70% ethanol, before and after use.
3. All disposable materials, including rubber gloves, plastic tissue culture plates, flasks and pipets will be placed in biohazard bags and autoclaved as appropriate.
4. Nondisposable materials (i.e. glassware) will be placed in plastic containers containing water saturated with Cloro bleach as a disinfectant. Materials will be washed and autoclaved for subsequent use.
5. Used cell culture media will be treated with Clorox bleach and then disposed.

iii) the protocol for decontaminating spills:

In the event of a liquid media spill, the area surrounding the spill will be cordoned off immediately, the liquid will be removed by absorbent paper towels and placed in a biohazard bag for autoclaving, and the area will be swabbed thoroughly with Clorox bleach disinfectant or 70% ethanol.

---

7. Does the protocol present conditions (e.g. handling of large volumes or high concentrations of pathogens) which could increase the hazards of the infectious agent (s)?

NO

---

8. Do procedures involving genetically engineered organisms have a history of safe use?

YES

---

9. What precautions are being taken to reduce production of infectious droplets and aerosols?

The laboratory does not use infectious agents. However, all cell culture is performed in biological safety laminar flow hoods. Noxious substances are used in University approved biological fume hoods.

---

10. List the biological safety cabinets to be used.

Building	Room No.	Manufacturer	Model No.	Serial No.	Date Certified
McIntyre Medical Science Bldg.	1141	Baker Company	1390-112	SP22885	June 14, 2002